

AD-A045 244

IOWA INST OF HYDRAULIC RESEARCH IOWA CITY
FIELD STUDY OF SEDIMENT TRANSPORT CHARACTERISTICS OF THE MISSIS--ETC(U)

F/6 8/8

JUL 77 T NAKATO, J F KENNEDY

UNCLASSIFIED

IIHR-201

NL

OF 2
AD
A045 244



BIBLIOGRAPHIC DATA SHEET		1. Report No. IIHR Report 201	2.	3. Recipient's Accession No.
4. Title and Subtitle Field study of sediment transport characteristics of the Mississippi River near Fox Island (RM 355-6) and Buzzard Island (RM 349-50)				5. Report Date July 1977
6.				7. Author(s) Tatsuaki Nakato & John F Kennedy
8. Performing Organization Rept. No.		9. Performing Organization Name and Address Iowa Institute of Hydraulic Research The University of Iowa Iowa City, Iowa 52242		10. Project/Task/Work Unit No.
11. Contract/Grant No.				12. Sponsoring Organization Name and Address U.S. Army Corps of Engineers Rock Island District Rock Island, Illinois
13. Type of Report & Period Covered				14.
15. Supplementary Notes <i>The field study was conducted in order to obtain a better understanding of the flow and sediment-transport mechanisms responsible for the recurrent shoaling that has been experienced in the vicinities of Fox Island (RM 355-6) and Buzzard Island (RM-349-50) in Pool 20 between Keokuk, Iowa, and Canton, Missouri, in the Mississippi River. Three sets of detailed data on transverse and streamwise distributions of flow velocity, suspended sediment discharge, bed-load discharge, bed-material properties, and flow depth were obtained for the high, intermediate, and low river stages during the period between May and September, 1976. The field data were used to establish empirical relationships between the sediment transport rates and hydraulic quantities in the study reaches. Based on the empirical sediment discharge formulas, closures of some side-channels to increase sediment-transport capacity in the main channel of the study reaches have been suggested.</i>				
16. Abstracts <i>The field study was conducted in order to obtain a better understanding of the flow and sediment-transport mechanisms responsible for the recurrent shoaling that has been experienced in the vicinities of Fox Island (RM 355-6) and Buzzard Island (RM-349-50) in Pool 20 between Keokuk, Iowa, and Canton, Missouri, in the Mississippi River. Three sets of detailed data on transverse and streamwise distributions of flow velocity, suspended sediment discharge, bed-load discharge, bed-material properties, and flow depth were obtained for the high, intermediate, and low river stages during the period between May and September, 1976. The field data were used to establish empirical relationships between the sediment transport rates and hydraulic quantities in the study reaches. Based on the empirical sediment discharge formulas, closures of some side-channels to increase sediment-transport capacity in the main channel of the study reaches have been suggested.</i>				
17. Key Words and Document Analysis. 17a. Descriptors sediment transport, river, field study				
17b. Identifiers/Open-Ended Terms				
17c. COSATI Field/Group				
18. Availability Statement	DISTRIBUTION STATEMENT A Approved for public release; Distribution Unlimited		19. Security Class (This Report) UNCLASSIFIED	21. No. of Pages 92
			20. Security Class (This Page) UNCLASSIFIED	22. Price

INSTRUCTIONS FOR COMPLETING FORM NTIS-35

(Bibliographic Data Sheet based on COSATI)

Guidelines to Format Standards for Scientific and Technical Reports Prepared by or for the Federal Government, PB-180 600).

1. **Report Number.** Each individually bound report shall carry a unique alphanumeric designation selected by the performing organization or provided by the sponsoring organization. Use uppercase letters and Arabic numerals only. Examples FASEB-NS-73-87 and FAA-RD-73-09.
2. Leave blank.
3. **Recipient's Accession Number.** Reserved for use by each report recipient.
4. **Title and Subtitle.** Title should indicate clearly and briefly the subject coverage of the report, subordinate subtitle to the main title. When a report is prepared in more than one volume, repeat the primary title, add volume number and include subtitle for the specific volume.
5. **Report Date.** Each report shall carry a date indicating at least month and year. Indicate the basis on which it was selected (e.g., date of issue, date of approval, date of preparation, date published).
6. **Performing Organization Code.** Leave blank.
7. **Author(s).** Give name(s) in conventional order (e.g., John R. Doe, or J. Robert Doe). List author's affiliation if it differs from the performing organization.
8. **Performing Organization Report Number.** Insert if performing organization wishes to assign this number.
9. **Performing Organization Name and Mailing Address.** Give name, street, city, state, and zip code. List no more than two levels of an organizational hierarchy. Display the name of the organization exactly as it should appear in Government indexes such as Government Reports Index (GRI).
10. **Project/Task/Work Unit Number.** Use the project, task and work unit numbers under which the report was prepared.
11. **Contract/Grant Number.** Insert contract or grant number under which report was prepared.
12. **Sponsoring Agency Name and Mailing Address.** Include zip code. Cite main sponsors.
13. **Type of Report and Period Covered.** State interim, final, etc., and, if applicable, inclusive dates.
14. **Sponsoring Agency Code.** Leave blank.
15. **Supplementary Notes.** Enter information not included elsewhere but useful, such as: Prepared in cooperation with . . . Translation of . . . Presented at conference of . . . To be published in . . . Supersedes . . . Supplements . . . Cite availability of related parts, volumes, phases, etc. with report number.
16. **Abstract.** Include a brief (200 words or less) factual summary of the most significant information contained in the report. If the report contains a significant bibliography or literature survey, mention it here.
17. **Key Words and Document Analysis.** (a) **Descriptors.** Select from the Thesaurus of Engineering and Scientific Terms the proper authorized terms that identify the major concept of the research and are sufficiently specific and precise to be used as index entries for cataloging. (b) **Identifiers and Open-Ended Terms.** Use identifiers for project names, code names, equipment designators, etc. Use open-ended terms written in descriptor form for those subjects for which no descriptor exists. (c) **COSATI Field/Group.** Field and Group assignments are to be taken from the 1964 COSATI Subject Category List. Since the majority of documents are multidisciplinary in nature, the primary Field/Group assignment(s) will be the specific discipline, area of human endeavor, or type of physical object. The application(s) will be cross-referenced with secondary Field/Group assignments that will follow the primary posting(s).
18. **Distribution Statement.** Denote public releasability, for example "Release unlimited", or limitation for reasons other than security. Cite any availability to the public, other than NTIS, with address, order number and price, if known.
- 19 & 20. **Security Classification.** Do not submit classified reports to the National Technical Information Service.
21. **Number of Pages.** Insert the total number of pages, including introductory pages, but excluding distribution list, if any.
22. **NTIS Price.** Leave blank.

FIELD STUDY OF SEDIMENT TRANSPORT
CHARACTERISTICS OF THE MISSISSIPPI RIVER
NEAR FOX ISLAND (RM 355-6) AND
BUZZARD ISLAND (RM 349-50)

by

10

Tatsuaki Nakato and John F. Kennedy

Submitted to

U.S. Army Corps of Engineers
Rock Island District
Rock Island, Illinois

DDC
202102
OCT 18 1977

14

IIHR - 201

Iowa Institute of Hydraulic Research
The University of Iowa
Iowa City, Iowa

DISTRIBUTION STATEMENT A

Approved for public release
Distribution Unlimited

11 Jul 77

12 95 p.

188 300 ✓

met

ABSTRACT

The field study was conducted in order to obtain a better understanding of the flow and sediment-transport mechanisms responsible for the recurrent shoaling that has been experienced in the vicinities of Fox Island (between RM 355 and RM 356) and Buzzard Island (between RM 349 and RM 350) in Pool 20 between Keokuk, Iowa, and Canton, Missouri, in the Mississippi River. Three sets of detailed data on transverse and streamwise distributions of flow velocity, suspended sediment discharge, bed-load discharge, bed-material properties, and flow depth were obtained for the high, intermediate, and low river stages during the period between May and September, 1976. The field data were used to establish empirical relationships between the bed-load discharge, Q_B (tons/day); and the water discharge, Q (cfs); and mean velocity, U (ft/s) in the study reaches. It was found that Q_B varies as approximately to fourth power of U or Q . The suspended-load discharge, Q_S (tons/day), was found to vary as the square, roughly, of Q . The unit total load, q_T (tons/ft/s), was found to vary as the square, approximately, of the unit water discharge, q (cfs/ft). In the vicinity of the Buzzard Island reach the Mississippi River flow was found to bifurcate, with in excess of 25 percent of the water discharge passing through the secondary side channel. This flow bifurcation and the attendant velocity reduction downstream from it in the main channel was found to be responsible in large measure for the recurrent shoaling in this reach. According to the empirical sediment-discharge formulas, closure of this side channel would roughly double the bed-load transport capacity of the reach. The sediment responsible for the recurrent shoaling in the study reaches was also found to originate from the Des Moines River (RM 361.5). The relatively large quantity of sand transported by the Des Moines River as both bed load and suspended load tends to be deposited downstream from the confluence of the two rivers due to relatively small energy slope of the Mississippi River. From examination made to determine the sensitivity of computed water- and sediment-discharge quantities to the number of sampling verticals, it was concluded that 8 to 10 sampling positions across a major Mississippi River section in the study reaches are adequate to yield reliable results.

ACKNOWLEDGEMENTS

This field study was conducted for, and sponsored by, the U.S. Army Corps of Engineers, Rock Island District Office, Rock Island, Illinois. The authors wish to express their special thanks to Messrs. Dudley Hansen, Richard Baker, and Steve VanderHorn of Corps of Engineers for their un-failing cooperation and assistance throughout the course of the study and for critically reviewing the manuscript. Valuable information concerning the present investigation was provided by the Rock Island District engineers. The authors also wish to acknowledge their gratitude to the U.S. Geological Survey, Iowa City District Office, for providing us with various sediment samplers, and especially Mr. Wilbur J. Matthes Jr. for training us in the best techniques for data collection and analysis of sediment. Finally, we wish to acknowledge Dr. C.T. Yang of Corps of Engineers, North Central Division, Chicago, Illinois for his critically reviewing the manuscript; Mr. Dale Harris and his shop staff for conducting the field work; Dr. John R. Glover for his assistance with the instrumentation; and Messrs. G-L Tyan, George Gay, and Steve Weber, who served as research assistants in the conduct of the study.

TABLE OF CONTENTS

	<u>Page</u>
I. INTRODUCTION	1
A. Background	1
B. Scope of the Study	4
II. EQUIPMENT AND DATA-SAMPLING TECHNIQUES	5
A. Field Equipment	5
1. Boat	5
2. Distance meter	5
3. Current meter	7
4. Suspended sediment sampler	7
5. Bed-load sampler	7
6. Bed-material sampler	9
B. Measurement Procedure	9
C. Sediment Analysis	12
III. PRESENTATION AND DISCUSSION OF FIELD DATA	13
A. Study Sections and Sampling Dates	13
B. Data Analysis	13
C. Presentation of Data	16
1. Velocity distributions	16
2. Channel cross sections	22
3. Lateral distributions of unit flow and sediment-transport quantities	28
4. Longitudinal distributions of averaged flow and sediment transport quantities	55
5. Effect of flow bifurcation on main-channel mean velocity	58
6. Effect of rainstorms on the Mississippi River sediment transport characteristics	59
7. Sediment transport characteristics of the Mississippi and Des Moines Rivers	64
8. Empirical sediment-discharge formulas	68
9. Evaluation of some existing sediment-discharge formulas	73

	<u>Page</u>
IV. SUMMARY AND CONCLUSIONS	78
LIST OF REFERENCES	83

LIST OF TABLES

Table 1. Sampling dates and number of sediment samples collected	13
Table 2. Summary of principal quantities obtained from the field data (1st trip)	17
Table 2. (2nd trip)	18
Table 2. (3rd trip)	19
Table 3. Effect of number of sampling verticals on major hydraulic and sediment-transport quantities for Sec. 2-1"	55
Table 4. Water discharges and mean velocities in Sec. 8-1 and Sec. 8-2	58
Table 5. Water and suspended-load discharges through the Mississippi and the Des Moines River study reaches	60
Table 6. Vertical distributions of suspended sediment concentrations at Sec. 8-1 and Sec. 9-1 from the first trip	64

LIST OF FIGURES

Figure 1(a). Fox Island study reach	2
Figure 1(b). Buzzard Island study reach	3
Figure 2. Photograph showing part of swing boom and cable attached to winch	6
Figure 3. Current meter attached to 50-lb weight	6
Figure 4. Suspended-load sampler and 1 pint milk bottle (US P-61)	8
Figure 5. Bed-load sampler (Helley-Smith)	8
Figure 6. Bed-material sampler (US BM-54)	10
Figure 7. Locations of transects in the Mississippi and Des Moines Rivers	14
Figure 7A. Definition sketch for variables	15A
Figure 8(a). Typical velocity distributions obtained at Sec. 5-1	20
Figure 8(b). Relationship between κ and \bar{C}	21
Figure 9. Comparison of flow discharges measured by IIHR with those measured by COE(RI)	23
Figure 10. Variations in cross-sectional bed profile (Fox Island Reach)	24
Figure 10. (Cont'd)	25

	<u>Page</u>
Figure 11. Variations in cross-sectional bed profile (Buzzard Island Reach)	26
Figure 11. (Cont'd)	27
Figure 12. Lateral distributions of d , \bar{u} , \bar{q} , \bar{q}_s , \bar{q}_B , and D_{50} for Sec. 1-2	29
Figure 13. Lateral distributions of d , \bar{u} , \bar{q} , \bar{q}_s , \bar{q}_B , and D_{50} for Sec. 2-1	30
Figure 14. Lateral distributions of d , \bar{u} , \bar{q} , \bar{q}_s , \bar{q}_B , and D_{50} for Sec. 3-2	31
Figure 15. Lateral distributions of d , \bar{u} , \bar{q} , \bar{q}_s , \bar{q}_B , and D_{50} for Sec. 4-1	32
Figure 16. Lateral distributions of d , \bar{u} , \bar{q} , \bar{q}_s , \bar{q}_B , and D_{50} for Sec. 5-1	34
Figure 17. Lateral distributions of d , \bar{u} , \bar{q} , \bar{q}_s , \bar{q}_B , and D_{50} for Sec. 6-1	35
Figure 18. Lateral distributions of d , \bar{u} , \bar{q} , \bar{q}_s , \bar{q}_B , and D_{50} for Sec. 7-2	36
Figure 19. Lateral distributions of d , \bar{u} , \bar{q} , \bar{q}_s , \bar{q}_B , and D_{50} for Sec. 8-1	37
Figure 20. Lateral distributions of d , \bar{u} , \bar{q} , \bar{q}_s , \bar{q}_B , and D_{50} for Sec. 2-1'	38
Figure 21. Lateral distributions of d , \bar{u} , \bar{q} , \bar{q}_s , \bar{q}_B , and D_{50} for Sec. 2-1'	39
Figure 22. Lateral distributions of d , \bar{u} , \bar{q} , \bar{q}_s , \bar{q}_B , and D_{50} for Sec. 3-2'	40
Figure 23. Lateral distributions of d , \bar{u} , \bar{q} , \bar{q}_s , \bar{q}_B , and D_{50} for Sec. 4-1'	41
Figure 24. Lateral distributions of d , \bar{u} , \bar{q} , \bar{q}_s , \bar{q}_B , and D_{50} for Sec. 5-1'	43
Figure 25. Lateral distributions of d , \bar{u} , \bar{q} , \bar{q}_s , \bar{q}_B , and D_{50} for Sec. 6-1'	44
Figure 26. Lateral distributions of d , \bar{u} , \bar{q} , \bar{q}_s , \bar{q}_B , and D_{50} for Sec. 7-2'	45
Figure 27. Lateral distributions of d , \bar{u} , \bar{q} , \bar{q}_s , \bar{q}_B , and D_{50} for Sec. 8-1'	46
Figure 28. Lateral distributions of d , \bar{u} , \bar{q} , \bar{q}_s , \bar{q}_B , and D_{50} for Sec. 1-2"	47
Figure 29. Lateral distributions of d , \bar{u} , \bar{q} , \bar{q}_s , \bar{q}_B , and D_{50} for Sec. 2-1"	48
Figure 30. Lateral distributions of d , \bar{u} , \bar{q} , \bar{q}_s , \bar{q}_B , and D_{50} for Sec. 3-2"	49
Figure 31. Lateral distributions of d , \bar{u} , \bar{q} , \bar{q}_s , \bar{q}_B , and D_{50} for Sec. 4-1"	50

	<u>Page</u>
Figure 32. Lateral distributions of d , \bar{u} , \bar{q} , \bar{q}_s , \bar{q}_B , and D_{50} for Sec. 5-1"	51
Figure 33. Lateral distributions of d , \bar{u} , \bar{q} , \bar{q}_s , \bar{q}_B , and D_{50} for Sec. 6-1"	52
Figure 34. Lateral distributions of d , \bar{u} , \bar{q} , \bar{q}_s , \bar{q}_B , and D_{50} for Sec. 7-2"	53
Figure 35. Lateral distributions of d , \bar{u} , \bar{q} , \bar{q}_s , \bar{q}_B , and D_{50} for Sec. 8-1"	54
Figure 36. Longitudinal variations of q , U , q_s , q_B , and \bar{D}_{50}	56
Figure 36A. Longitudinal variations of Q , Q_s , and Q_B	57A
Figure 37. Relationship between Q and Q_s for the Des Moines River	62
Figure 38. Variations in cross-sectional bed profile for the Des Moines River	63
Figure 39. Typical vertical distributions of suspended-sediment concentration obtained at Sec. 1-2 and Sec. 9-1 (1st trip)	66
Figure 39. (Cont'd) (2nd and 3rd trips)	67
Figure 39A. Typical size distribution curves for bed-material samples obtained at Sec. 6-1 (approximately 600 ft from the right bank)	68A
Figure 40. Relationship between U and Q_B	69
Figure 41. Relationship between Q and Q_B	71
Figure 42. Relationship between Q and Q_s	72
Figure 43. Relationship between q and q_T	74
Figure 44(a). Evaluation of sediment-discharge formulas (Engelund-Hansen, Inglis-Lacey, and Einstein-Brown formulas)	75
Figure 44(b). Evaluation of sediment-discharge formulas (Engelund-Hansen, Inglis-Lacey, and Einstein-Brown formulas)	76
Figure 45(a). Evaluation of total sediment discharges using Toffaleti formula	77
Figure 45(b). Evaluation of bed-load discharges using Toffaleti formula	79
Figure 46. Evaluation of total sediment discharges using Colby's relation	80

LIST OF SYMBOLS

The following symbols are used in this report:

a = distance above river bed to sampler intake nozzle when suspended sediment sampler is at the lowest vertical position;

A = cross-sectional area of channel;

C = point-integrated local suspended sediment concentration;

\bar{C} = mean suspended sediment concentration averaged over depth;

d = local flow depth;

\bar{d} = mean flow depth (A/W)

D_{50} = median size of bed sediment;

\bar{D}_{50} = mean median size of bed sediment;

D_g = geometric mean size of bed sediment;

q = water discharge per unit width (Q/W);

Q = water discharge;

q_B = bed-load discharge per unit width (Q_B/W);

q_i = water discharge for i-th subsection of transect;

q_s = suspended-load discharge per unit width (Q_s/W)

q_T = total sediment discharge per unit width (Q_T/W);

Q_B = bed-load discharge;

Q_s = suspended-load discharge;

Q_T = total sediment discharge (Q_B+Q_s);

q_{Bi} = bed-load for i-th subsection of transect;

q_{si} = suspended load for i-th subsection of transect;

\bar{q} = water discharge per unit width (q_i/W_i);

\bar{q}_B = bed-load per unit width (q_{Bi}/W_i);

\bar{q}_s = suspended-load per unit width (q_{si}/W_i);

S = slope of energy gradient;

T = surface water temperature;

u = local flow velocity;

U = mean flow velocity (Q/A);

\bar{u} = mean flow velocity at vertical;

u_* = shear velocity;

w = fall velocity of sediment particle;

W = channel width;

w_i = width of i -th subsection of transect;
 y = distance above river bed;
 z = Rouse number ($w/\beta \kappa u_*$);
 β = ratio of ϵ_s to ϵ_m (ϵ_s/ϵ_m);
 ϵ_m = diffusion coefficient for momentum;
 ϵ_s = diffusion coefficient for sediment;
 κ = Kármán constant; and
 σ_g = geometric standard deviation of particle size.

LIST OF U.S. CUSTOMARY-SI CONVERSION FACTORS

To convert	To	Multiply by
inches (in.)	millimeters (mm)	25.40
inches (in.)	centimeters (cm)	2.540
inches (in.)	meters (m)	0.0254
feet (ft)	meters (m)	0.305
miles (mi)	kilometers (km)	1.61
yards (yd)	meters (m)	0.91
cubic inches (cu in.)	cubic centimeters (cm^3)	16.4
cubic feet (cu ft)	cubic meters (m^3)	0.028
cubic yards (cu yd)	cubic meters (m^3)	0.765
pounds (lb)	kilograms (kg)	0.453
tons (ton)	kilograms (kg)	1000.0

FIELD STUDY OF SEDIMENT TRANSPORT CHARACTERISTICS OF
THE MISSISSIPPI RIVER NEAR FOX ISLAND (RM 355-6) AND
BUZZARD ISLAND (RM 349-50)

I. INTRODUCTION

A. Background. The field study reported herein was directed primarily towards elucidating the mechanisms and processes responsible for the recurrent shoaling which has been experienced in the reaches of the Mississippi River in the vicinities of Fox Island (between RM 355 and RM 356) and Buzzard Island (between RM 349 and RM 350), in Pool 20 between Keokuk, Iowa, and Canton, Missouri. The locations of the Fox Island and Buzzard Island study reaches are shown in figures 1(a) and 1(b). They lie approximately 9 mi and 15 mi, respectively, downstream from Lock and Dam 19 (Keokuk, Iowa). The chronic shoaling these reaches historically have experienced has given rise to the necessity of periodic dredging by the Army Corps of Engineers, Rock Island District [COE(RI)], of large quantities of river-bed material in order to maintain the 9-foot navigation channel. Dredging records show, for example, that 132,471 cu yd of sediment was dredged from the Fox Island reach in 1975, and 68,075 cu yd was removed from the Buzzard Island reach in 1976. The average annual dredging volume required to maintain the navigation channel in the Mississippi River between Guttenberg, Iowa, and Saverton, Missouri, a river distance of approximately 315 miles, amounts to approximately one million cubic yards. Concomitant with these large quantities of dredging are two major problems. First, the cost of dredging has increased sharply in recent years. The average unit dredging costs for the aforementioned reaches of the Mississippi River for the years 1973, 1974, 1975, and 1976 were about \$0.27/yd³, \$0.49/yd³, \$0.77/yd³, and \$1.88/yd³, respectively. Here it should be noted that the radical increase in the unit cost for the last two years was due to some extent to the reduced dredging volumes. The second major problem is arising from disposal of dredge spoil in shallow backwater areas away from the main channel, or on natural islands. This practice recently has come under severe attack from environmentalists because of the purported adverse impact of the turbidity produced by the dredging and spoil deposition on wildlife

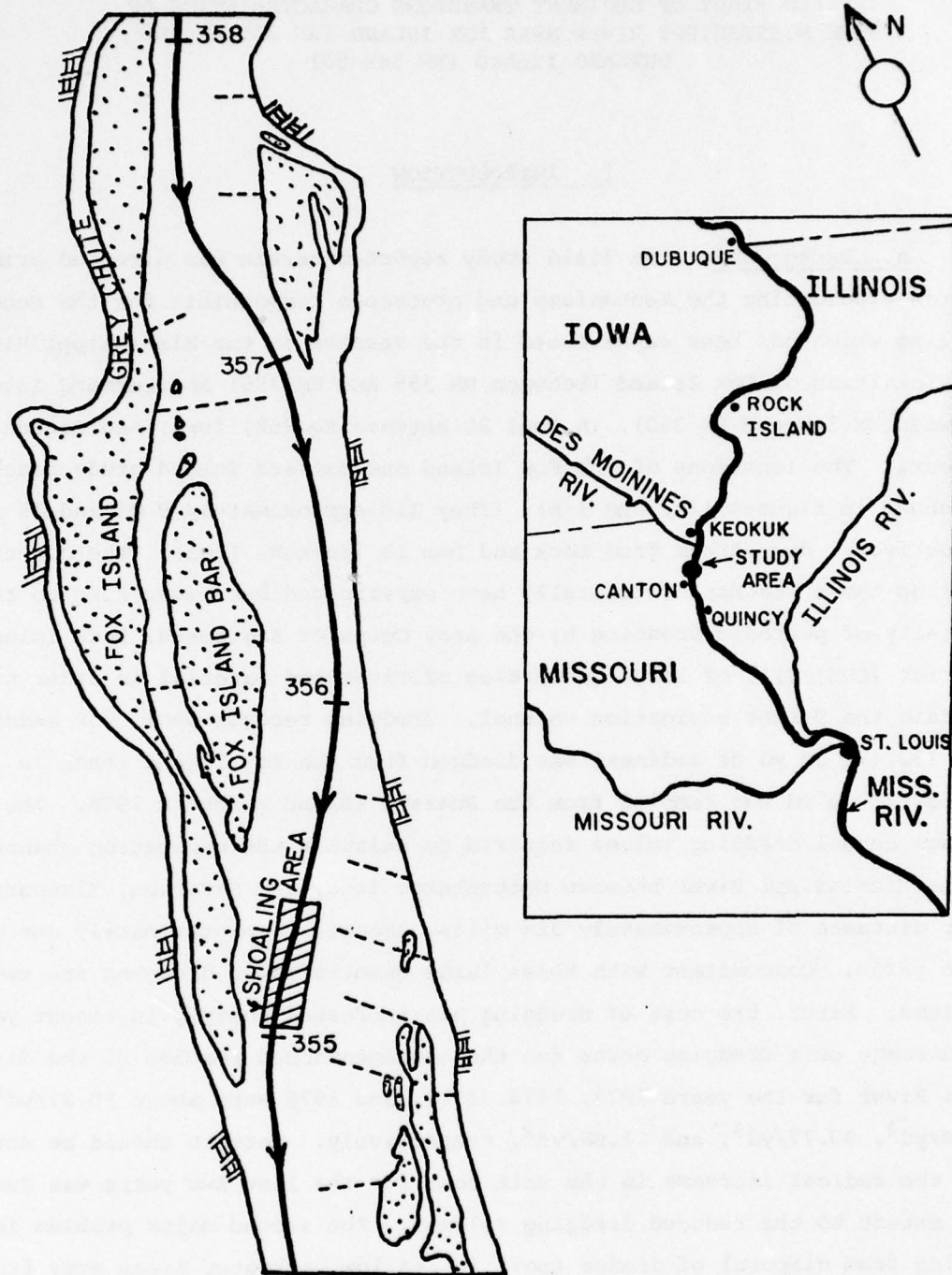


Figure 1(a). Fox Island study reach

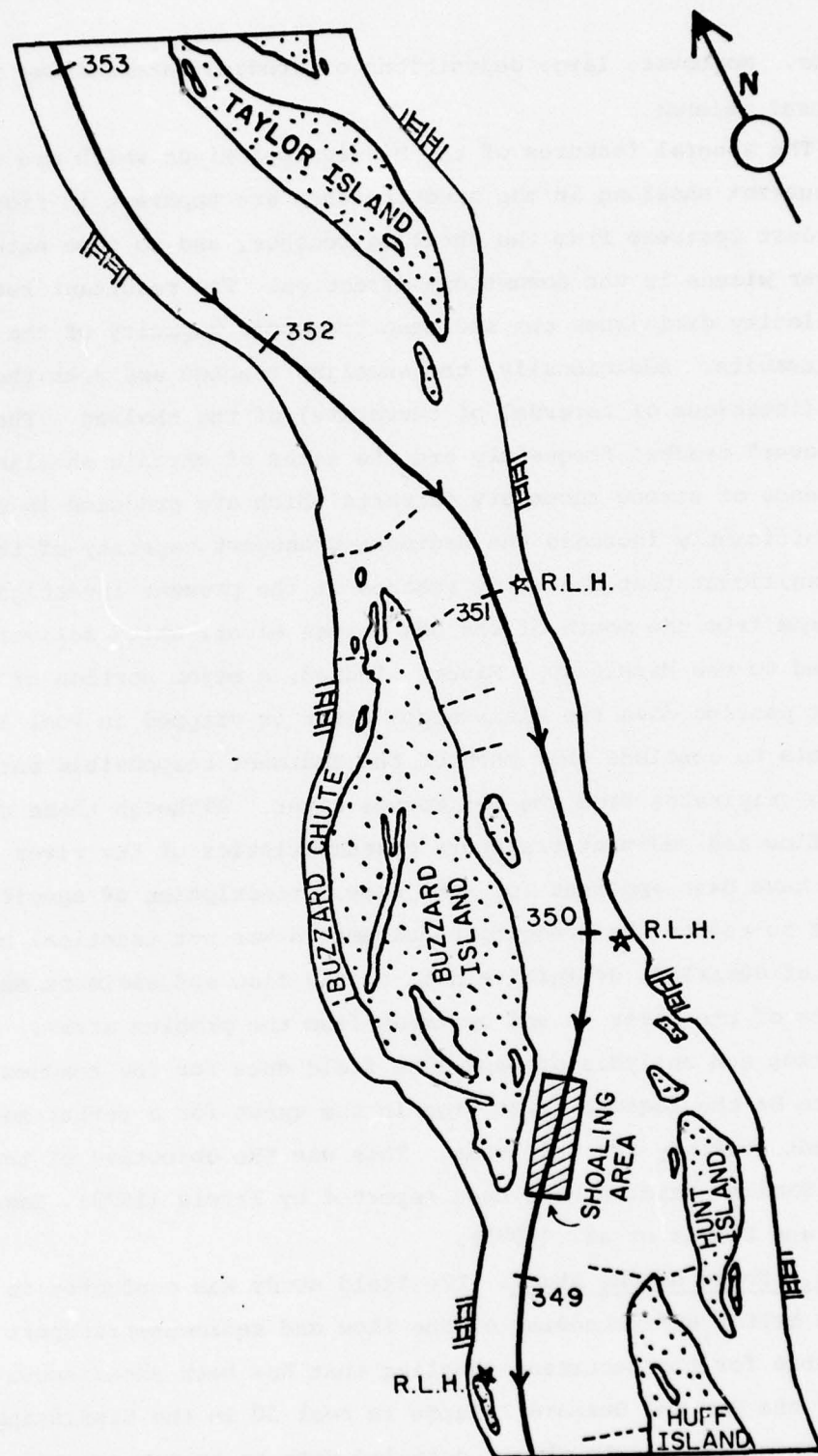


Figure 1(b). Buzzard Island study reach

habitats. Moreover, large depositions of dredged material may injure trees in natural islands.

The general features of the Mississippi River which are responsible for the recurrent shoaling in the study reaches are apparent in figures 1(a) and 1(b). Just upstream from the shoaling reaches, and to some extent along them, the river widens in the downstream direction. The resultant reduction in the mean velocity diminishes the sediment-transport capacity of the flow, and deposition results. Additionally, the shoaling reaches are near the inflection points (locations of reversal of curvature) of the thalweg. These so-called "cross-over" reaches frequently are the sites of chronic shoaling, because of the absence of strong secondary currents which are produced in channel bends and significantly increase the sediment-transport capacity of the flow. It is also significant that the study reaches of the present investigation are just downstream from the mouth of the Des Moines River, which delivers a large sediment load to the Mississippi River. Indeed, a major portion of the coarser sediment passing down the Mississippi River is trapped in Pool 19, and it is reasonable to conclude that much of the sediment responsible for the problem shoaling originates from the Des Moines River. Although these general features of the flow and sediment-transport characteristics of the river in the study reaches have been apparent for some time, prescription of specific corrective measures to reduce the dredging requirements was not practical because of the absence of detailed, definitive data on the flow and sediment movement characteristics of the river in and upstream from the problem areas. Accordingly, acquisition and analysis of base-line field data for the reaches were concluded to be the logical first step in the quest for a better sediment-management strategy for the areas. This was the objective of the present study. Similar studies have been reported by Isfeld (1973), Lagasse et al. (1976), and Simons et al. (1975).

B. Scope of the Study. The field study was conducted in order to obtain a better understanding of the flow and sediment-transport mechanisms responsible for the recurrent shoaling that has been experienced in the vicinities of the Fox and Buzzard Islands in Pool 20 in the Mississippi River. The primary objective was to obtain detailed data on transverse and streamwise distributions of flow velocity, suspended sediment discharge, bed-load

discharge, bed-material properties, and flow depth. A concomitant objective was establishment of a sediment-transport formula which could be used to describe the local unit (per unit width) sediment discharge of the stream and its dependence on the local flow properties and bed characteristics. A third objective was to develop, from these recommendations for corrective measures which could be implemented to reduce the frequency and volume of dredging required to maintain the 9-foot navigation channel. A final objective was to evaluate the reliability of several existing sediment-discharge formulas as predictors for the local unit sediment discharge of this stretch of the Mississippi River.

II. EQUIPMENT AND DATA-SAMPLING TECHNIQUES

A. Field Equipment. The principal items of equipment employed in the measurement of the field data were as follows:

1. Boat. The Iowa Institute of Hydraulic Research (IIHR) data-collection boat was used for all field work. This is an 18-foot Jon-boat (monArk: Model MV-18, weight capacity = 2,100 lbs) equipped with a 50 HP outboard motor (Mercury: Model 500). A swing-boom attached to the bottom of the boat was used to suspend the current meter and sediment samplers at any desired vertical position through a steel cable (1/8-in. Ellsworth reverse-lay cable) which was attached to a winch fitted with a dial gauge. Figure 2 shows the winch and part of the boom. The boat was equipped with a removable canvas cover which was found to be invaluable in protecting the crew and equipment from the elements. However, the cover had to be removed on windy days, because the wind drag on it caused the boat to drift from the sampling position.

2. Distance meter. An optical-type distance meter (Hewlett-Packard: Model 3800B) was utilized to determine boat positions along the measurement transects. The instrument was positioned along the bank, and the reflector was attached to a staff mounted on the boat bow. The instrument emits a modulated infrared light beam, and determines distance by counting the integral number of light-beam intensity variations, plus a residual number, between the instrument and reflector. The range of the instrument is 3,000 m, and the mean-square error in distance determination is \pm (5 mm + 7 mm per km) for temperatures between -10°C and 40°C .

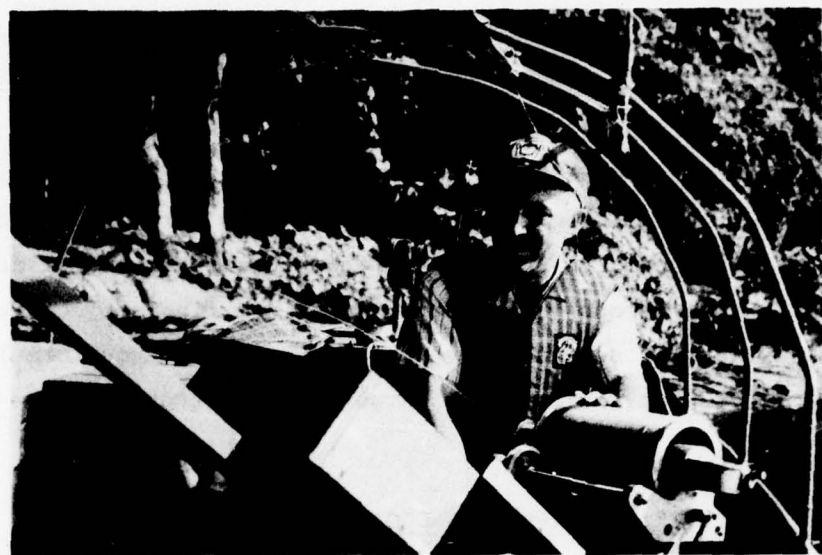


Figure 2. Photograph showing part of swing boom and cable attached to winch



Figure 3. Current meter attached to 50-lb weight

3. Current meter. Velocities were measured by means of a propeller-type current meter (A. OTT Kempten Universal Current Meter: Model 10.002) which is shown in figure 3. Each revolution of the propeller produced an electrical signal, which was counted and displayed by a digital counter (Hewlett-Packard: Model 5300A Measuring System). A measurement time of 60 sec was used. The current meter was calibrated against a measured distance in the uniform velocity distribution in a flow of known width and depth in one of the laboratory flumes of IIHR. The estimated accuracy of the field velocity measurements is \pm 5 percent. The major impediment to achieving better accuracy was movement of the boat.

4. Suspended sediment sampler. Suspended sediment samples were obtained by means of a US P-61 point-integrating suspended-sediment sampler (Guy and Norman 1970, Vanoni 1975) which was borrowed from the U.S.G.S. District Office, Iowa City. The sampler is shown in figure 4. It weighed 100 lbs; was fitted with a 3/16-in. diameter intake nozzle which collected the sample in a one-pint milk bottle in its body; and was equipped with a solenoid activated valve and an equalizing air compression chamber. When the solenoid valve was not energized, the air chamber in the body was connected to the cavity in the sampler head which was connected, in turn, through the valve to the sample bottle; the intake and exhaust passages then were closed. When the solenoid was energized, the valve as well as the intake and exhaust passages were opened. The US P-61 was designed to sample isokinetically; i.e., the water-sediment sample enters the nozzle at the local ambient flow velocity. The solenoid was activated by means of four 12-volt batteries which were connected to the sampler through a switch and electrical cable.

5. Bed-load sampler. Bed-load samples were obtained with a 50-lb Helleys-Smith bed-load sampler, which also was borrowed from the U.S.G.S. District Office in Iowa City. The sampler, which is shown in figure 5, consists of a pipe-frame, a stainless-steel inlet section connected to a 125 μ -mesh nylon trap net, and large tail fins which align the axis of the sampler with the flow. The hanger is so positioned that as the sampler is lowered, its tail section reaches the bed first. In this way the inlet section can be carefully lowered to the bed without disturbing the bed surface. Bed-load sediment moving into the 3-in. wide and 3-in. high inlet mouth passes through a diverging section before entering the trapping net. The sediment is

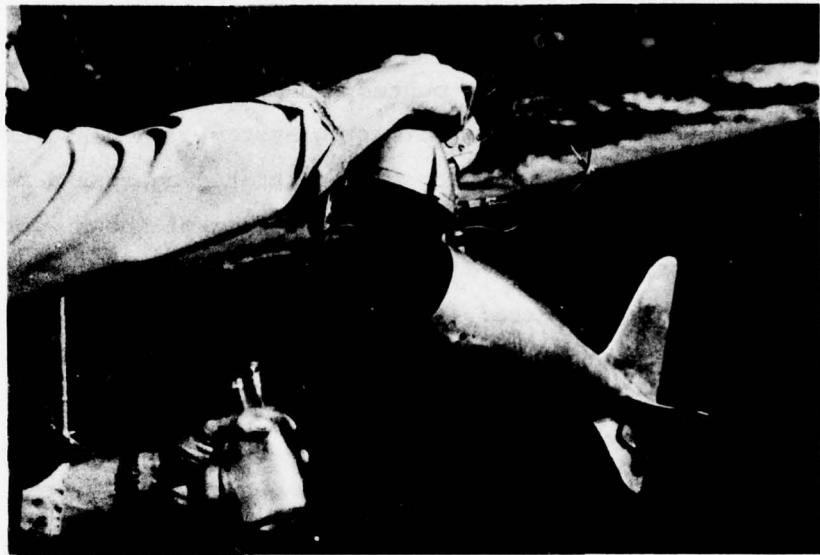


Figure 4. Suspended-load sampler and 1 pint milk bottle (US P-61)

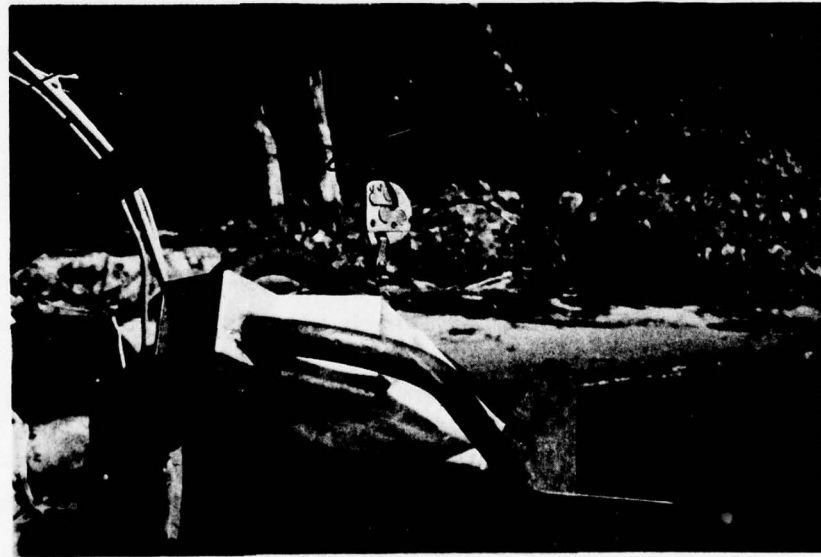


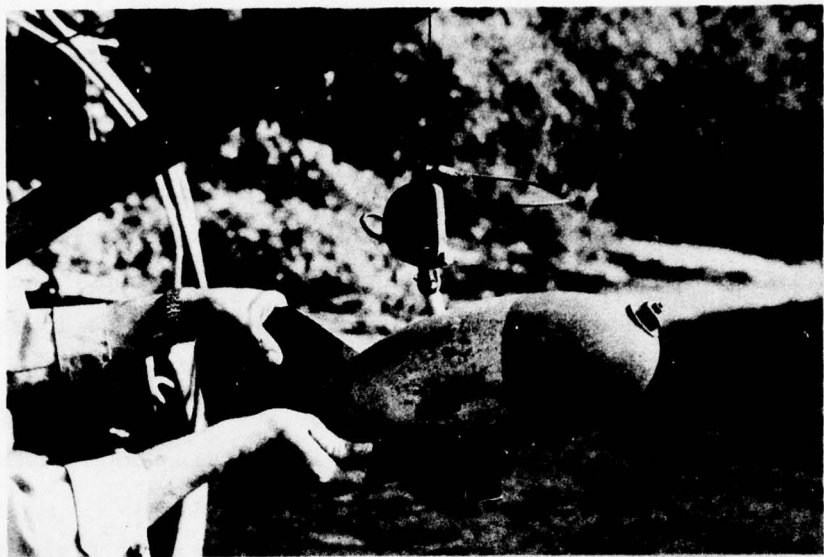
Figure 5. Bed-load sampler (Holley-Smith)

retained in the net, while the water passes through it.

6. Bed-material sampler. Bed-material samples were collected by means of a US BM-54 bed-material sampler (Guy and Norman 1970, Vanoni 1975) borrowed from the U.S.G.S. District Office in Iowa City. Figure 6 presents a photograph of the sampler, which weighs 100 lbs; is equipped with tail fins to align it with the flow; and is designed to collect a 3-in. wide bed-material sample from the top 2 in. of the stream bed by means of a metal scoop. The retractable scoop is placed in the open position before the sampler is lowered to the bed. When tension in the supporting cable is released by resting the sampler on the bed, a coil spring rotates the scoop through 180°, thereby trapping the sample. When the scoop is in the closed position, its cutting edge rests against a rubber gasket so that none of the sediment sample is lost.

B. Measurement Procedure. Before the program of field-data collection was initiated, a survey trip was made to the study sites to select the locations of the transects along which data would be collected. Note that the word "transect" hereinafter will be used to refer to lines extending clear across the river. Major and secondary sections along each transect were established perpendicular to the principal axis of the river along the Fox Island and Buzzard Island reaches. The ends of the sections were marked by surveyor's stakes close to which 4-foot red-white targets attached to steel posts were installed. Targets and sections were identified by means of large black numbers. Attached to each target was a public notice giving the purpose of the marker and the study and asking that the targets not be damaged. Throughout the course of the study, none of the targets or stakes was disturbed.

Operation of field work proceeded as follows. The distance meter was set up near the shoreline to measure water-surface width. The width of the major section then was divided into 8 to 10 subsections. Samples were collected at the midpoint of each subsection. Before collecting data, the boat was located and anchored at the desired position. This was accomplished through dual-radio communication between the boat crew and the shoreman. Trial and error methods were used; however, after obtaining some experience the boat crew could position the boat on the first try to within a few meters of the desired position. Two anchors, one each attached to the stern and bow, were used to secure the boat. The two-anchor system was found to be especially useful on windy days.



(scoop being set)



(after sampling)

Figure 6. Bed-material sampler (US BM-54)

Flow velocities were measured first, at distances y above the bed of 0.5 ft, 1.0 ft, 1.5 ft, 2.0 ft, 3.0 ft, 4.0 ft, 5.0 ft, 7.0 ft, 10.0 ft, 15.0 ft, 20.0 ft, etc. Point-integrated samples of suspended-sediment then were taken at these positions. The required filling time for the sampler was determined from the velocity measurements so that each sample bottle was nearly filled but did not overflow. Special care was taken not to let the sampler come into contact with the bed, because the outlet holes of the air-equalizing chamber located on the bottom of the sampler body might have been clogged with sediment. Bed-load samples were collected next. The sampling time for these was 5 min, except during flood stage, when a sampling time of only 2 to 3 min was used because of the heavy bed load. During the sampling process the suspension cable of the sampler was maintained loose, to preclude agitation of the sampler by the wind and the wave induced motion of the boat. It was found that even a slight shift in the position of the boat during bed-load sampling could result in the sampler being dragged along the bed and scooping bed material into the net when the sampler was raised. Therefore, extreme care was taken to position the boat so that the bed-load sampler was raised vertically upward from the bed. Sampling was repeated on the spot when the judgement and experience of the field crew indicated that the size of the sample was unreasonable. There was always some question concerning the orientation of the bed-load sampler when it rested on the bed, although the fins presumably aligned the sampler opening parallel to the local flow direction. It is apparent that the local bed-load transport rate varies with position along a bed form, and achieves its maxima at or near the crests of the dunes and its minima in the vicinities of the troughs. It was found, in fact, during the period of the spring flood recession that bed-load samples collected consecutively at the same position varied considerably, presumably due to the migration of the bed forms. Because of these uncertainties, at least two bed-load samples were collected at each measurement position along a section, in an attempt to obtain more reliable estimates of the bed-load transport rate. Finally, a bed-material sample was collected to complete the measurement sequence at a station. The boat was then moved to the next sampling position along the section and the process was repeated. Collection of a complete set of data at each position required approximately 45 min.

C. Sediment Analysis. A total of 1,380 samples (suspended load, bed load, and bed material) were collected during the study. Of these, approximately one third were analyzed in the sediment laboratory of the U.S.G.S. District Office in Iowa City; the others were analyzed in the IIHR sediment laboratory. The procedures followed were the generally accepted ones (Guy 1969, Vanoni 1975).

Because the suspended-material sample was extremely fine, the suspended-load samples were allowed to settle in the sampling milk bottles for at least two weeks before they were analyzed. During this time, the bottles were sealed to prevent evaporation. Most of the suspended-load samples which contained only silt and clay were analyzed by the filtration method. The sediment-water mixture first was weighed; supernatant water was decanted from the bottle by a vacuum pump; and the remainder of the sample was washed into a porcelain crucible with distilled water. The crucible was fitted with a glass-fiber filter and connected to a vacuum system to accelerate filtration. The filtered sample then was dried in an oven, cooled in a desiccator, and weighed on a Sartorius electronic balance to an accuracy of ± 0.0008 gm. The sediment concentration in each sample then was computed, in ppm (mg/l) units. Samples which contained readily visible quantities of sand were analyzed using a split method. The sand portion of the sample was collected on a 62μ wet sieve and subjected to size-distribution analysis by means of the visual accumulation tube (VA) method. The remainder of the sample (i.e., the finer material) then was dried in an oven of 200°F and weighed. No size analysis was made of the material finer than 62μ because the samples were too small for use of the pipette method.

The bed-load samples were placed in plastic bags in the field. In the laboratory, these were washed into beakers and any organic material (mainly dead leaves) was removed by adding a few drops of a 30 percent hydrogen peroxide solution to the water-sediment mixture. Samples larger than approximately 10 gm were sieve analyzed to determine their size distributions, while for smaller samples the VA method was employed.

Organic material first was removed from the bed-material samples, by means of hydrogen peroxide. Material finer than 62μ was separated by a wet sieve. The silt and clay portions of the sample then were dry weighed, while the sand fractions were size-analyzed by means of a sieve.

III. PRESENTATION AND DISCUSSION OF FIELD DATA

A. Study Sections and Sampling Dates. The field data in the Fox Island and Buzzard Island areas were collected along four major transects in each study reach; one located just upstream and a second just downstream from the reaches requiring frequent dredging; and two which transversed the stretches of heavy shoaling. In addition to these principal transects, two others were established to obtain input information on the flow and sediment discharges to the study reaches; one each across the Des Moines and Mississippi Rivers just upstream from their confluence. Each transect consisted of a major section which extended across the main channel; in some cases these were extended by one or more minor sections which covered adjacent small channels around the islands. The locations and the numbers of the individual sections are shown in figure 7. Data were collected during three different periods between May and September 1976, to obtain sets of measurements at a relatively high, an intermediate, and a relatively low river stage. The dates of each data collection trip and the number of samples obtained are given in table 1.

Table 1. Sampling dates and number of sediment samples collected

Trip No.	Period	No. of sus.- load samples	No. of bed- load samples	No. of bed- mate. samples
1	May 5 - May 26, 1976	415	159	50
2	June 17 - July 2, 1976	214	65	37
3	Aug 17 - Sept 9, 1976	316	68	57
	TOTAL:	945	292	143

B. Data Analysis. The procedures employed in the calculation of the water and sediment discharges from the measured data were as follows (Vanoni 1975): The local measured velocity, u , was plotted against the logarithm of elevation above the river bed, y . The mean velocity, \bar{u} , for the vertical then was obtained from the straight line through the data points at $y = 0.37d$, where d is the flow depth for the vertical. The sectional water discharge, q , for each subsection delineated by the bisectors between verticals was obtained

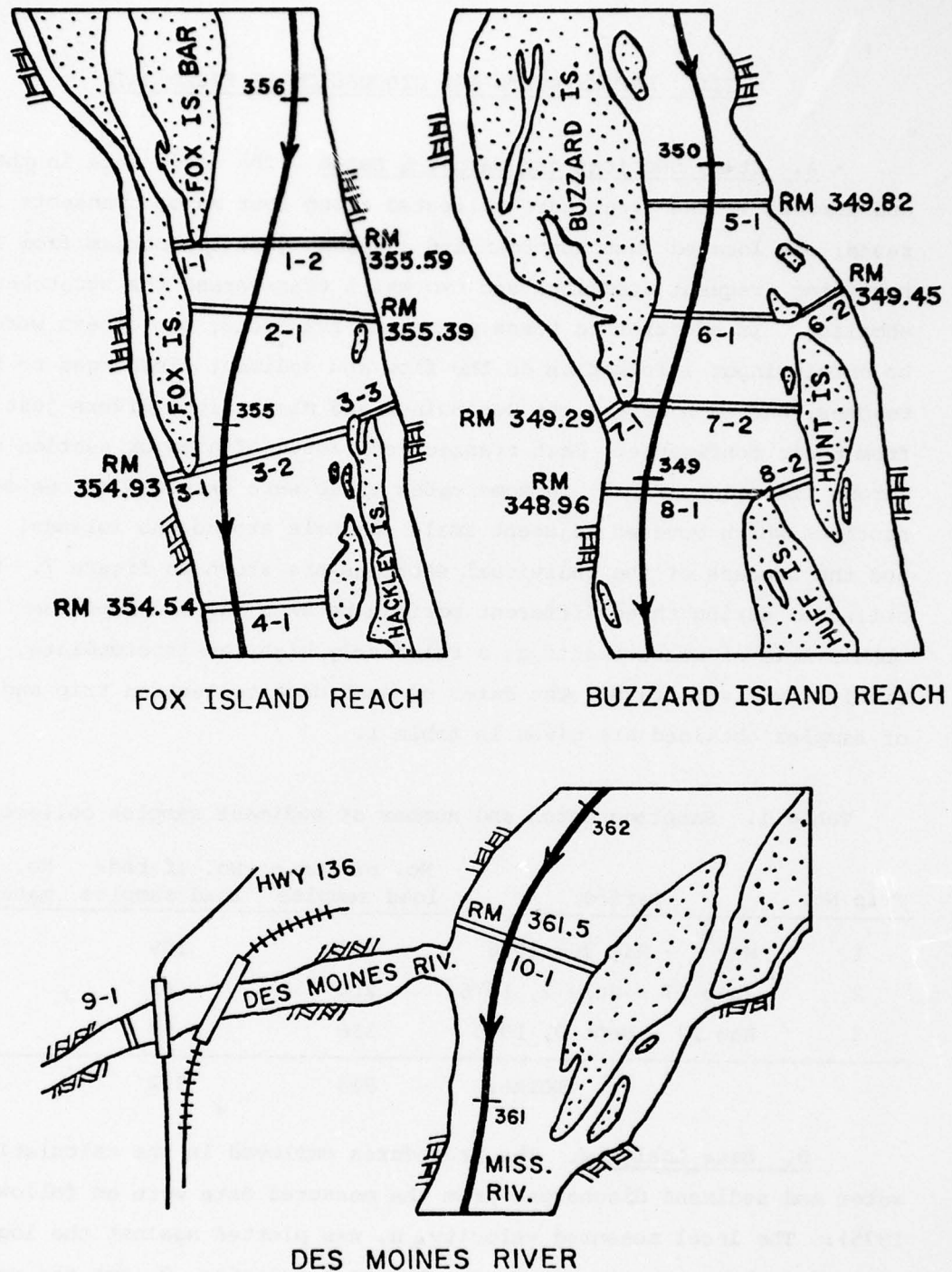


Figure 7. Locations of transects in the Mississippi and Des Moines Rivers

as the product of \bar{u} and the area of the subsection, determined from the measured water surface elevation and plotted transverse bed profile. The total flow discharge for the transect, Q , was obtained by summing the section discharges for the transect.

A mean suspended-sediment concentration at the i -th vertical of the transect, \bar{C}_i , was determined by numerical integration over the measured depth of the vertical of the local concentration, C ; i.e.,

$$\bar{C}_i = \frac{1}{d-a} \int_a^d C dy \approx \frac{1}{d-a} \sum_j [C(y_j) + C(y_j + \Delta y_j)] \Delta y_j / 2 \quad \dots \dots \dots \quad (1)$$

in which a is the distance above the river bed to the sampler intake nozzle when the sampler was at its lowest vertical position ($a = 0.5$ ft for the present study), and $C(y_j)$ and $C(y_j + \Delta y_j)$ denote concentrations measured at the j -th vertical position ($y=y_j$) and the $(j+1)$ -th vertical position ($y=y_j + \Delta y_j$), respectively, in which Δy_j is the distance between two adjacent vertical positions (see figure 7A).

The discharge of suspended sediment (i.e. the suspended load) for the subsection centered on the i -th vertical, q_{si} , was calculated as the product of the sectional flow discharge, q_i , and the mean suspended-sediment concentration, \bar{C}_i ; i.e.,

$$\bar{q}_{si} = q_i \bar{C}_i \quad \dots \dots \dots \dots \dots \dots \quad (2)$$

and the average suspended load per unit width as

$$\bar{q}_{si} = (q_i \bar{C}_i) / W_i \quad \dots \dots \dots \dots \dots \dots \quad (2')$$

in which W_i is the width of the i -th subsection. The total suspended load for the entire cross-section covered by the section, Q_s , was obtained by summing q_{si} over all i (i.e. over all subsections). Here it should be pointed out that no attempt was made to estimate the unmeasured sediment load in the interval $0 < y < a$, by application of, for example, the modified Einstein method, because the amounts of sand present in the suspended load samples were too small to permit determination of their size distributions.

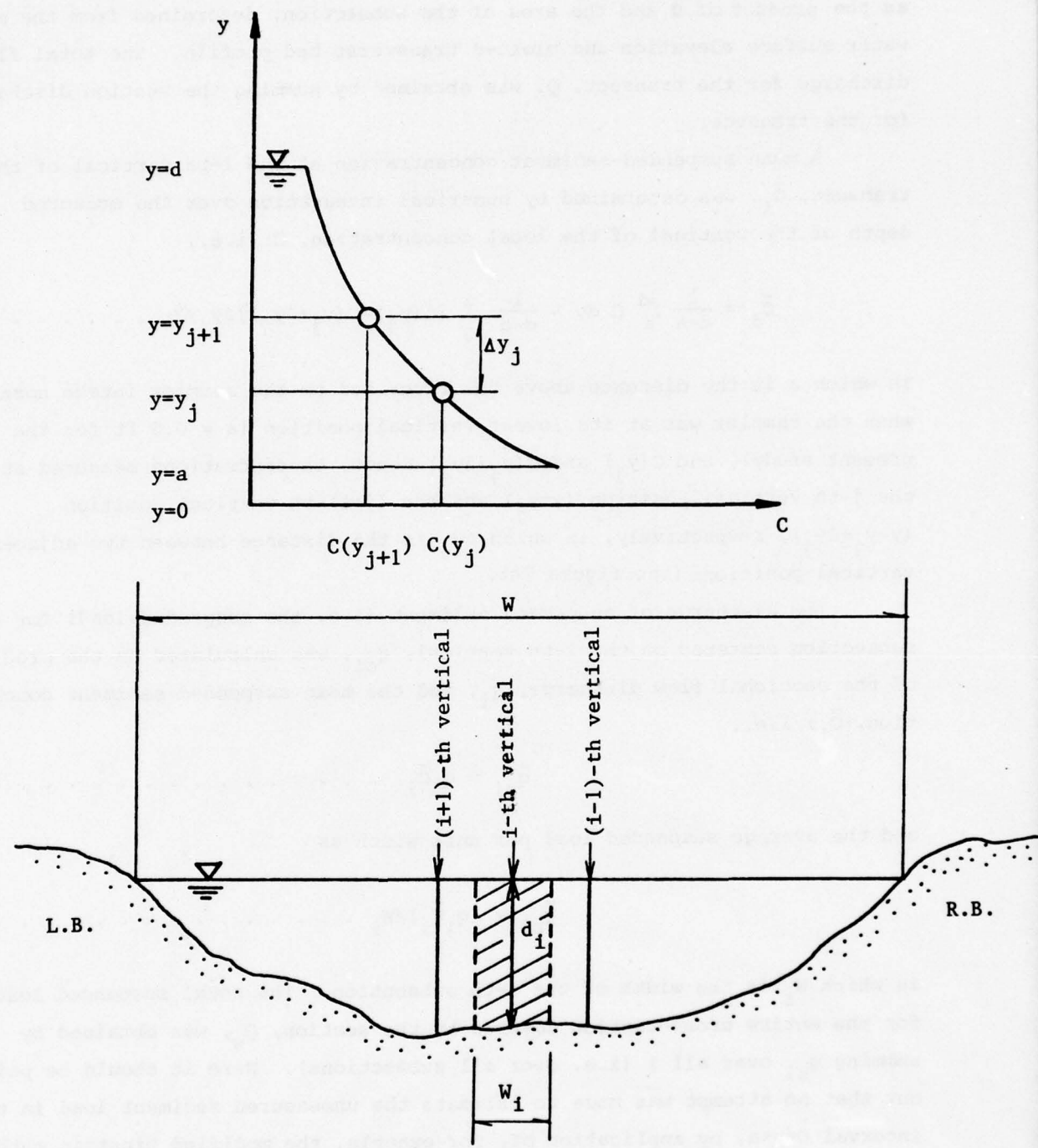


Figure 7A. Definition sketch for variables

The bed load for the i -th subsection of a transect, q_{Bi} , was obtained by assuming that the unit rate of sediment transport and bed load over the entire subsection was equal to the value measured through the 3-in. square bed-load sampler inlet. The total bed load for the cross-section was obtained as the sum of q_{Bi} for the individual verticals.

C. Presentation of Data. Table 2 presents a summary of principal quantities obtained from the field data. Therein the first, second, and third sampling groups (trips) are identified by 0, 1, and 2 primes affixed to the section number. Note that section numbers without primes also will be used in the text to refer to entire sections. The footnote to table 2 defines the notation.

1. Velocity distributions. Typical vertical distributions of local velocity obtained at the vertical 1,130 ft from the right bank of Sec. 5-1 are shown in figure 8(a) for the three different trips. It is seen therein that the velocity distributions are adequately described by the well known logarithmic relation,

$$\frac{u}{u_*} = \frac{1}{\kappa} \ln \frac{y}{d} = \frac{2.3}{\kappa} \log \frac{y}{d} \dots \dots \dots \dots \quad (3)$$

where $u_* = \sqrt{gds}$, g is the gravitational constant, S is the slope of the energy gradient, and κ is the Kármán's constant. The quantity $2.3u_*/\kappa$ was determined from the velocity increment over a logarithmic cycle of y in the plotted velocity profile. The shear velocity, u_* , was obtained from the water surface slope recorded by COE(RI) along a 21-mile reach between Keokuk, Iowa, and Canton, Missouri, and the depth at the vertical. Note that water-surface elevations averaged over 24-hours were used in calculating the water-surface slopes. Finally, κ was obtained from the known values of $2.3 u_*/\kappa$ and u_* . These data, together with \bar{u} and \bar{C} determined as described above, are shown for each profile included in figure 8(a). Figures 8(b) presents the relationship between Kármán's constant, κ , and mean suspended sediment concentration, \bar{C} . Only the data from the first and second trips are shown in the figure, because the mean concentrations from the third trip were generally lower than 40 ppm and the κ -values varied between 0.05 and 0.35; in the figure these would appear as a congested vertical band. It is seen in the figure that the Kármán

Table 2 Summary of principal quantities obtained from the field data (1st trip)

Date	Sec. No.	T (F°)	W (ft)	U (ft/s)	\bar{d} (ft)	S	Q (cfs)	Q_s (tons/day)	Q_B (tons/day)	\bar{D}_{50} (mm)	D_g (mm)	σ_q
050576	1-1	56	394	3.00	10.6	7.278×10^{-5}	12,526	7,767	42.1	0.53	0.69	1.47
050776	1-2	54	2,297	3.19	18.6	6.999×10^{-5}	136,486	77,095	1,943.1	0.69	1.18	3.00
051176	2-1	61	2,792	2.75	13.7	5.691×10^{-5}	105,017	28,564	966.0	0.61	0.70	1.84
051376	3-1	63	289	1.09	5.4	5.565×10^{-5}	1,701	346	0.1	0.45	0.45	1.51
051276	3-2	62	2,703	2.86	11.9	5.610×10^{-5}	91,991	22,395	966.8	0.65	0.74	1.86
051376	3-3	63	515	2.51	4.5	5.565×10^{-5}	5,881	1,642	6.9	0.35	0.37	1.22
051476	4-1	63	2,415	2.58	12.0	5.628×10^{-5}	74,739	14,739	248.5	0.63	0.73	2.10
051876	5-1	65	2,096	2.81	16.6	5.348×10^{-5}	97,546	138,672	174.6	0.38	0.41	2.79
051976	6-1	65	2,200	2.57	14.1	5.610×10^{-5}	79,590	44,911	460.9	0.50	0.70	2.20
052076	6-2	68	738	1.50	6.4	5.610×10^{-5}	6,963	1,858	1.5	0.50	0.51	1.59
052176	7-1	69	387	1.51	5.4	5.528×10^{-5}	3,126	1,210	11.9	0.54	0.67	2.09
052176	7-2	67	2,477	2.58	12.1	5.528×10^{-5}	77,357	19,088	467.3	0.54	0.60	1.81
052376	8-1	65	2,625	1.98	10.2	3.842×10^{-5}	53,084	8,519	123.7	0.45	0.50	1.77
052676	8-2	65	797	2.20	6.7	3.598×10^{-5}	11,726	1,002	32.8	0.50	0.52	1.59
051376	9-1	63	531	3.28	6.2	2.487×10^{-4}	10,797	5,149	565.4	0.76	1.23	2.85
052676	9-1	66	541	2.96	6.0	3.073×10^{-4}	9,636	6,316	215.5	0.73	0.64	2.36

T=surface water temperature
W=water surface width
U=mean flow velocity
 \bar{d} =mean flow depth

\bar{D}_{50} =mean median size of bed sediment
 D_g =geometric mean size of bed sediment
 Q_s =suspended load discharge
 Q_B =bed load discharge

S=slope of water surface
Q=water discharge
 σ_g =geometric standard deviation of sediment sizes

Table 2 Cont'd (2nd trip)

Date	Sec. No.	T (F°)	W (ft)	U (ft/s)	\bar{d} (ft)	S	Q (cfs)	Q_s (tons/day)	Q_B (tons/day)	\bar{D}_{50} (mm)	D_g (mm)	σ_g
061776	1-1'	78	328	0.86	5.9	2.597×10^{-5}	1,668	1,149	0.7	0.60	0.62	1.58
061776	1-2'	75	2,297	2.26	12.6	2.597×10^{-5}	65,518	33,048	30.6	0.62	1.10	2.66
062176	2-1'	74	2,733	1.80	10.9	1.587×10^{-5}	53,429	7,154	25.3	0.59	0.69	1.92
062276	3-1'	77	285	0	-	1.723×10^{-5}	0	0	0	-	-	-
062276	3-2'	77	2,694	1.71	9.0	1.723×10^{-5}	41,648	5,409	22.4	0.60	0.66	1.87
062176	3-3'	73	509	1.59	5.3	1.587×10^{-5}	4,255	346	0.7	0.38	0.36	1.33
062376	4-1'	77	2,388	1.85	11.4	1.631×10^{-5}	50,365	5,884	28.5	0.63	0.77	2.14
062476	5-1'	73	2,083	1.48	16.4	1.668×10^{-5}	50,532	6,325	0.8	0.45	0.46	1.65
062576	6-1'	73	2,208	1.26	15.1	1.687×10^{-5}	42,124	4,130	6.4	0.43	0.46	1.77
062576	6-2'	79	699	0.86	7.0	1.687×10^{-5}	4,206	441	0	0.33	0.36	1.56
070276	7-1'	77	387	0.56	7.6	1.154×10^{-5}	1,643	1,581	0	0.51	0.41	2.71
070176	7-2'	79	2,493	1.18	12.3	1.254×10^{-5}	36,183	58,147	8.2	0.74	0.89	2.29
070276	8-1'	77	2,582	1.16	10.8	1.154×10^{-5}	32,334	21,773	4.8	0.43	0.52	1.83
070276	8-2'	77	696	1.29	10.0	1.154×10^{-5}	8,994	5,521	0.1	0.46	0.49	1.54
061876	9-1'	74	541	3.65	5.9	2.788×10^{-4}	11,603	22,395	230.0	0.43	0.66	2.56

Table 2 Cont'd (3rd trip)

Date	Sec. No.	T (F°)	W (ft)	U (ft/s)	\bar{d} (ft)	S	Q (cfs)	Q_B (tons/day)	D_{50} (mm)	Dg (mm)	g
083176	1-1"	80	394	0.38	5.8	3.608×10^{-7}	870	102	0.2	0.54	0.51
083176	1-2"	80	2,300	0.73	13.1	3.608×10^{-7}	21,811	1,393	1.9	0.72	1.27
090176	2-1"	80	2,756	0.70	11.5	1.804×10^{-7}	22,083	1,204	0.5	0.59	0.77
090376	3-1"	79	315	0	-	1.263×10^{-6}	0	0	0	-	-
090276	3-2"	79	2,720	0.73	10.8	1.263×10^{-6}	21,468	1,258	0.8	0.52	0.59
090376	3-3"	79	525	0.56	7.5	1.263×10^{-6}	2,178	101	0	0.37	0.37
090376	4-1"	79	2,392	0.56	11.8	1.263×10^{-6}	15,721	772	1.0	0.53	0.53
081776	5-1"	77	2,106	0.75	18.2	2.886×10^{-6}	28,626	1,647	1.3	0.60	0.66
081876	6-1"	77	2,211	0.62	15.9	2.074×10^{-6}	21,670	1,241	2.6	0.44	0.43
081876	6-2"	77	768	0.48	6.6	2.074×10^{-6}	2,414	148	0	0.32	0.31
081976	7-1"	79	413	0.35	8.8	1.894×10^{-6}	1,269	109	0	0.59	0.58
081976	7-2"	77	2,552	0.58	13.5	1.894×10^{-6}	19,943	1,199	1.8	0.57	0.64
082076	8-1"	77	2,618	0.52	11.7	1.623×10^{-6}	15,931	794	1.5	0.57	0.67
082076	8-2"	79	722	0.61	9.5	1.623×10^{-6}	4,144	162	0.5	0.46	0.51
090776	9-1"	73	525	0.12	3.4	2.033×10^{-4}	222	29	0	0.43	0.46
090776	10-1"	79	2,362	0.40	9.5	3.608×10^{-7}	9,027	304	0	2.17	1.86

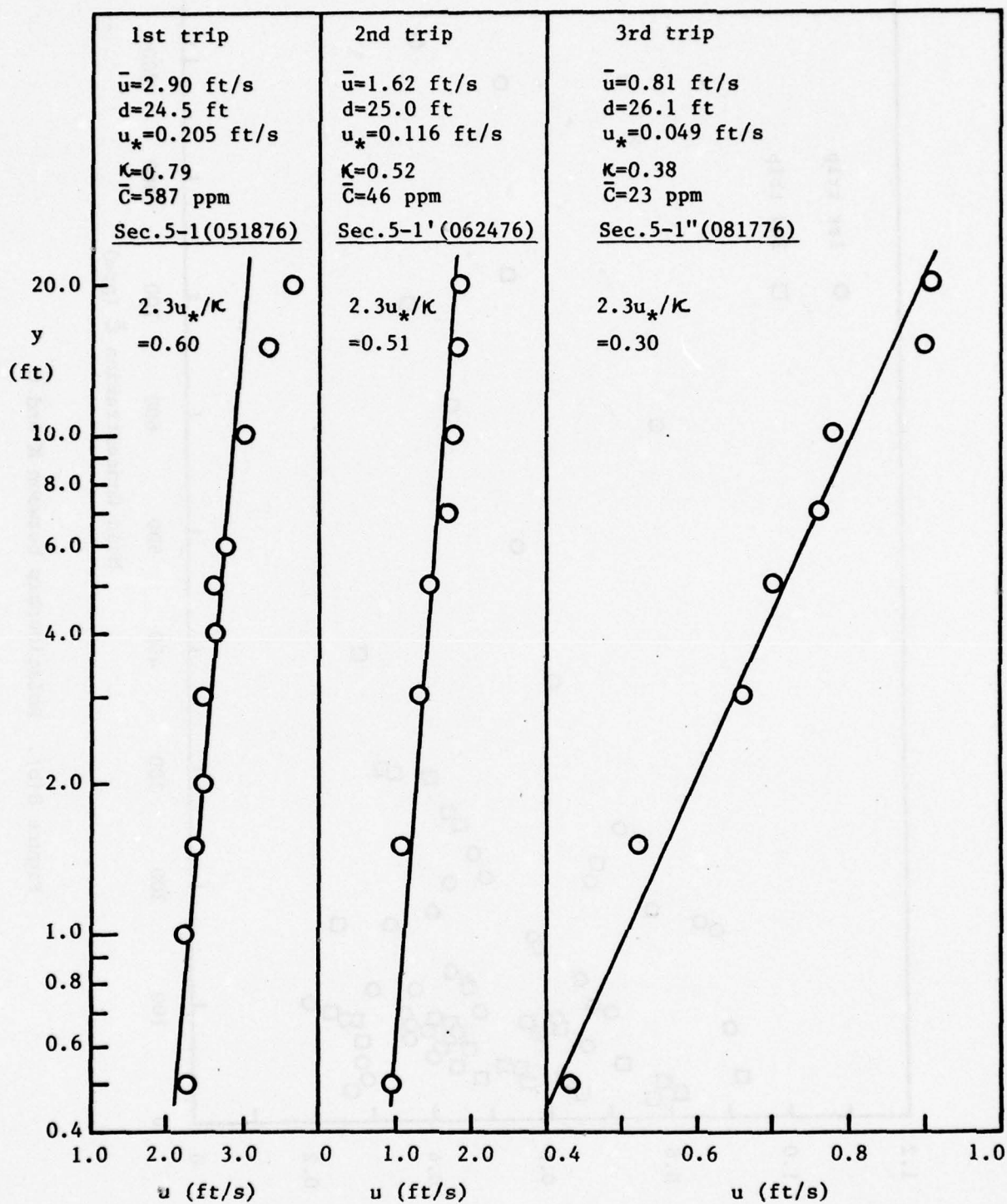


Figure 8(a). Typical velocity distributions obtained at Sec. 5-1

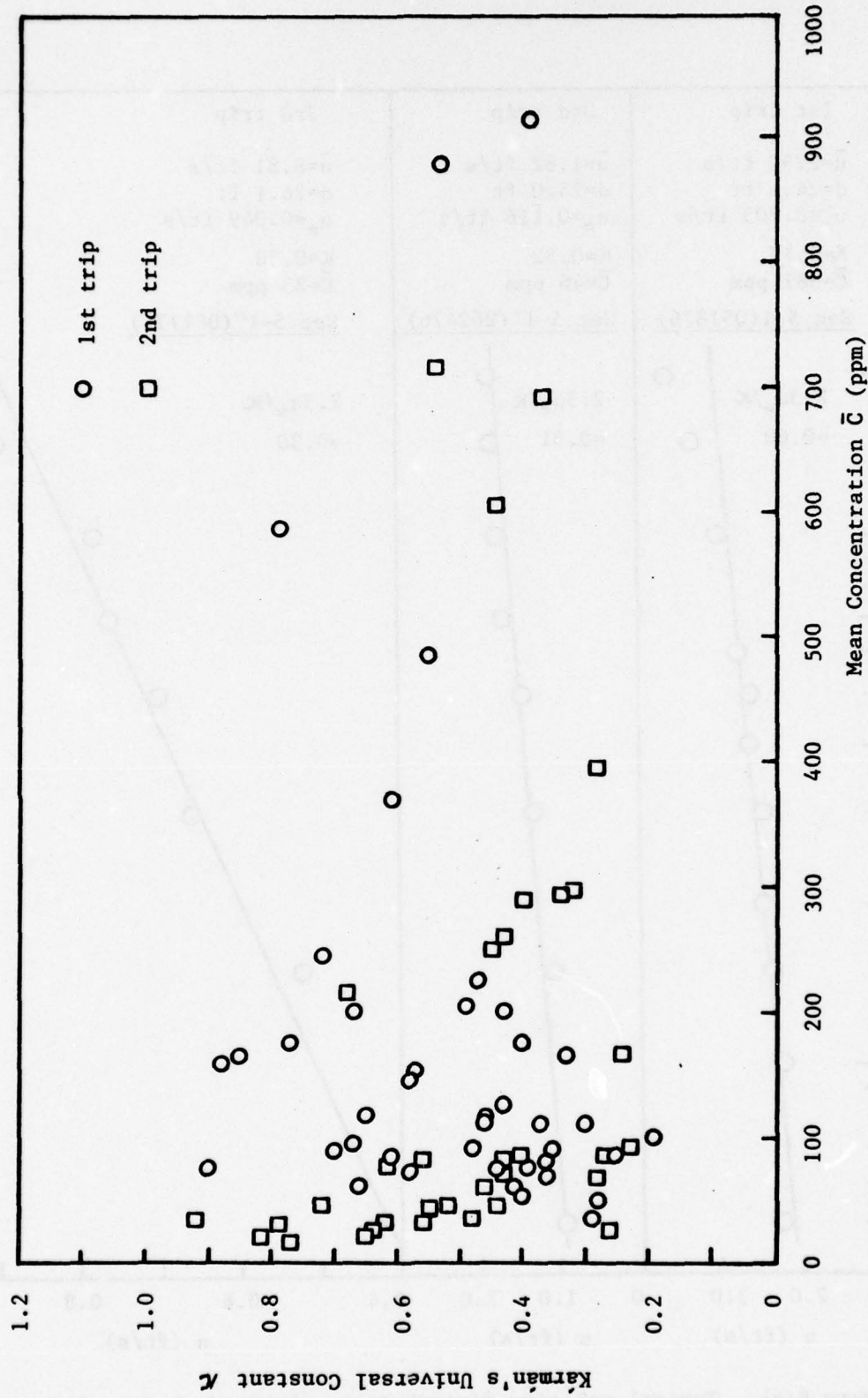


Figure 8(b). Relationship between K and \bar{C}

constant varies widely at low concentration, but κ is generally larger than 0.4 for the higher mean concentrations. Since the range of the mean concentration reported herein is very narrow (15 ppm - 925 ppm), a conclusive statement concerning the concentration effect on κ cannot be made. It appears, however, that κ varies significantly when the mean suspended sediment concentration is lower than approximately 200 ppm.

Water discharges reported by COE(RI) for the Des Moines River at St. Francisville (15.1 mi upstream from the mouth) and for the Mississippi River at Keokuk were added and compared with those computed from the field data using the method described above. Figure 9 shows a comparison of the COE values and those obtained from the present study for each of the eight principal transects and each of the three data-collection trips. The agreement is seen to be, on the whole, quite satisfactory. The values determined by IIHR from the measured velocity distributions are judged to be more accurate than those determined from gaging station rating curves and head drops across dam gates.

2. Channel cross sections. The channel cross sections measured along the transects in the Fox Island reach during the three field trips are shown in figures 10. It is seen in figure 7 that Secs. 1-2, 2-1, and 3-2 lie along the river reach in which the thalweg is crossing the channel, and at Sec. 4-1 the crossing is largely completed and the thalweg is close to the right bank. The progressive migration of the thalweg from the left to the right bank along this reach is apparent in the cross sections shown in the measured cross sections. Figures 10 show that the top width of the river is practically constant over the range of discharge that occurred during the study. This is a consequence of the dam gates being operated so as to minimize the stage variations. One of the most interesting features demonstrated by figures 10 is that at some locations, the changes in bed elevation are practically as great as those of the water surface. Between trips 1 and 3, as the water discharge diminished, deposition occurred over much of Secs. 1-2 and 2-1; the deposition-scour pattern was somewhat erratic across Sec. 3-2 (the site of chronic shoaling); and Sec. 4-1 was essentially stable. It should be recalled that no dredging was required along this reach in 1976. The transects across the Buzzard Island reach were quite stable during the study period, as figures 11 attest. Note also that the stage variations along the Buzzard Island reach were somewhat smaller

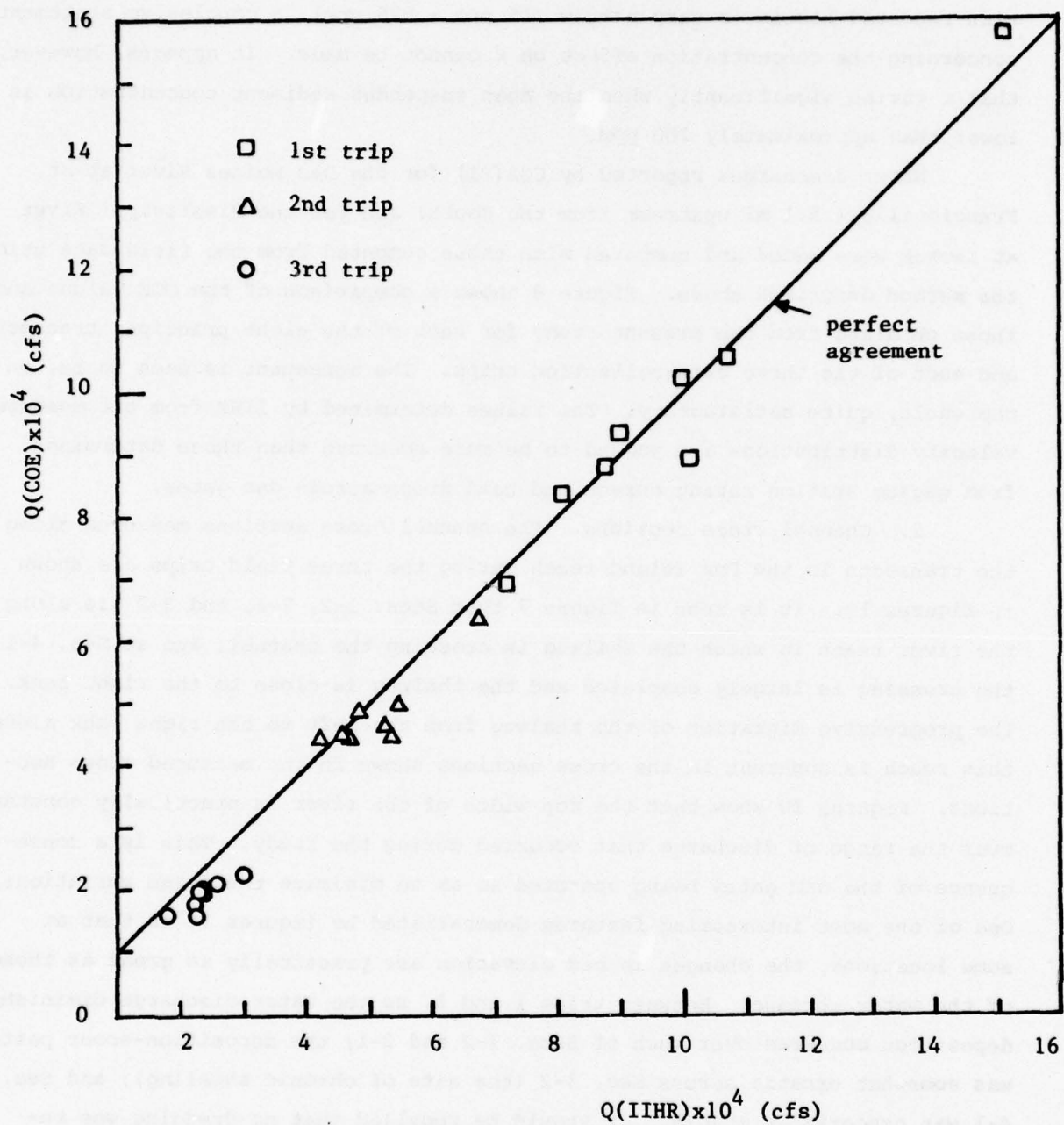
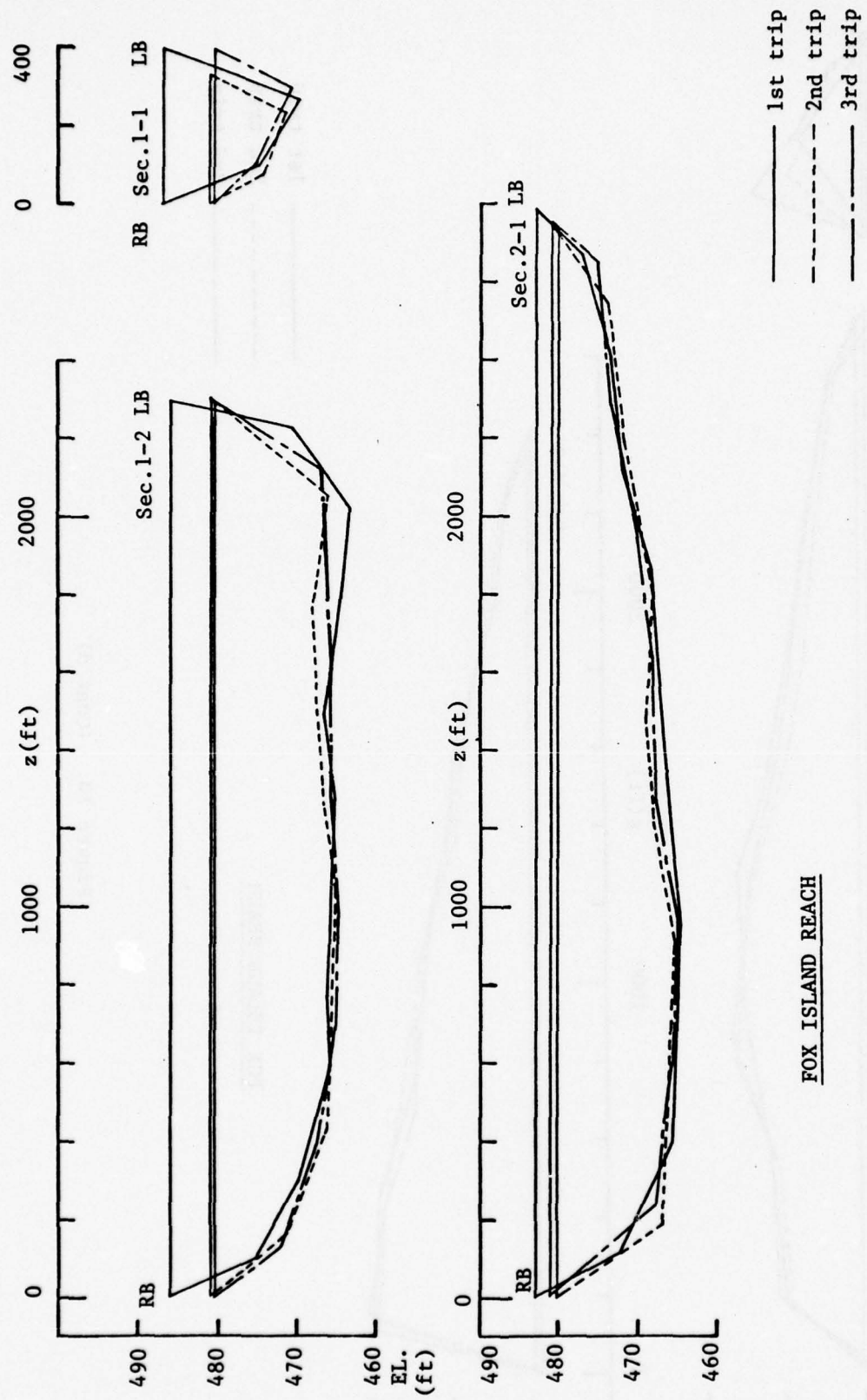


Figure 9. Comparison of flow discharges measured by IIHR with those measured by COE(RI)



Note: All elevations are in reference to M.S.L. 4th G.A.

Figure 10. Variations in cross-sectional bed profile (Fox Island reach)

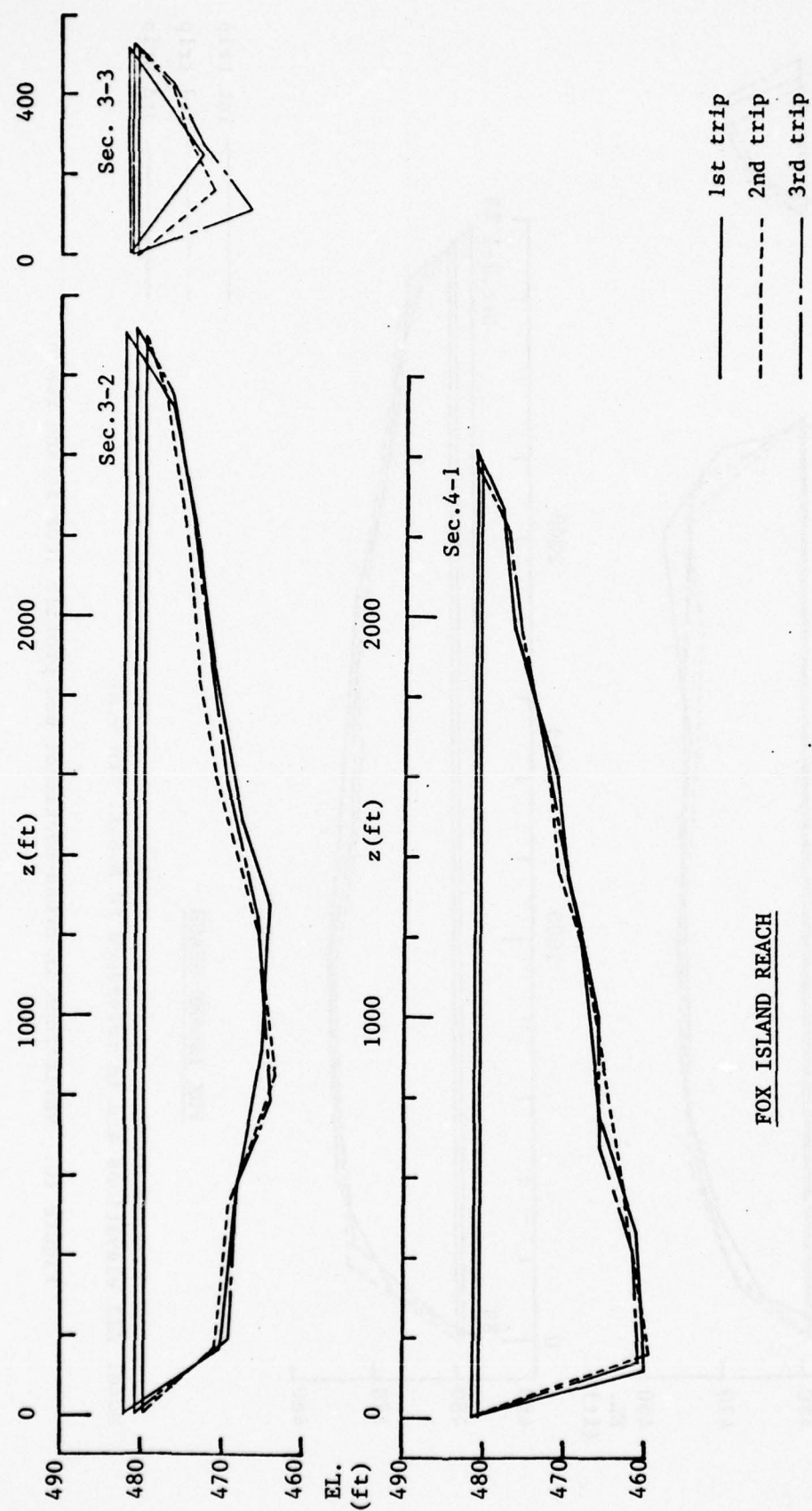


Figure 10. (Cont'd)

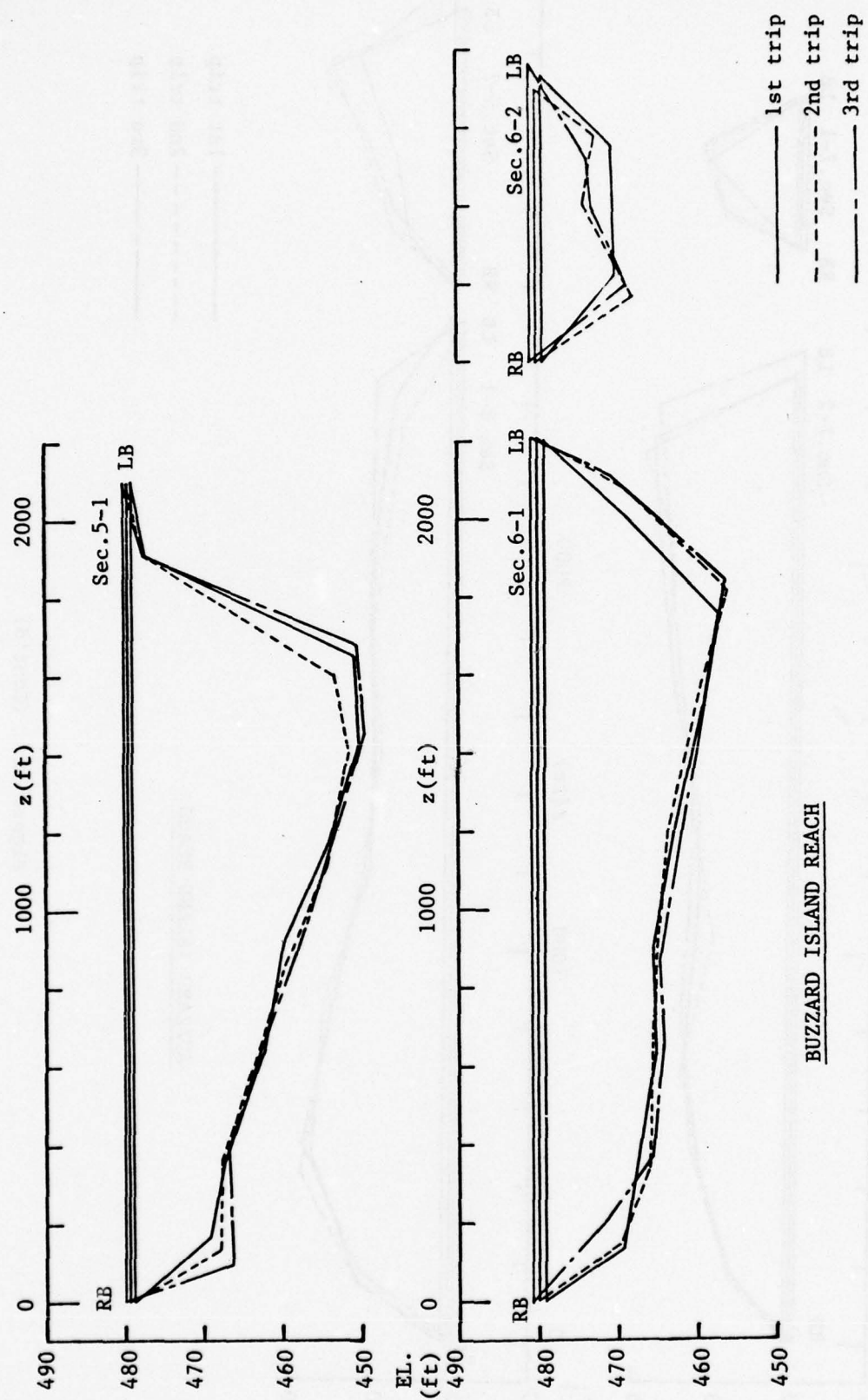


Figure 11. Variations in cross-sectional bed profile (Buzzard Island reach)

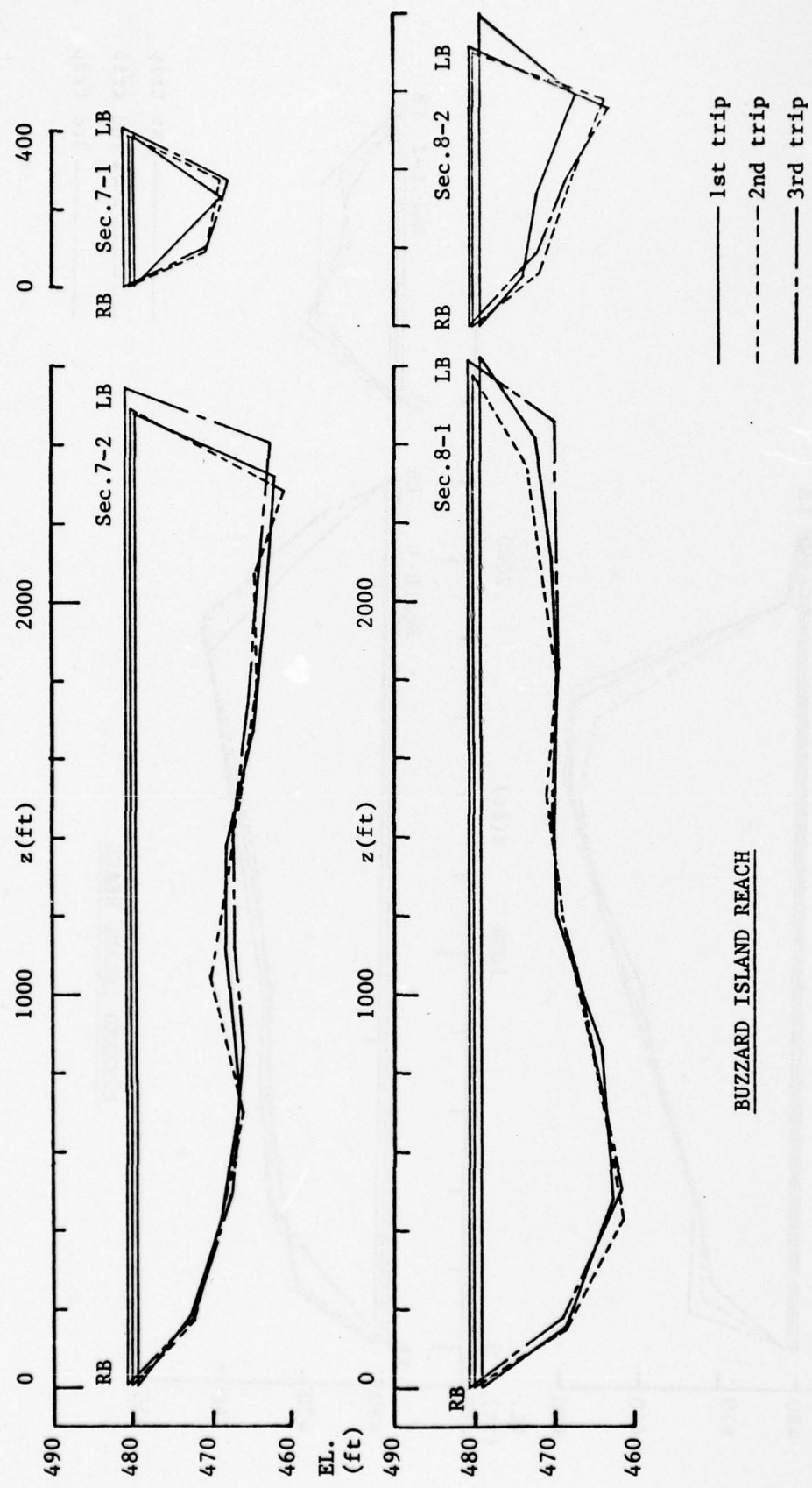


Figure 11. (Cont'd)

BUZZARD ISLAND REACH

than those along the Fox Island reach; this is a consequence of the shorter distance between the former and Lock and Dam 20 at Canton, Missouri, which is only about 6 mi downstream from Sec. 7-2. During 1976, COE(RI) dredged approximately 68,000 yd³ of river-bed sediment from a 250-ft wide, 3,250-ft long stretch of the navigation channel extending from just downstream of Sec. 6-1 to just upstream from Sec. 8-1. The third field trip was made just prior to this dredging operation. It is seen in figures 11 that the available depth along the sailing line was greater than 9 ft at the time of the third field trip. The dredging was done to assure adequate depth for navigation at the time of the anticipated minimum water surface elevation (477.2 ft at Sec. 7-2) during the period of very low discharge which was expected later in 1976. Indeed, inadequate depth did prove to be a major impediment to navigation from late summer until the river was closed by ice in 1976.

3. Lateral distributions of unit flow and sediment-transport quantities. Figures 12 through 35 present the lateral (cross-channel) variations of local depth (d), mean velocity (\bar{u}), mean suspended sediment concentration (\bar{C}), unit water discharge (\bar{q}), unit suspended-load discharge (\bar{q}_s), unit-bed-load discharge (\bar{q}_B), and median diameter of bed material (D_{50}) computed from the data obtained on each of the three field trips at the eight sections across the major channel in the Fox and Buzzard Island reaches. These distributions now will be discussed.

Figures 12 through 15 show the distributions computed from the first-trip data for the Fox Island reach. It is seen that for the relatively high water discharge that occurred at this time, \bar{u} is quite uniform across the channel. Accordingly, \bar{q} is seen to vary linearly with d . The mean sediment concentration, \bar{C} , is higher near the right bank of the river because the heavy sediment load delivered to the Mississippi River by the Des Moines River had not been transported far enough downstream to become distributed across the Mississippi River channel. Here it should be mentioned that during the field study, the turbid water entering the Mississippi River from the Des Moines River easily could be seen along the right bank of the Mississippi River for distances of up to 12 mi from the confluence. The distribution of \bar{q}_s is seen to be very similar to that of \bar{q} except for Sec. 1-2. The unit bed-load discharge, \bar{q}_B , is greater over the right-hand portion of the channel, where D_{50} is smaller.

*: All elevations are in reference to M.S.L. 4th G.A.

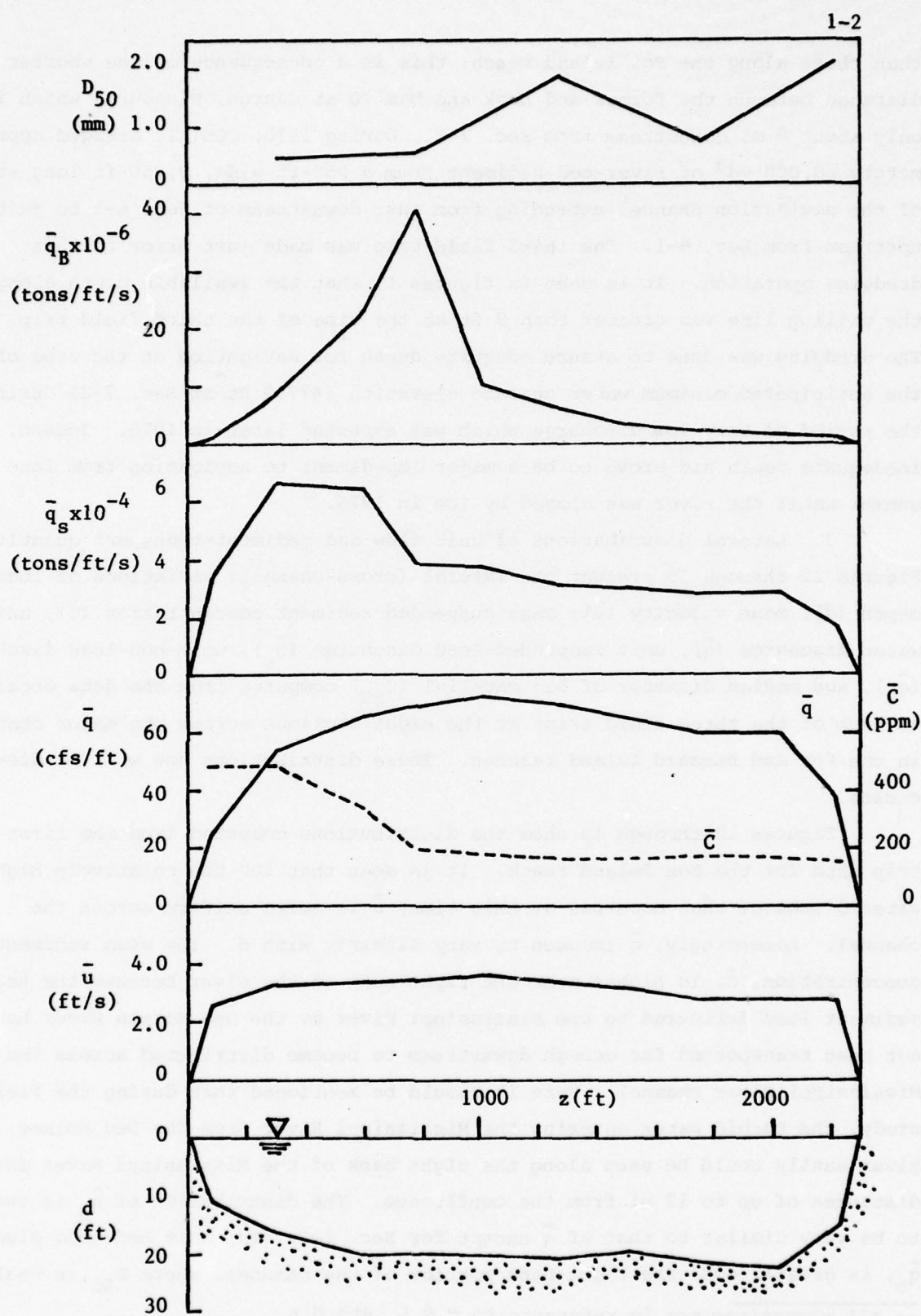


Figure 12. Lateral distributions of d , \bar{u} , \bar{q} , \bar{q}_s , \bar{q}_B , and D_{50} for Sec. 1-2

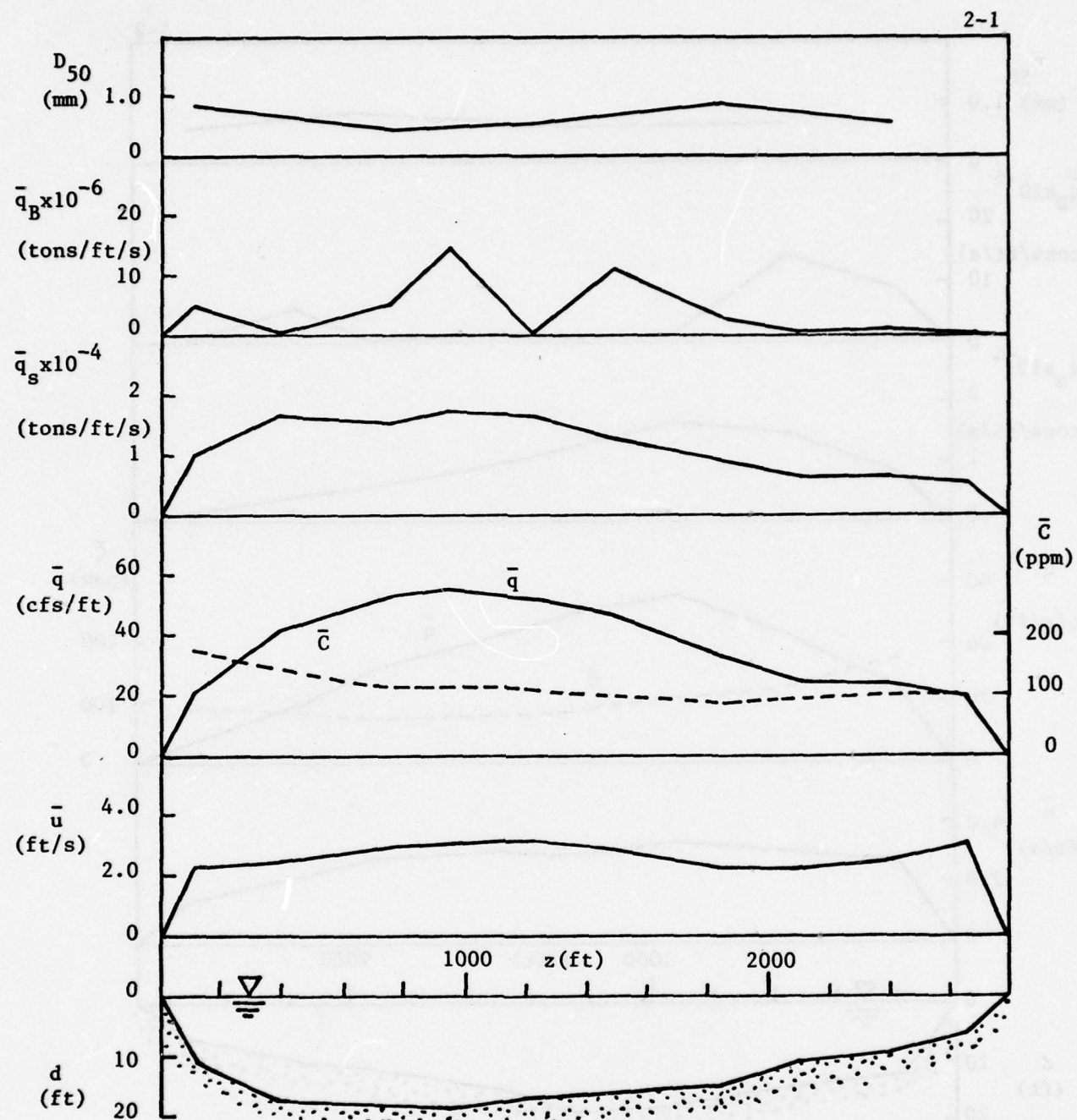


Figure 13. Lateral distributions of d , \bar{u} , \bar{q} , \bar{q}_s , \bar{q}_B , and D_{50} for Sec. 2-1

3-2

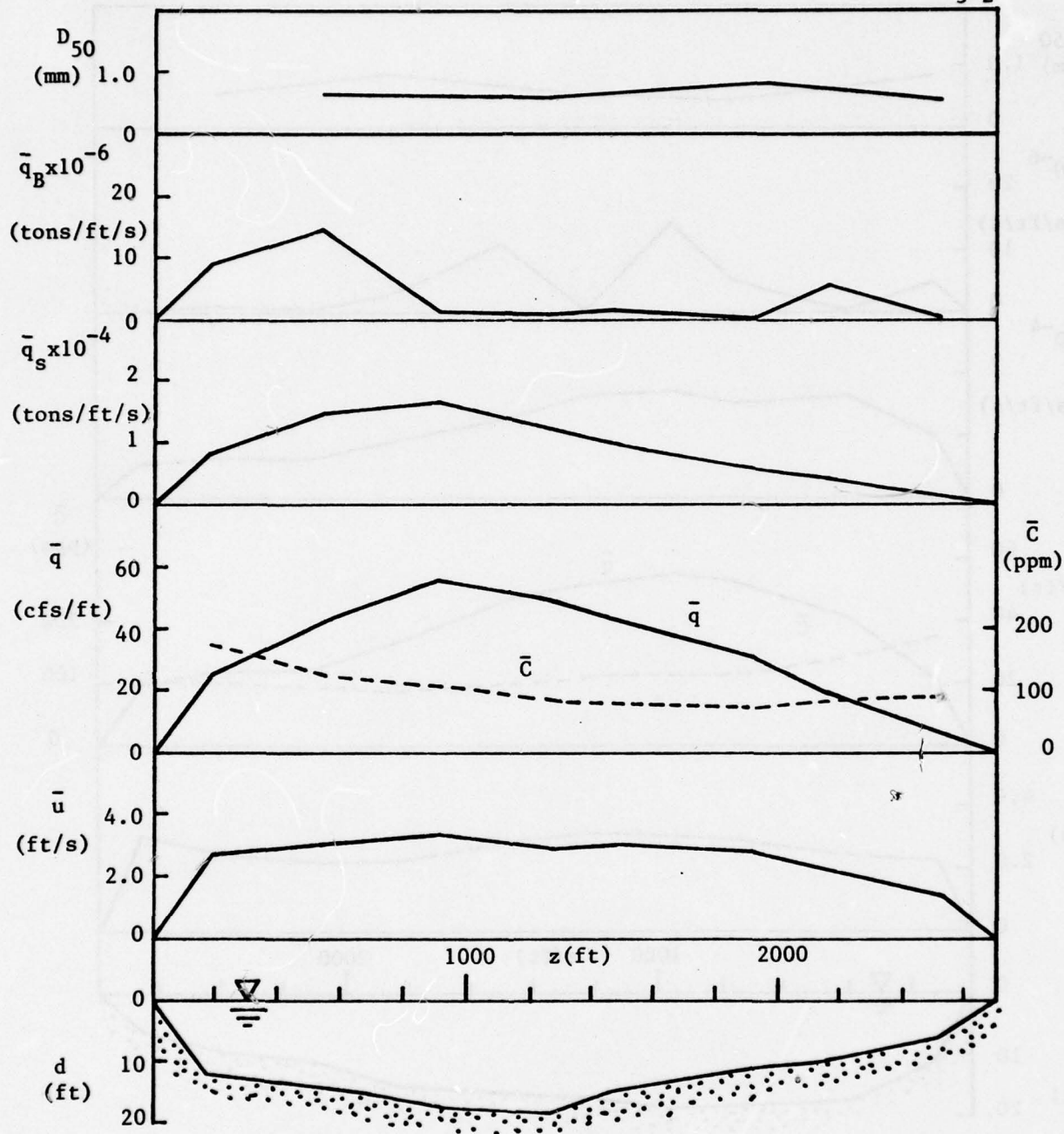


Figure 14. Lateral distributions of d , \bar{u} , \bar{q} , \bar{q}_s , \bar{q}_B , and D_{50} for Sec. 3-2

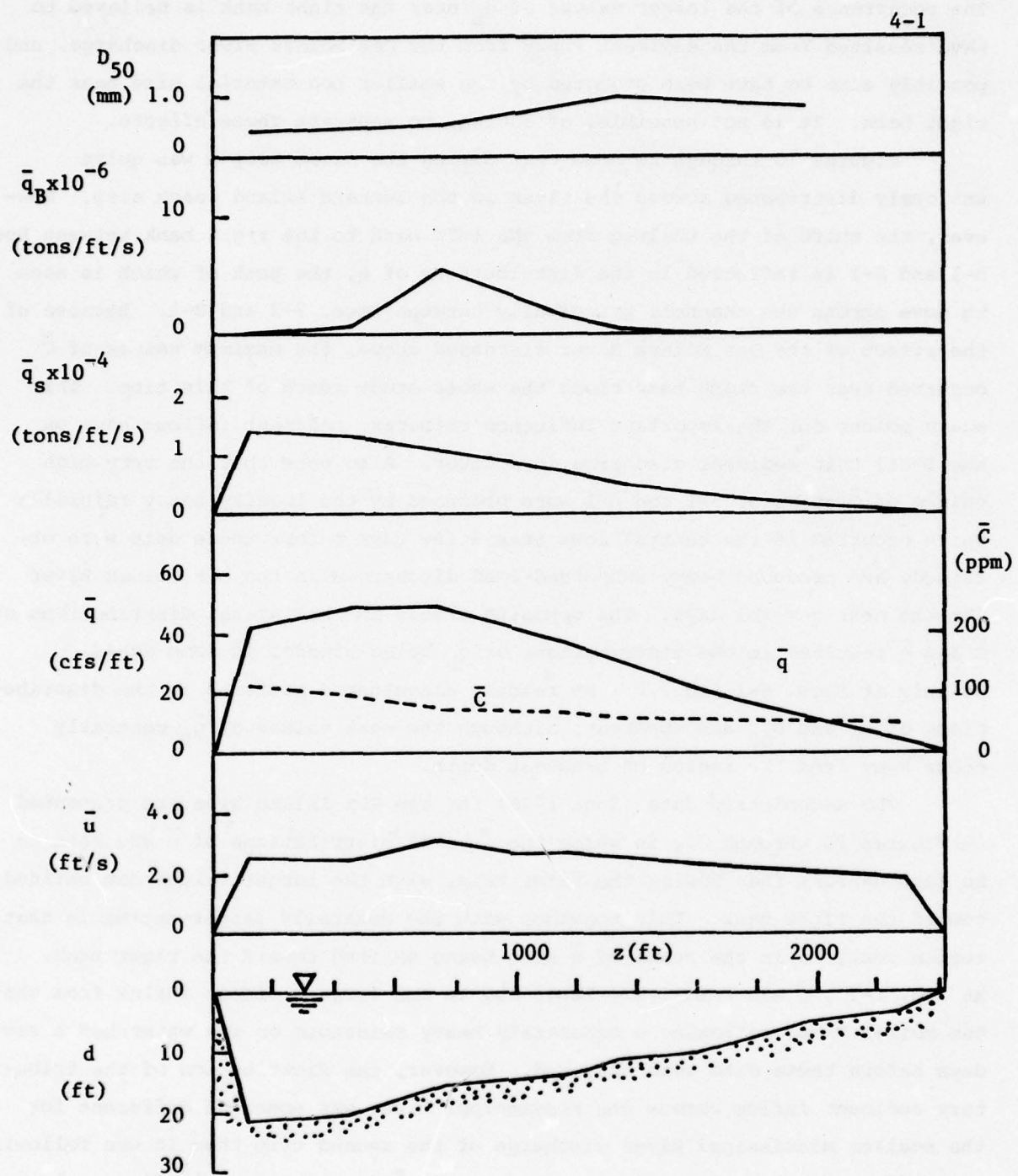


Figure 15. Lateral distributions of d , u , \bar{q} , \bar{q}_s , \bar{q}_B , and D_{50} for Sec. 4-1

The occurrence of the larger values of \bar{q}_B near the right bank is believed to have resulted from the sediment input from the Des Moines River discharge, and possibly also to have been promoted by the smaller bed material size near the right bank. It is not possible, of course, to separate these effects.

Figures 16 through 19 show that during the first trip \bar{u} was quite uniformly distributed across the river in the Buzzard Island reach also. However, the shift of the thalweg from the left bank to the right bank between Secs. 5-1 and 8-1 is reflected in the distributions of \bar{q} , the peak of which is seen to move across the channel, principally between Secs. 7-2 and 8-1. Because of the effect of the Des Moines River discussed above, the maximum values of \bar{C} occurred near the right bank along the whole study reach of this time. This again points out the important influence tributary sediment inflows have on the local unit sediment discharge in a river. Also note that the very high values of \bar{C} at Secs. 5-1 and 6-1 were produced by the locally heavy rainfalls which occurred in the central Iowa area a few days before these data were obtained, and produced heavy suspended-load discharges in the Des Moines River for the next several days. The opposing trends in the lateral distributions of \bar{C} and \bar{q} resulted in the distributions of \bar{q}_s being binodal in some cases, notably at Secs. 6-1 and 7-2. No readily discernable patterns in the distributions of \bar{q}_B and D_{50} are apparent, although the peak values of \bar{q}_B generally occur away from the region of greatest depth.

The second-trip data (June 1976) for the Fox Island area are presented in figures 20 through 23, in which the lateral distributions of \bar{u} are seen to be less uniform than during the first trip, with the larger values now shifted toward the right bank. This together with the generally larger depths in that region resulted in the peaks of \bar{q} also being shifted toward the right bank. At Sec. 1-2', \bar{C} was relatively large due to the large sediment influx from the Des Moines River following a moderately heavy rainstorm on its watershed a few days before these data were obtained. However, the distribution of the tributary sediment inflow across the Mississippi River was somewhat different for the smaller Mississippi River discharge of the second trip than it was following a runoff event during the first trip (compare \bar{C} distributions in figures 12 and 20). The relatively higher Mississippi River velocities during the first trip deflected the Des Moines River inflow abruptly and caused it to remain concen-

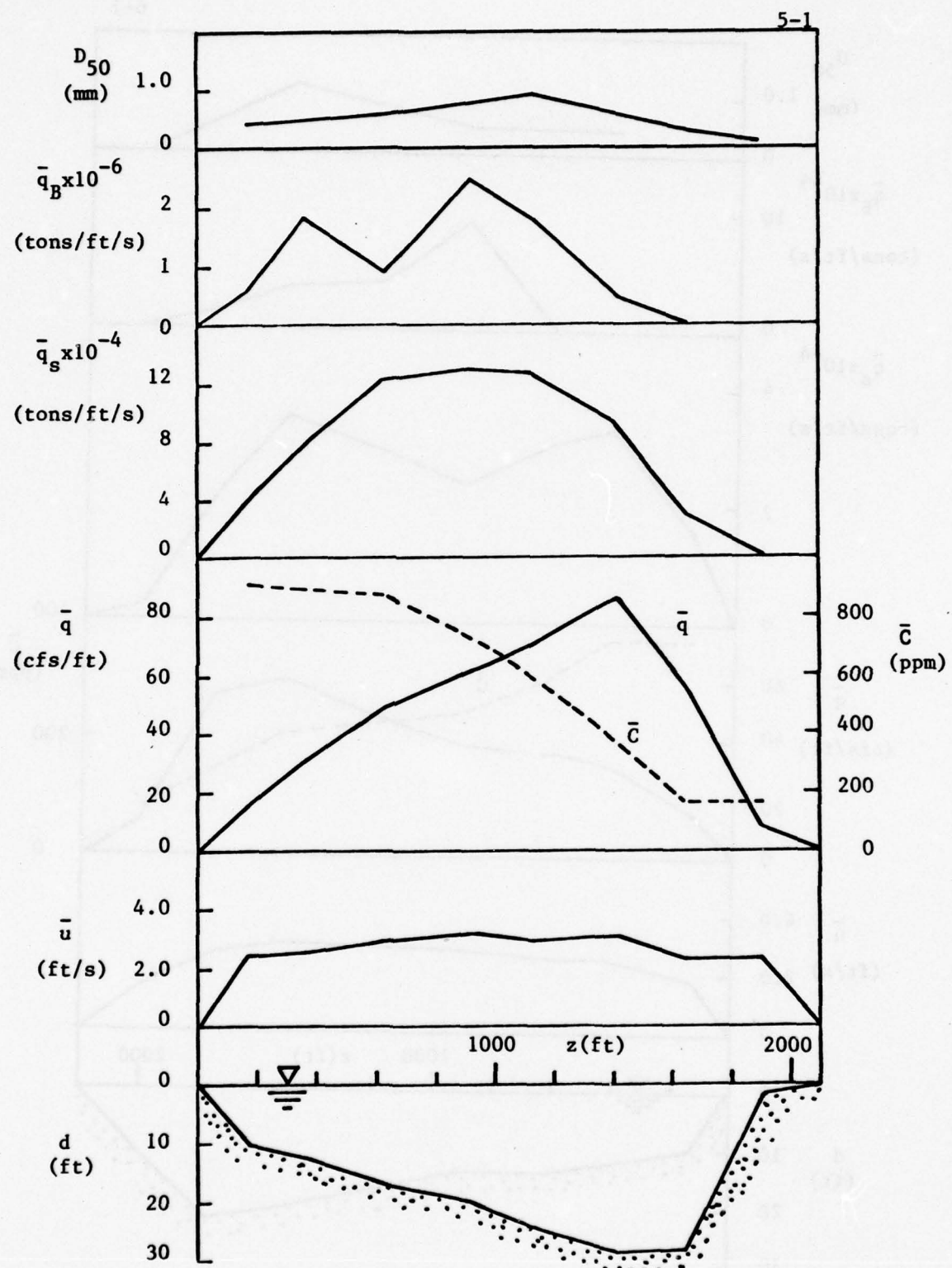


Figure 16. Lateral distributions of d , \bar{u} , \bar{q} , \bar{q}_s , \bar{q}_B , and D_{50} for Sec. 5-1

6-1

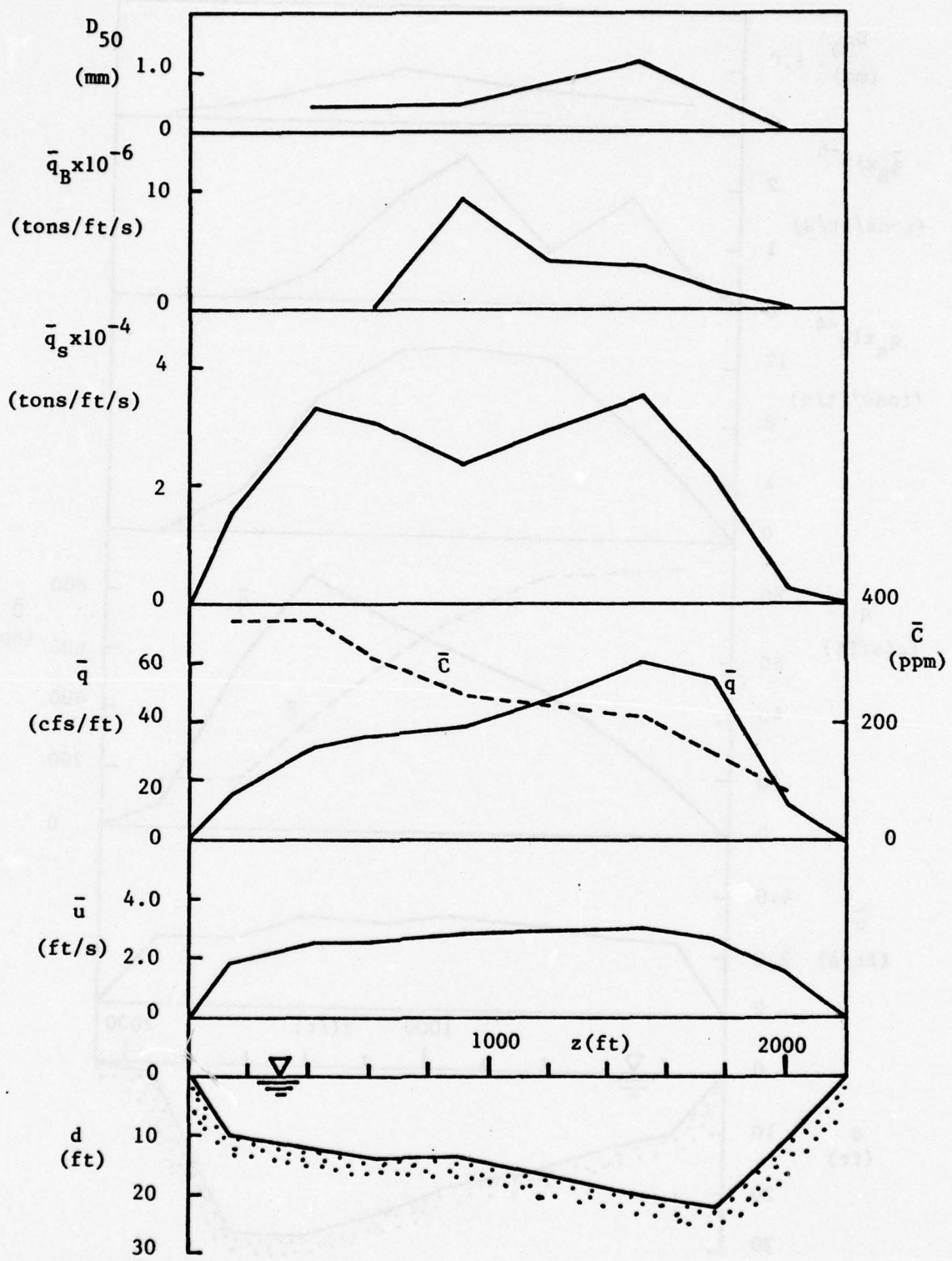


Figure 17. Lateral distributions of d , \bar{u} , \bar{q} , \bar{q}_s , \bar{q}_B , and D_{50} for Sec. 6-1

7-2

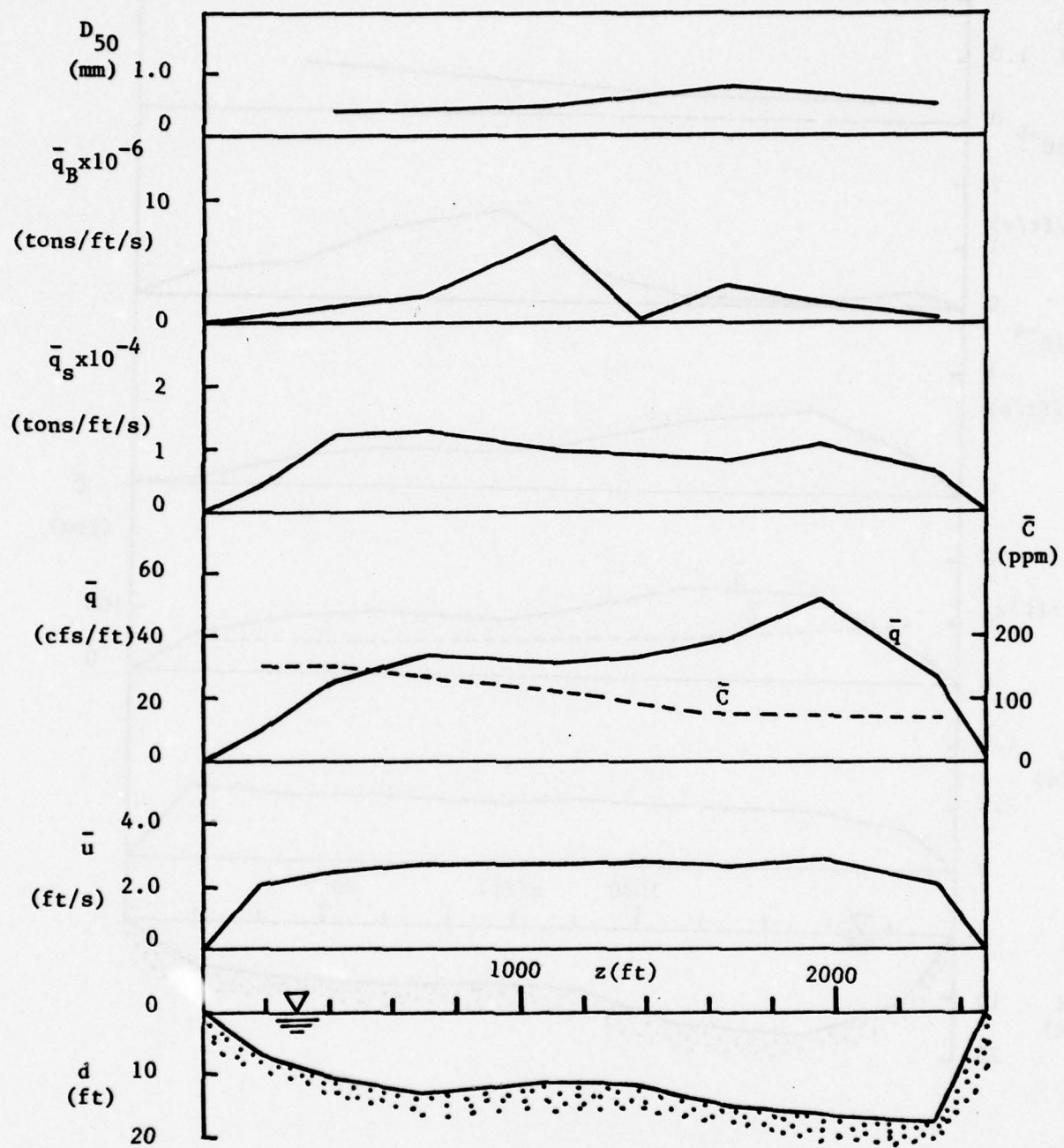


Figure 18. Lateral distributions of d , \bar{u} , \bar{q} , \bar{q}_s , \bar{q}_B , and D_{50} for Sec. 7-2

8-1

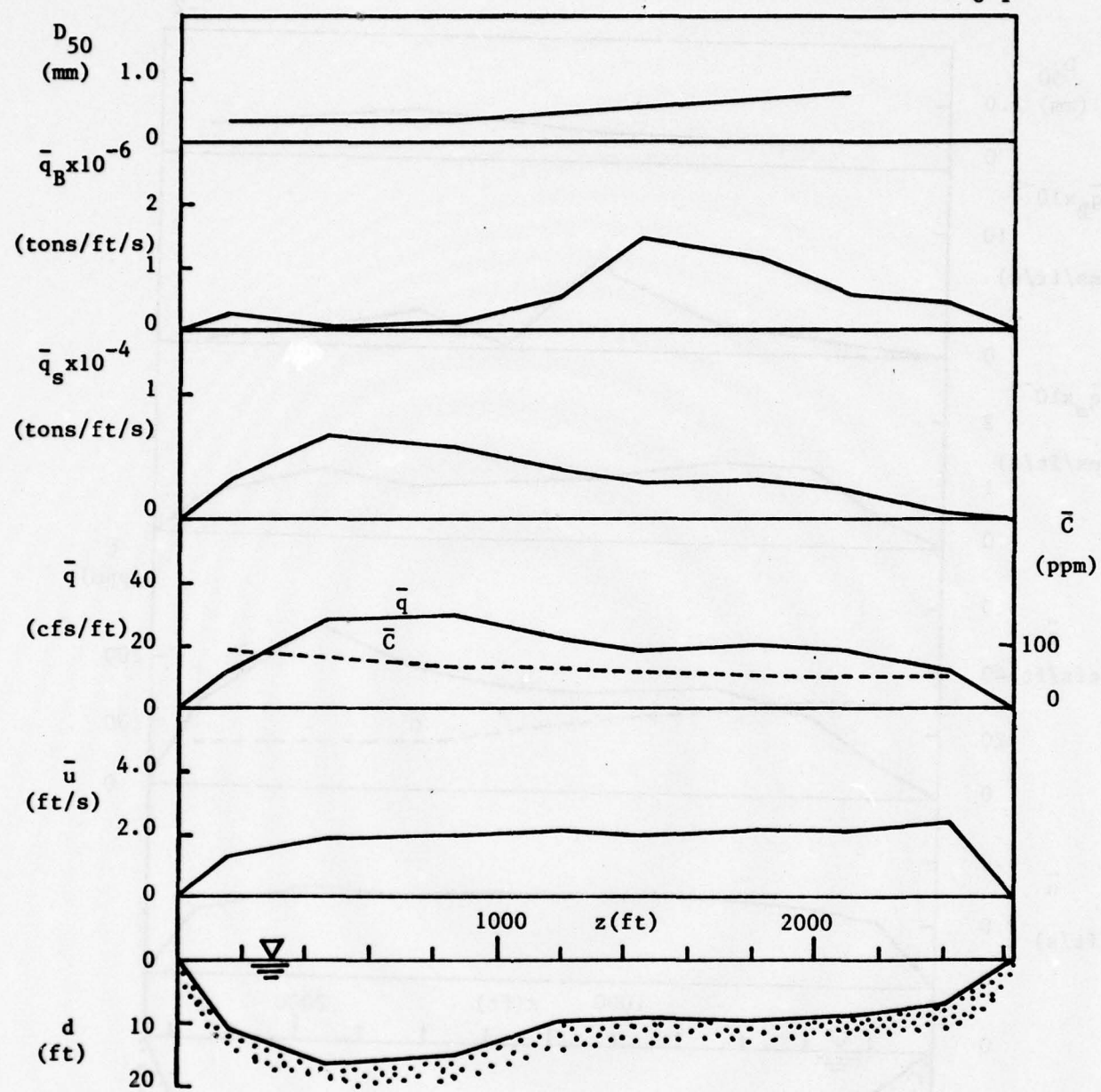


Figure 19. Lateral distributions of d , \bar{u} , \bar{q} , \bar{q}_s , \bar{q}_B , and D_{50} for Sec. 8-1

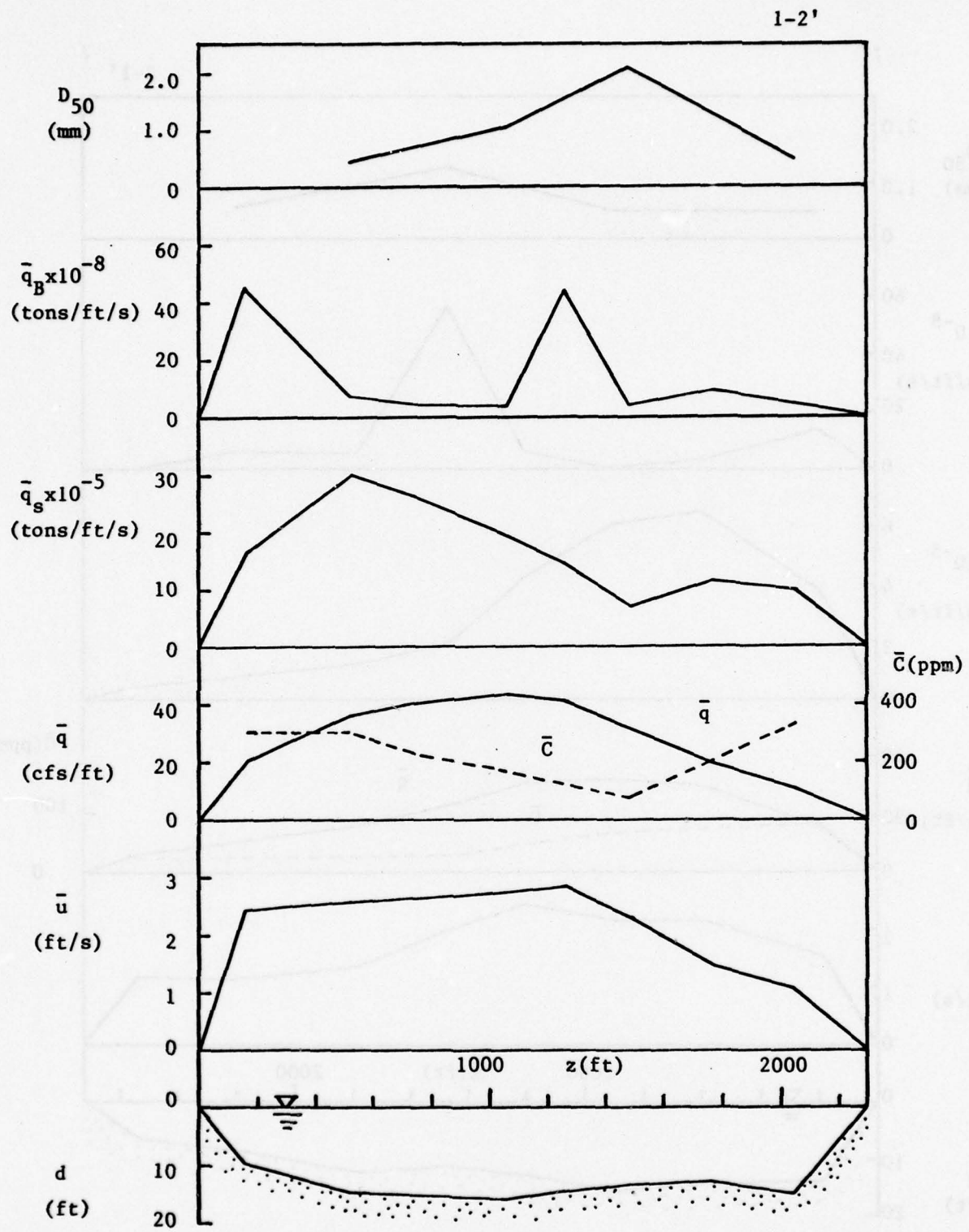


Figure 20. Lateral distributions of d , \bar{u} , \bar{q} , \bar{q}_s , \bar{q}_B , and D_{50} for Sec. 1-2'

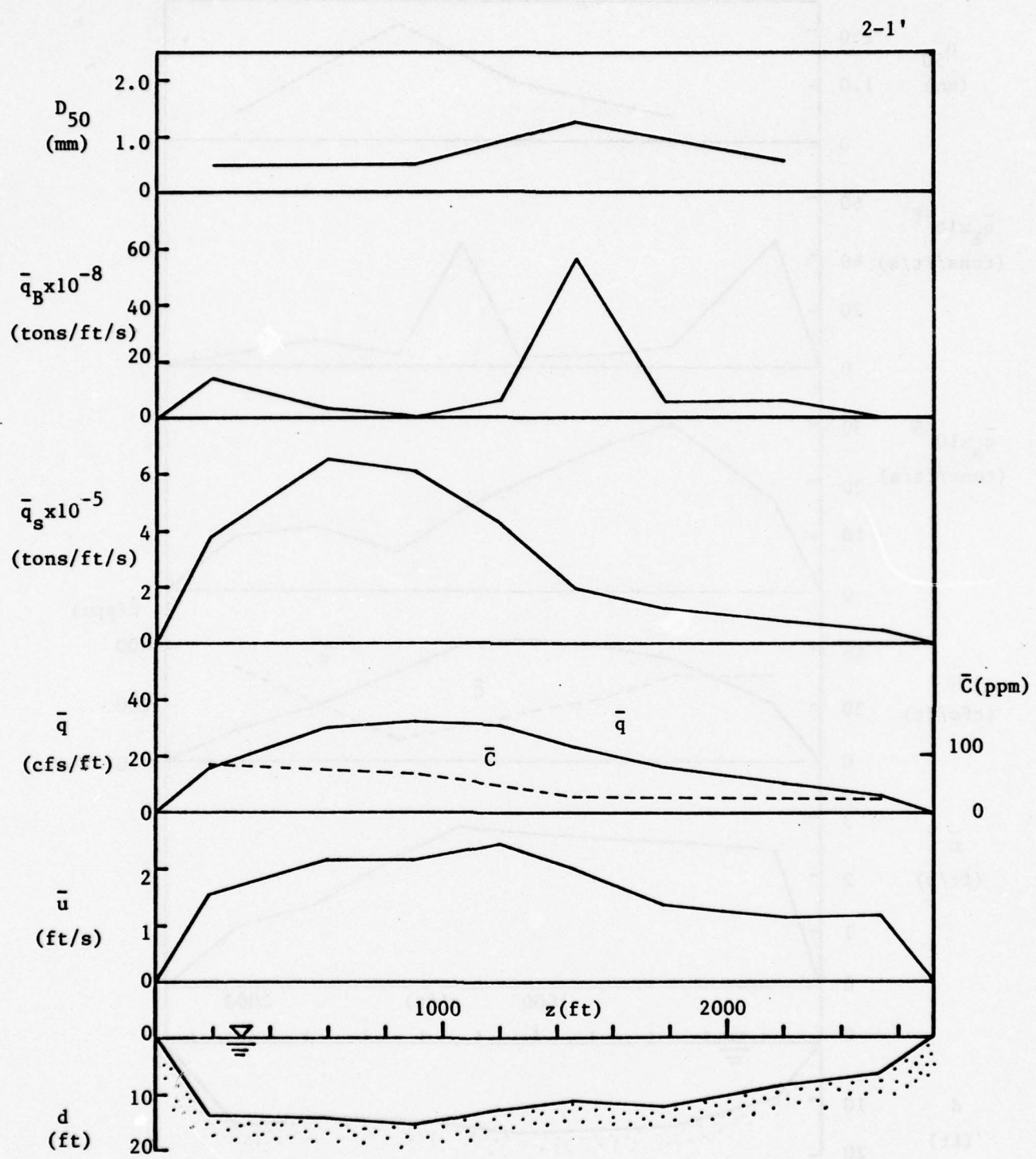


Figure 21. Lateral distributions of d , \bar{u} , \bar{q} , \bar{q}_s , \bar{q}_B , and D_{50} for Sec. 2-1'

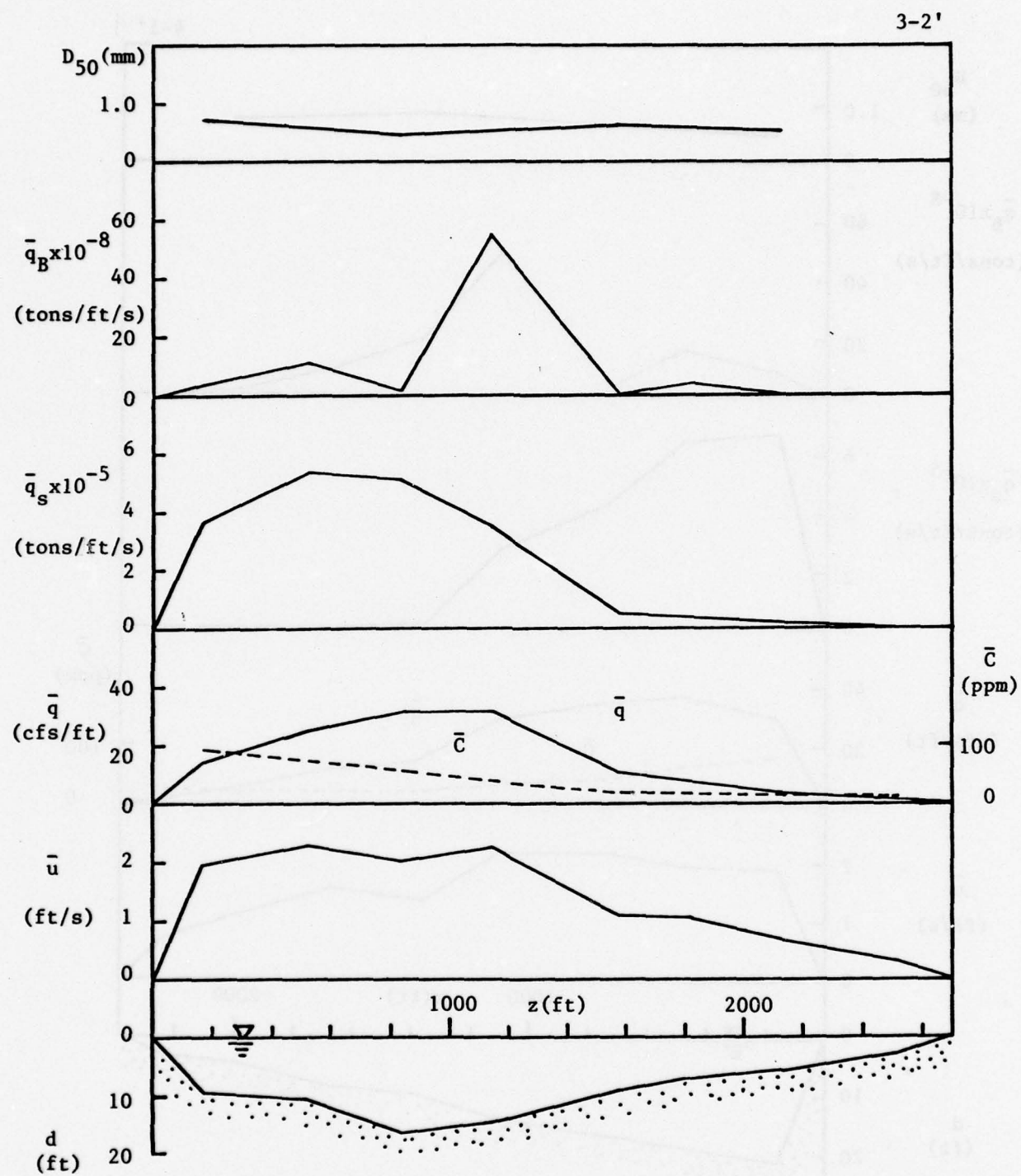


Figure 22. Lateral distributions of d , \bar{u} , \bar{q} , \bar{q}_s , \bar{q}_B , and D_{50} for Sec. 3-2'

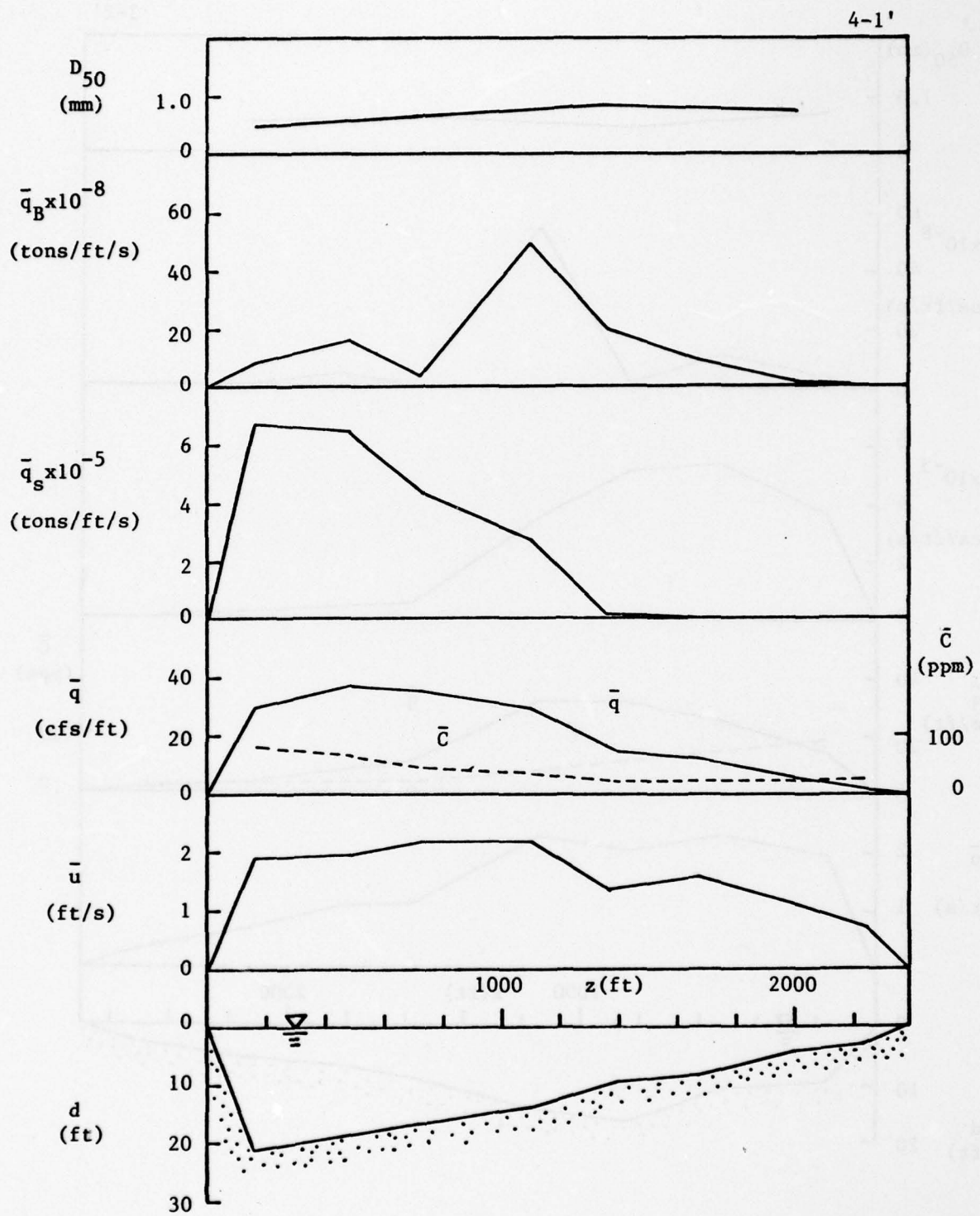


Figure 23. Lateral distributions of d , \bar{u} , \bar{q} , \bar{q}_s , \bar{q}_B , and D_{50} for Sec. 4-1'

trated along the right bank and to mix more slowly across the Mississippi River channel. It is also seen that the values of \bar{q}_s and \bar{q}_B are significantly lower than they were during the first trip, typically by factors of the order of 10, and 100, respectively.

The distributions of the quantities under consideration along the Buzzard Island reach during the second trip are shown in figures 24 through 27. The heavy sediment concentrations reflected in the large values of \bar{C} for Secs. 7-2' to 8-1' were a consequence of the Des Moines River runoff from a rainstorm, as discussed in the preceding paragraph. The seemingly anomalous feature is that larger values of \bar{C} occurred near the left bank at Sec. 7-2', while \bar{C} was nearly uniformly distributed across Sec. 8-1'. During the first trip the mean sediment concentrations were significantly larger near the right bank at both Secs. 7-2 and 8-1. The increased rate of lateral mixing, reflected in the more uniform lateral distributions of \bar{C} for the second-trip than for the first trip, again was attributed to the smaller Mississippi River discharge and velocity during the second trip, which permitted the Des Moines River inflow to penetrate farther across the Mississippi River channel. The two prominent peaks seen in the distributions of \bar{q} , \bar{q}_s , and \bar{q}_B in figure 26 are believed to have resulted from the bifurcation of the flow around Huff Island, which is just downstream from Sec. 7-2 (see figure 7). As can be seen in table 2, the discharge through Sec. 8-2' was approximately 28 percent of that through the main channel, Sec. 8-1'. It is believed that the chronic shoaling which occurs along part of Buzzard Island is a result of the streamwise reduction of velocity resulting from the diversion of a significant part of the flow from the main channel around the side of Huff Island; this point is expanded upon later.

The third trip data for Fox Island and Buzzard Island study reaches are shown in figures 28 through 31 and figures 32 through 35, respectively. The Buzzard Island data (Secs. 5-1" athrough 8-1") were obtained in mid-August 1976, just prior to the dredging operation, and the Fox Island measurements were made in early September 1976. During this period the flows in the Mississippi and Des Moines Rivers were extremely low, because of the record-breaking drought that was occurring in the upper midwest. Accordingly, all of the flow-related quantities shown in figures 28 through 35 are very small. Indeed, because of the severity of the drought it is reasonable to conclude

5-1'

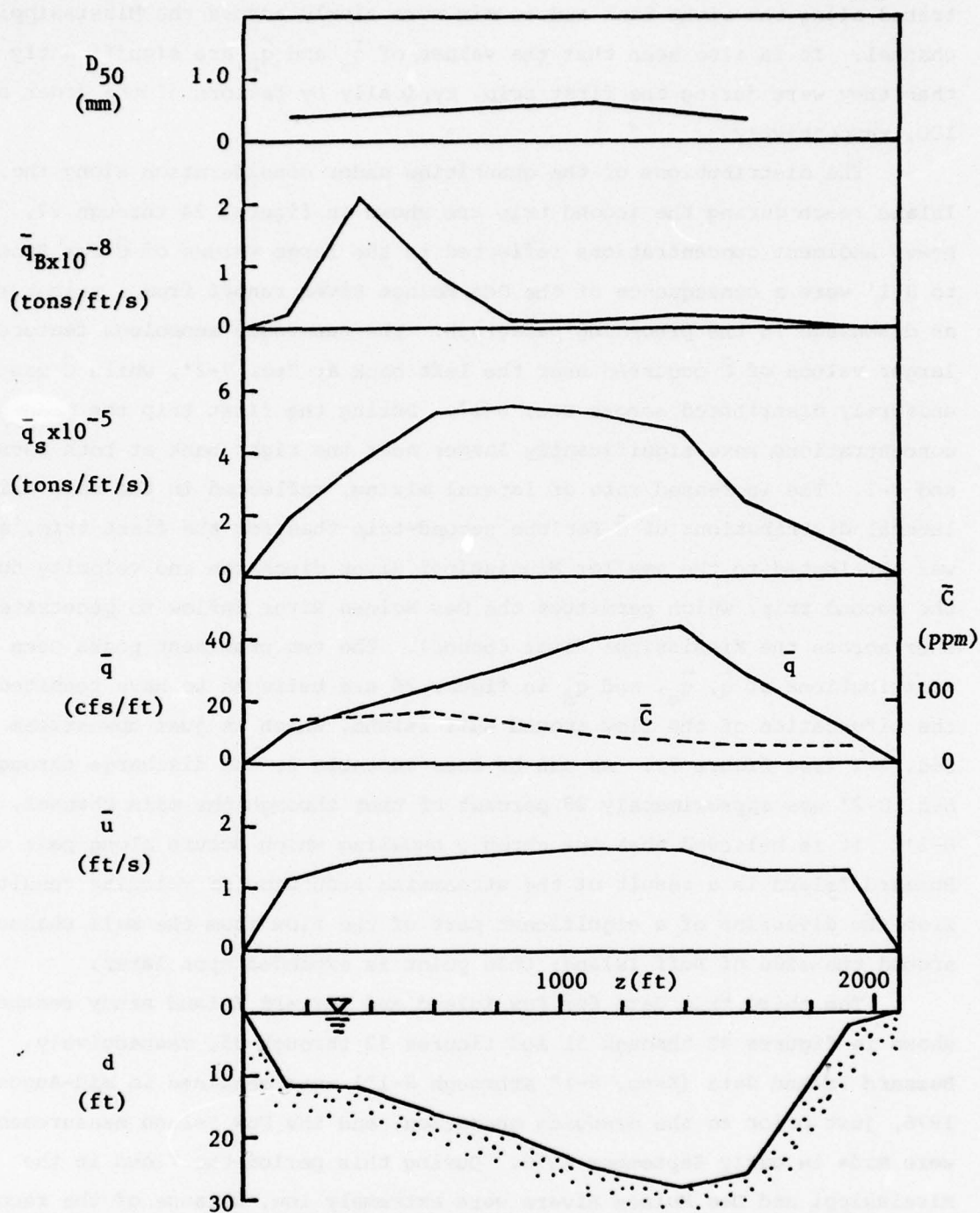


Figure 24. Lateral distributions of d , \bar{u} , \bar{q} , \bar{q}_s , \bar{q}_B , and D_{50} for Sec. 5-1'

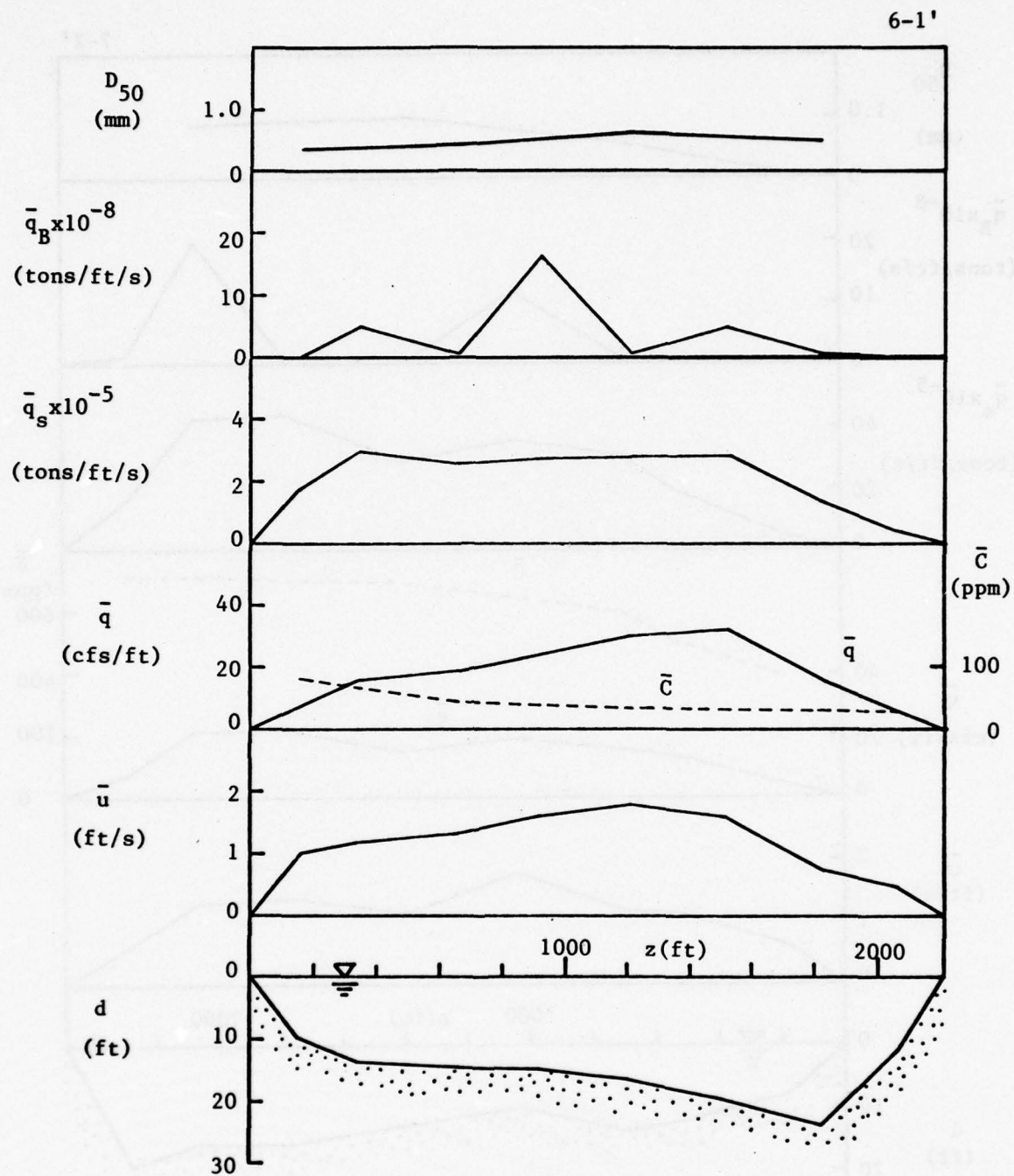


Figure 25. Lateral distributions of d , \bar{u} , \bar{q} , \bar{q}_s , \bar{q}_B , and D_{50} for Sec. 6-1

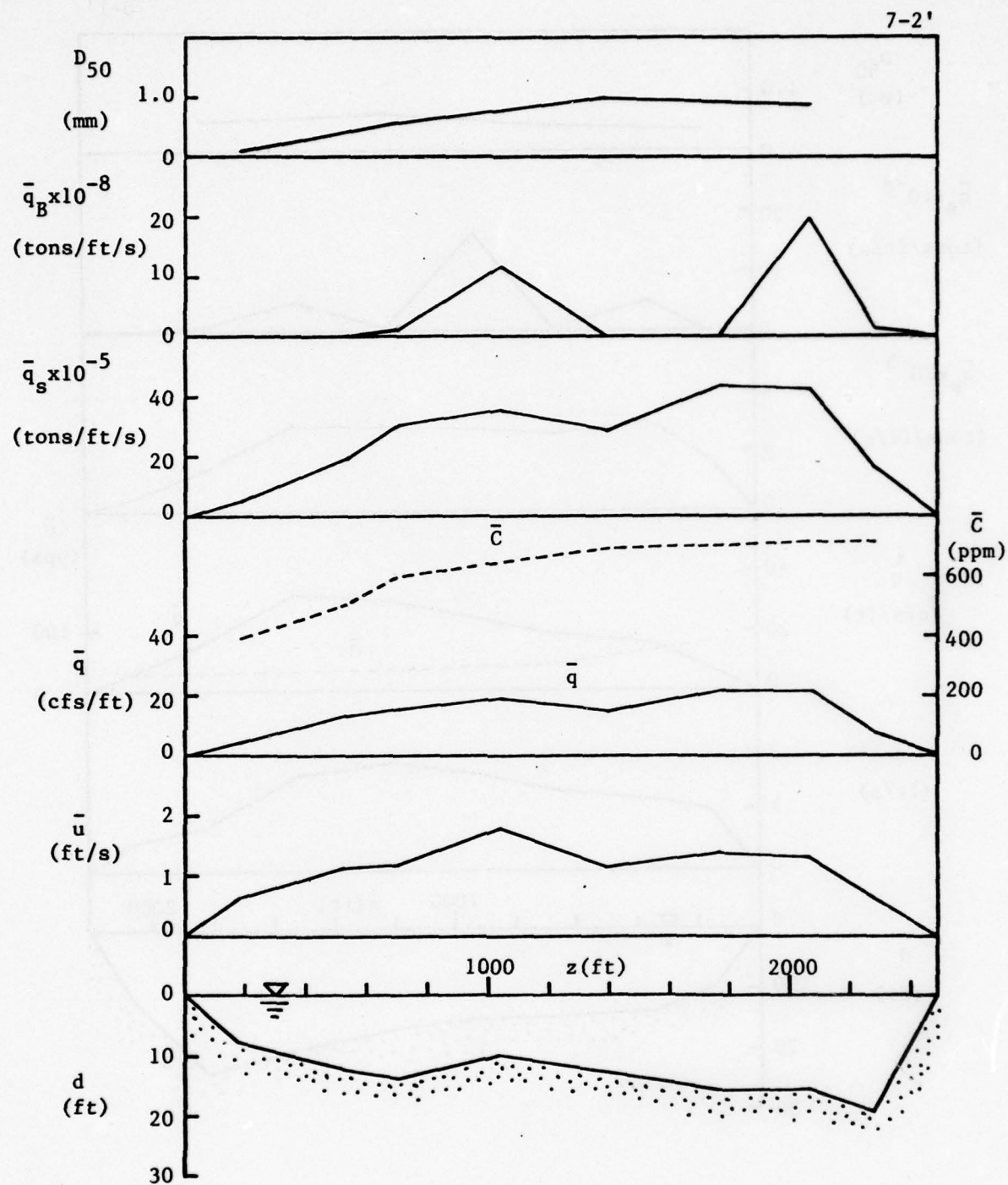


Figure 26. Lateral distributions of d , \bar{u} , \bar{q} , \bar{q}_s , \bar{q}_B , and D_{50} for Sec. 7-2'

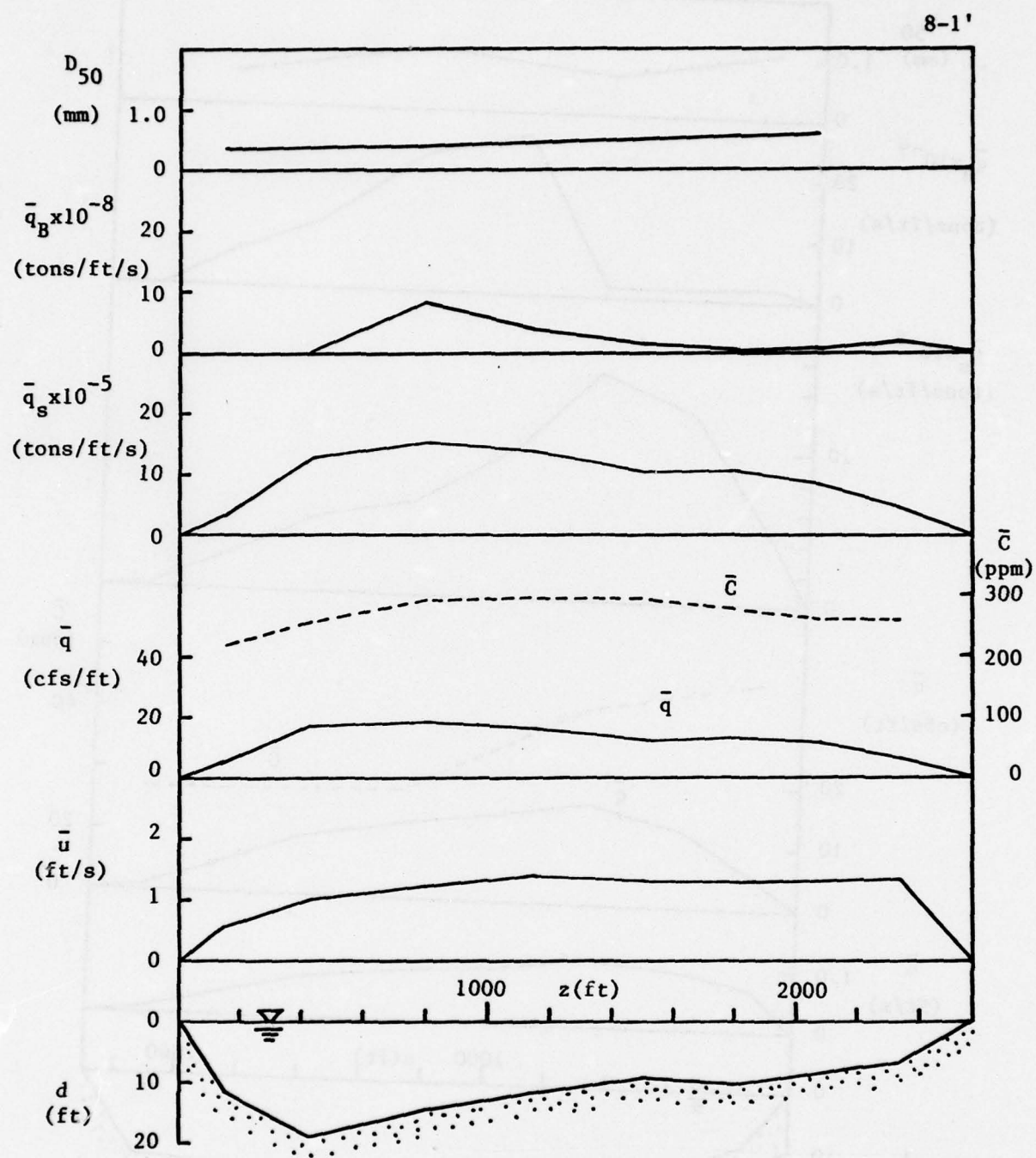


Figure 27. Lateral distributions of d , \bar{u} , \bar{q} , \bar{q}_s , \bar{q}_B , and D_{50} for Sec. 8-1'

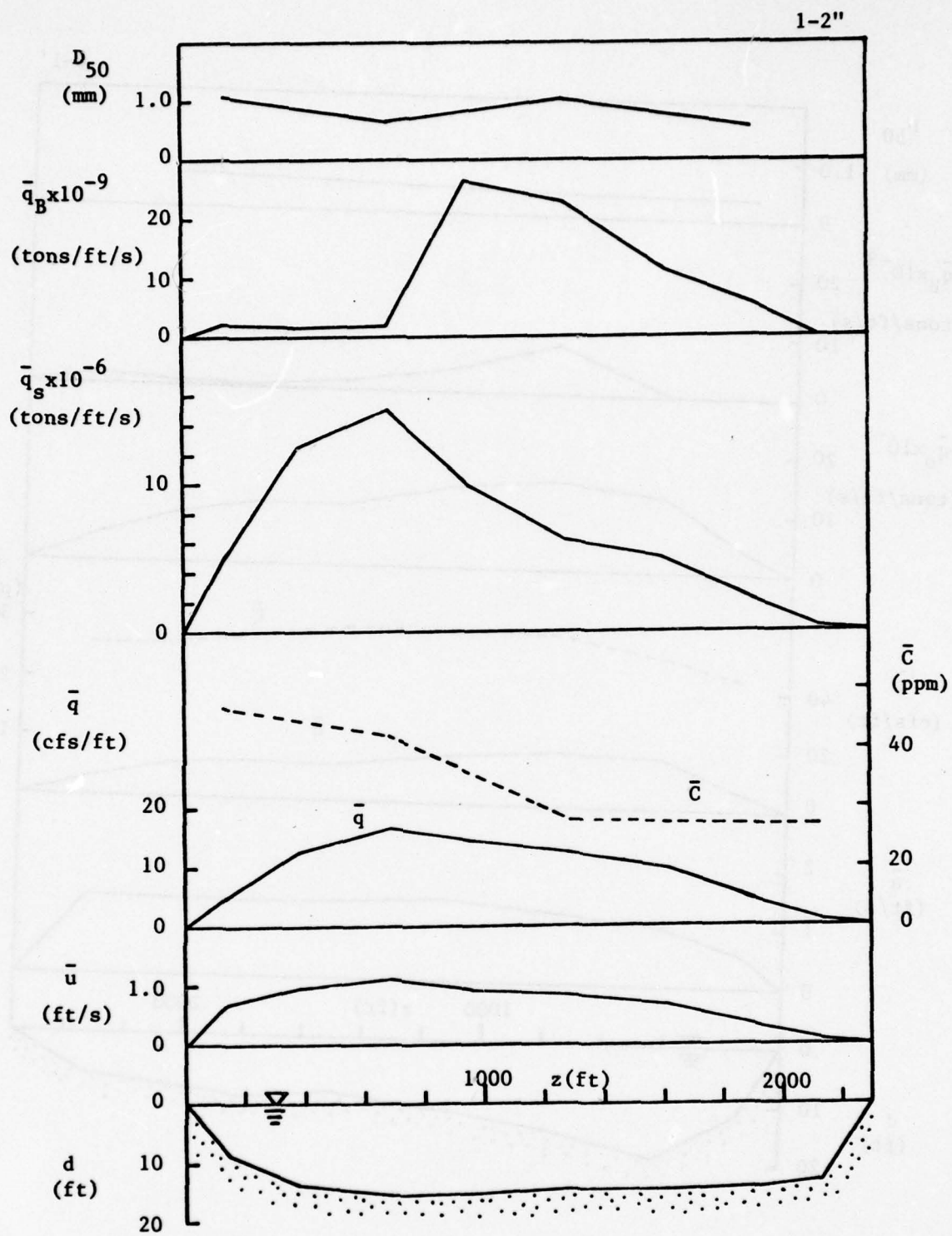


Figure 28. Lateral distributions of d , \bar{u} , \bar{q} , \bar{q}_s , \bar{q}_B , and D_{50} for Sec. 1-2"

2-1"

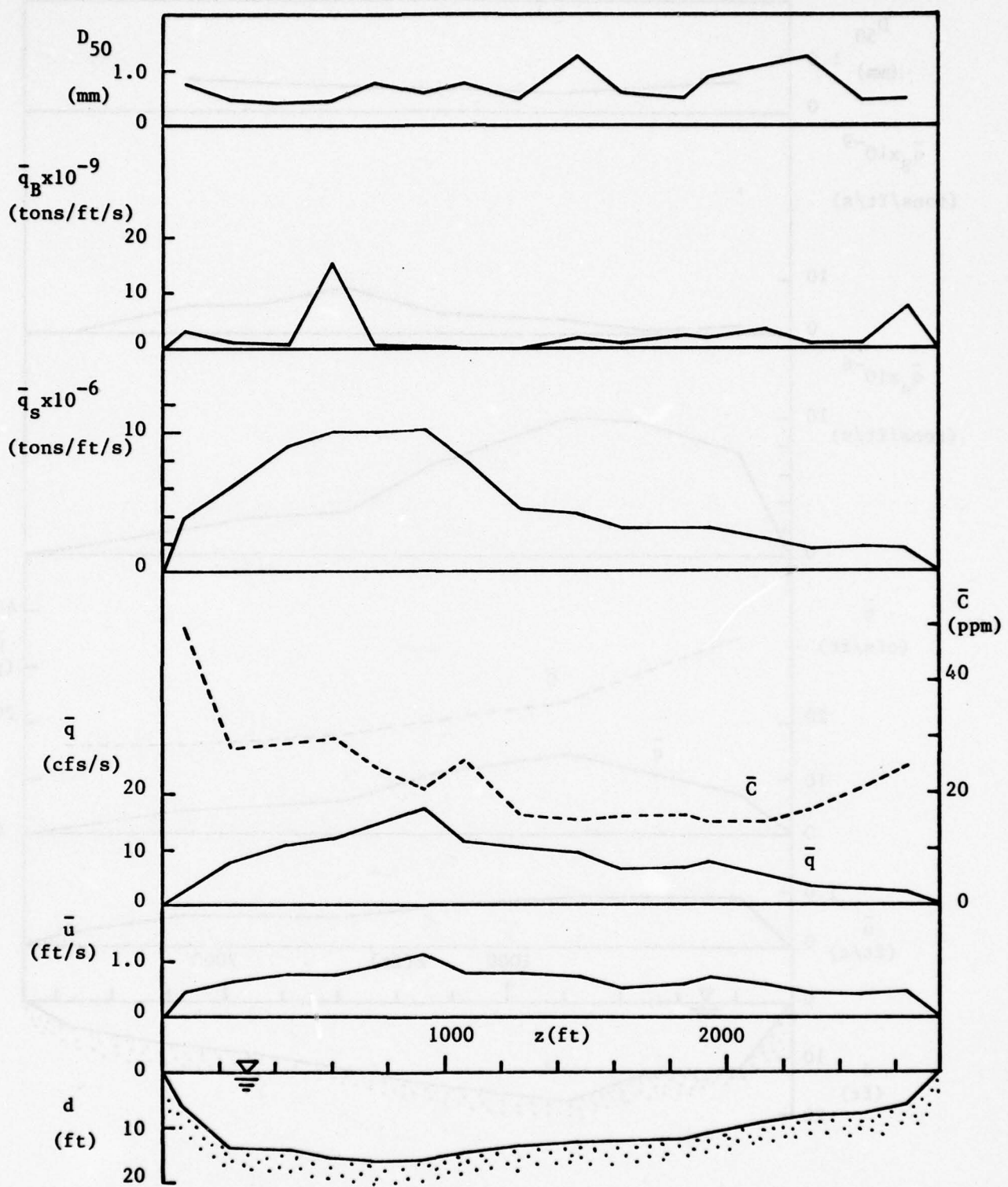


Figure 29. Lateral distributions of d , \bar{u} , \bar{q} , \bar{q}_s , \bar{q}_B , and D_{50} for Sec. 2-1"

3-2"

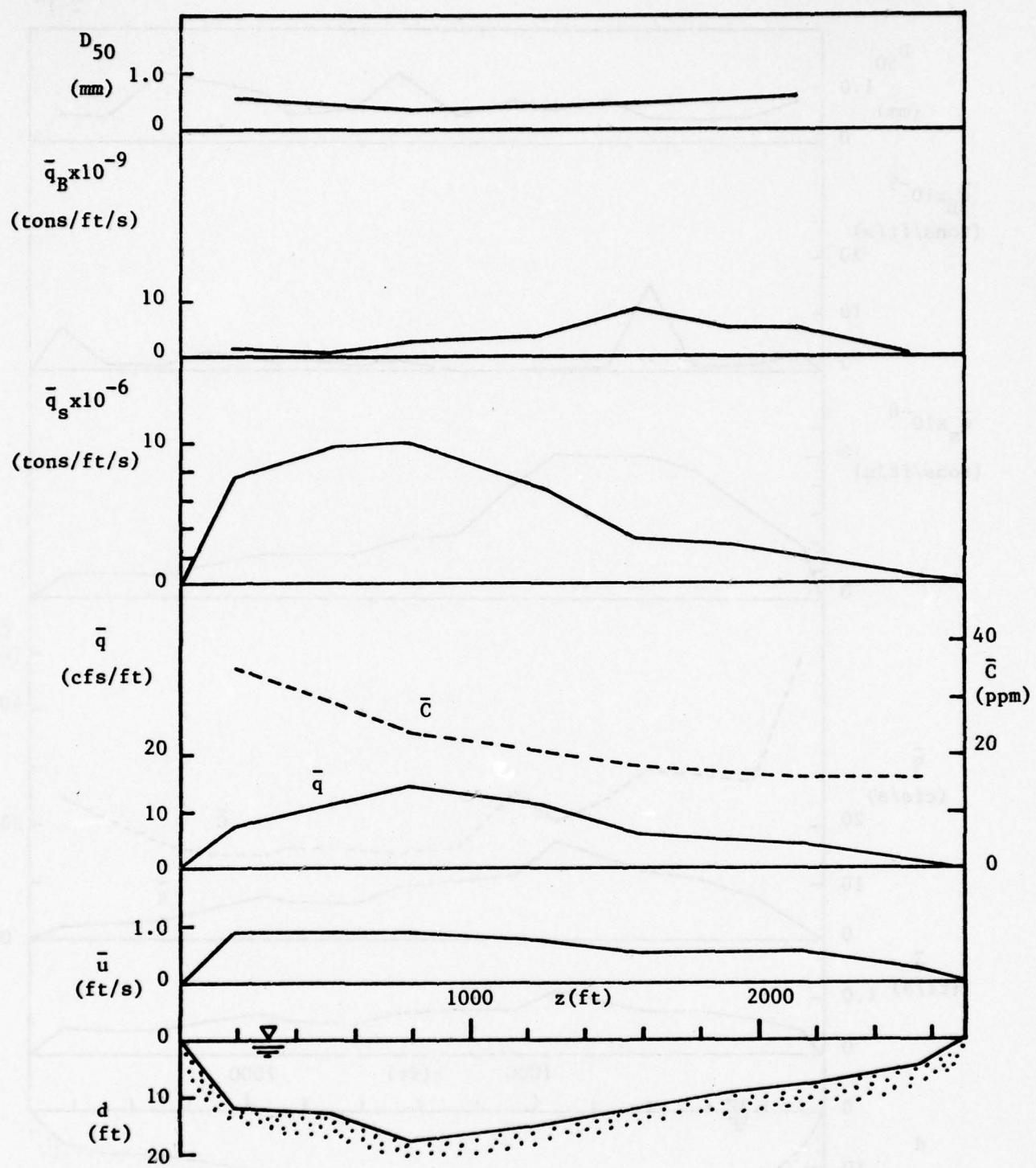


Figure 30. Lateral distributions of d , \bar{u} , \bar{q} , \bar{q}_s , \bar{q}_B , and D_{50} for Sec. 3-2"

4-1"

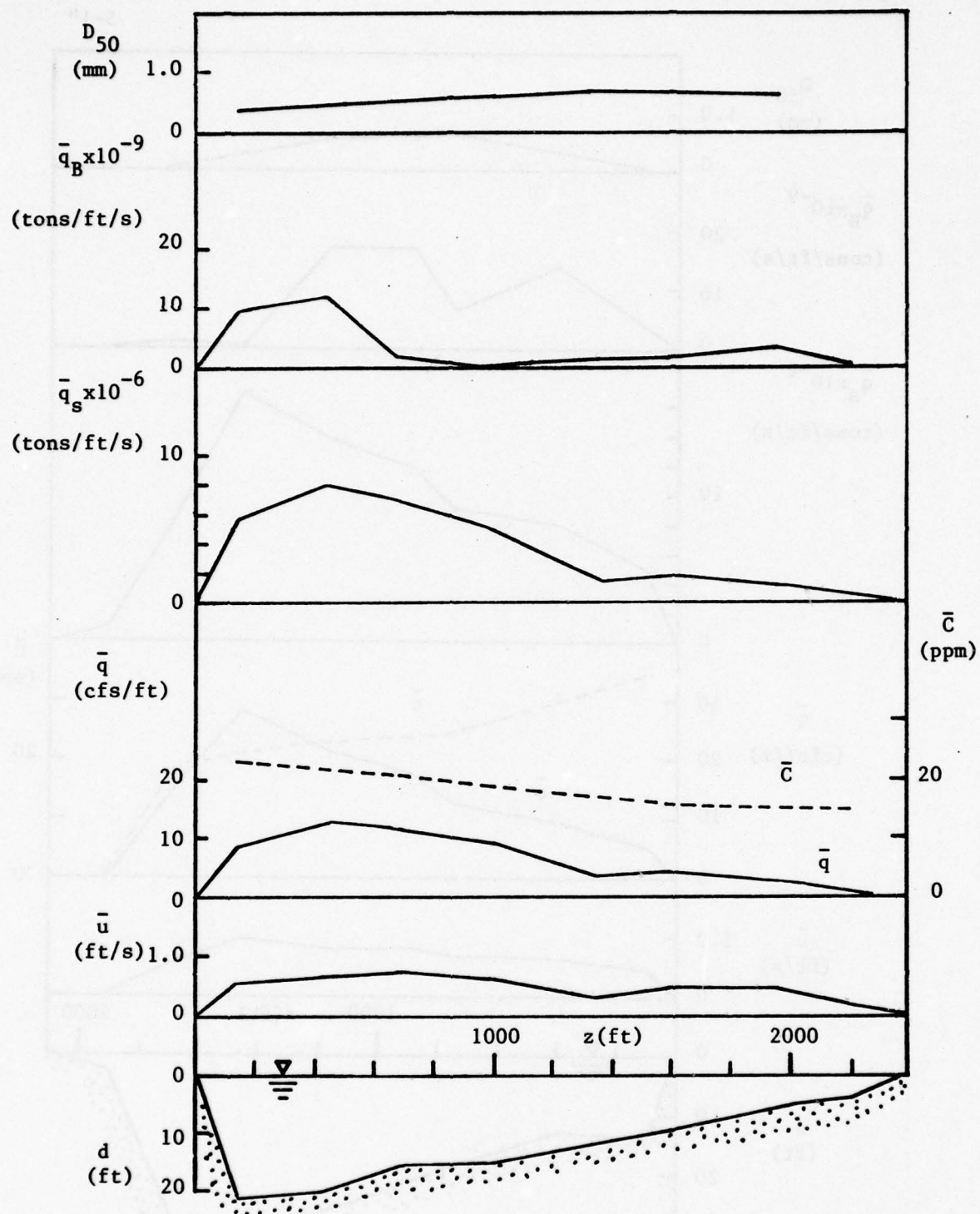


Figure 31. Lateral distributions of d , \bar{u} , \bar{q} , \bar{q}_s , \bar{q}_B , and D_{50} for Sec. 4-1"

5-1"

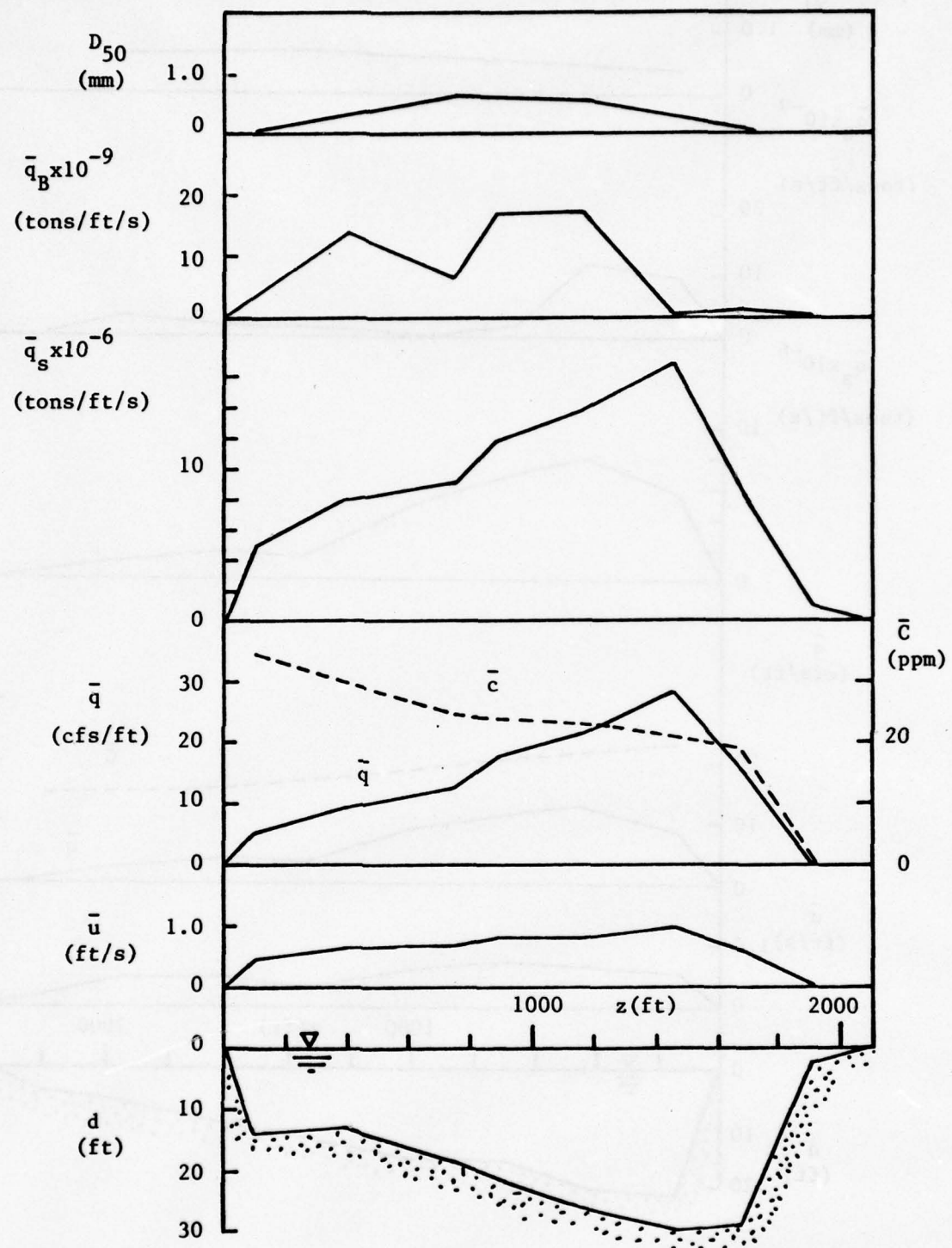


Figure 32. Lateral distributions of d , \bar{u} , \bar{q} , \bar{q}_s , \bar{q}_B , and D_{50} for Sec. 5-1"

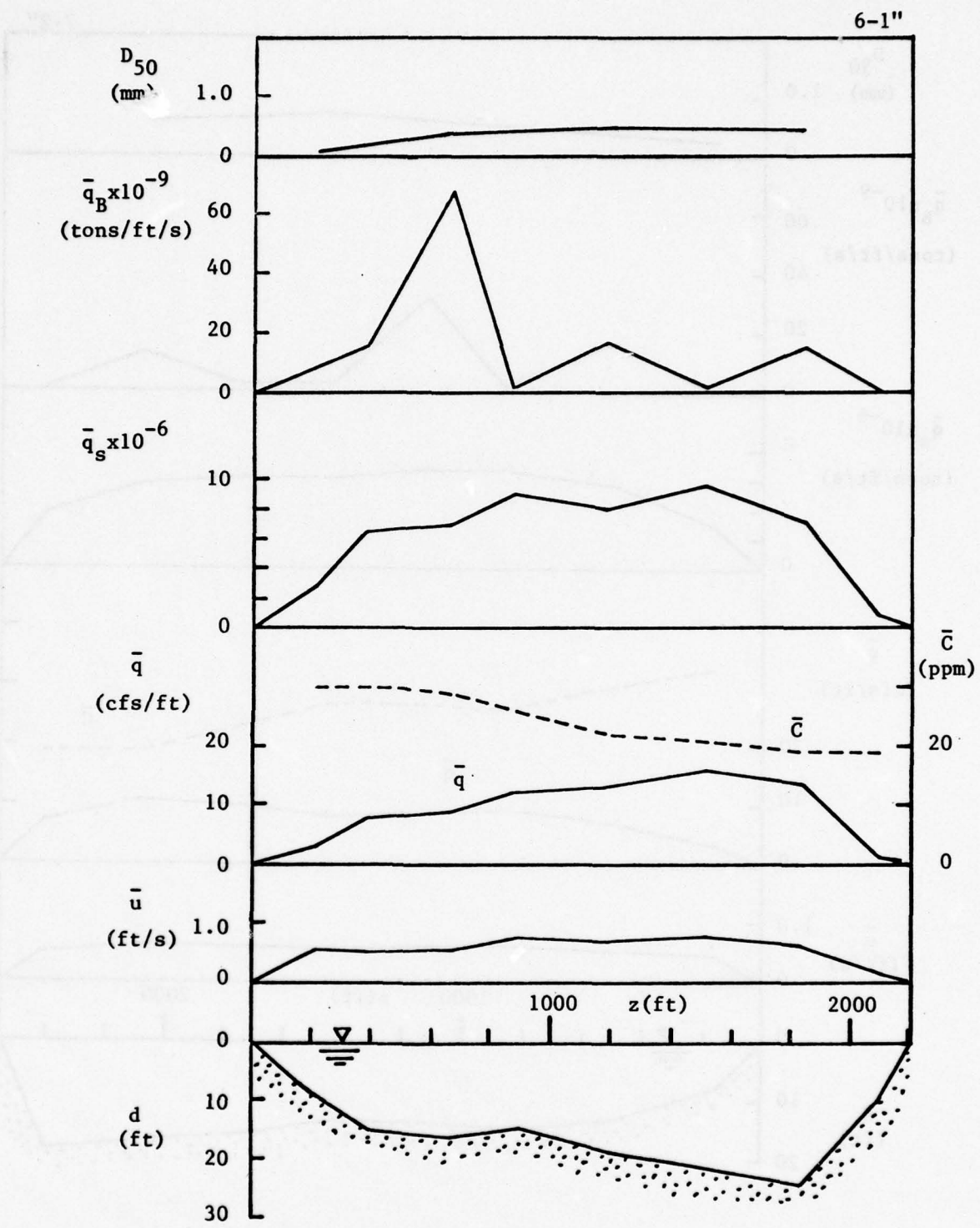


Figure 33. Lateral distributions of d , u , \bar{q} , \bar{q}_s , \bar{q}_B , and D_{50} for Sec. 6-1"

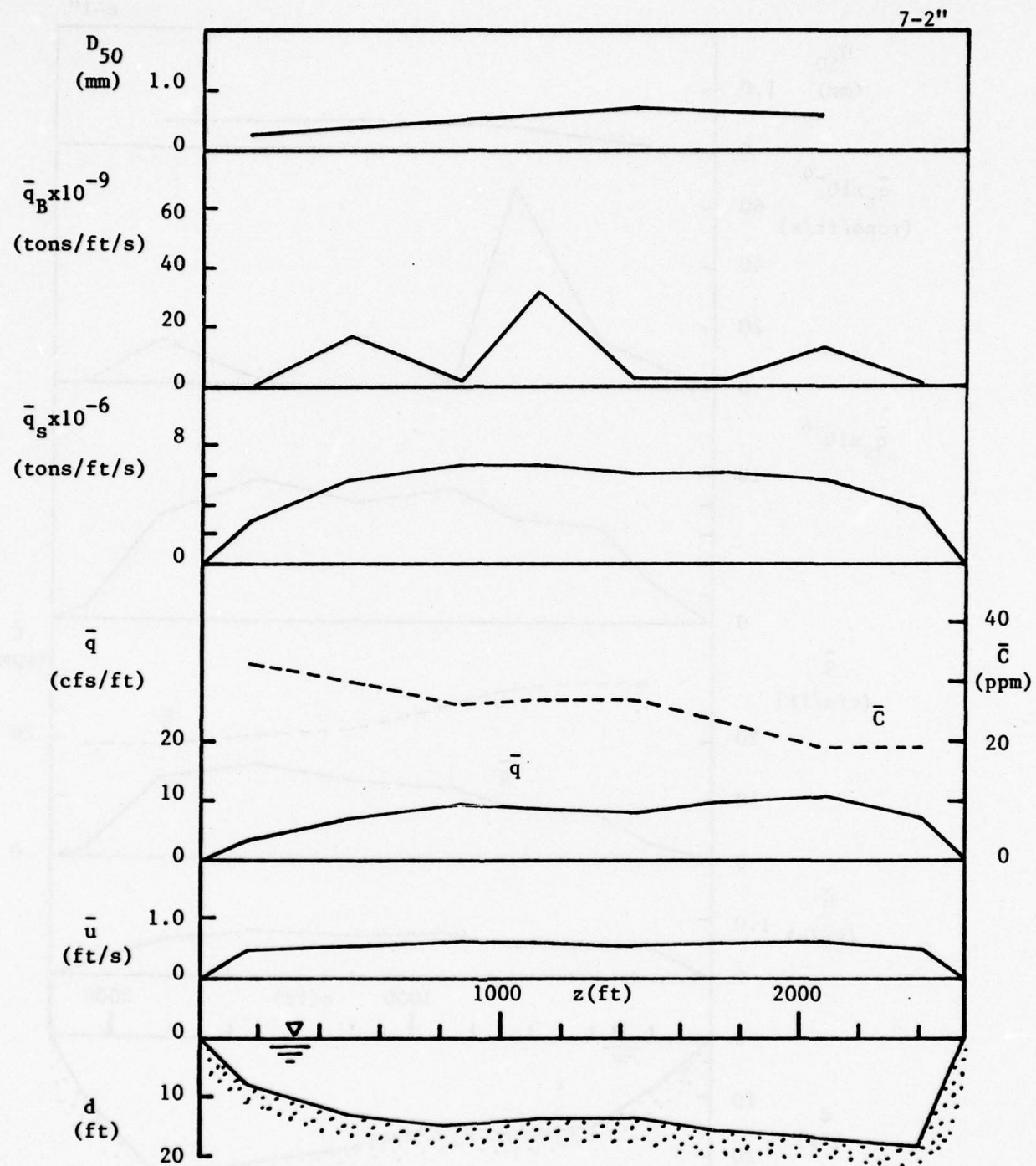


Figure 34. Lateral distributions of d , \bar{u} , \bar{q} , \bar{q}_s , \bar{q}_B , and D_{50} for Sec. 7-2"

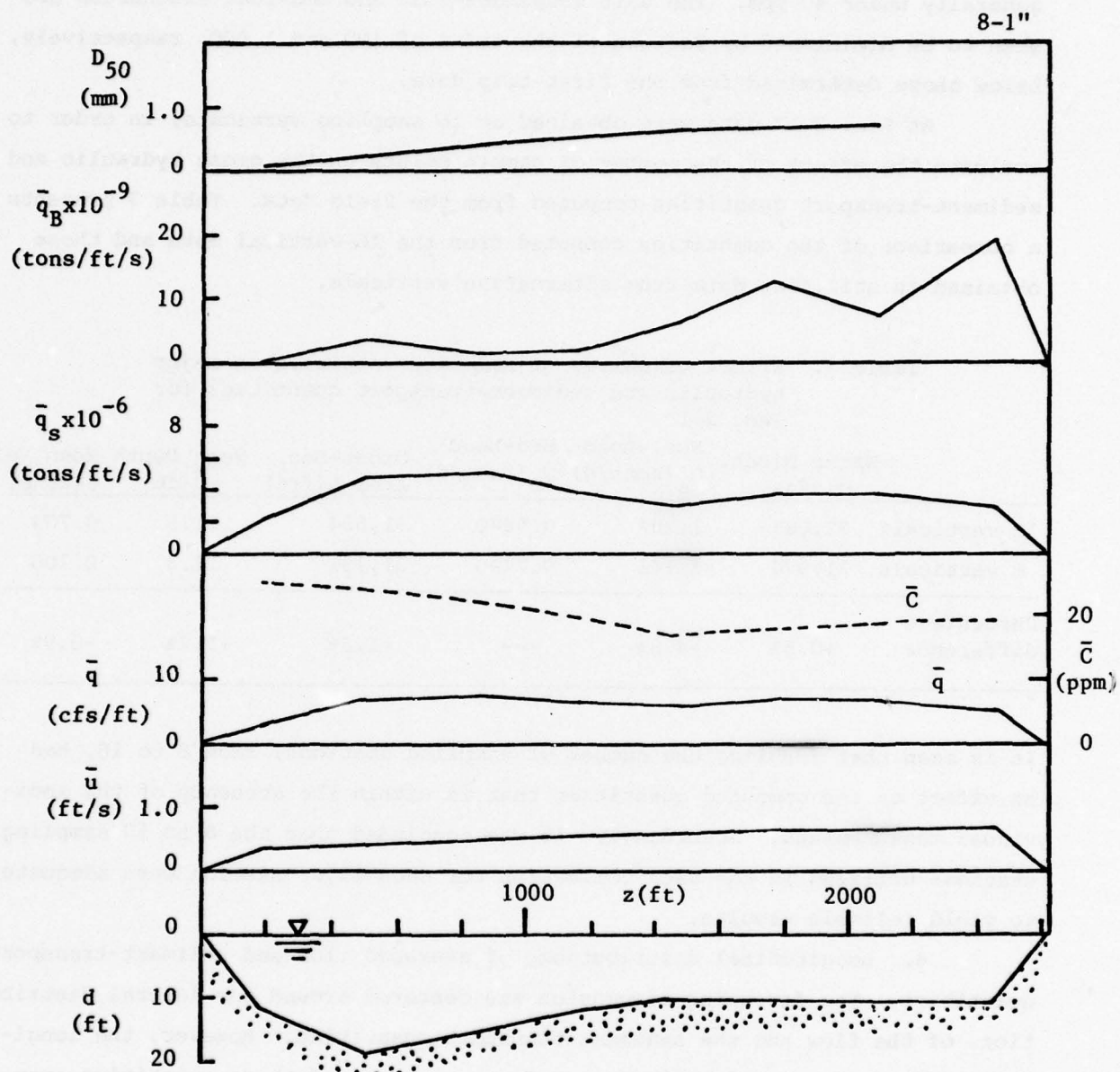


Figure 35. Lateral distributions of d , \bar{u} , \bar{q} , \bar{q}_s , \bar{q}_B , and D_{50} for Sec. 8-1"

that the water and sediment discharges were at or near the lows for the past several decades. The mean velocities were lower than 1 ft/sec and \bar{C} was generally under 40 ppm. The unit suspended-load and bed-load discharges are seen to be diminished by factors of the order of 100 and 1,000, respectively, below those determined from the first-trip data.

At Sec. 2-1" data were obtained at 16 sampling verticals, in order to evaluate the effect of the number of sample points on the gross hydraulic and sediment-transport quantities computed from the field data. Table 3 presents a comparison of the quantities computed from the 16-vertical data and those obtained in utilizing data from alternative verticals.

Table 3. Effect of number of sampling verticals on major hydraulic and sediment-transport quantities for Sec. 2-1"

	Water Disch. Q (cfs)	Sus.-Load Q_s (tons/d)	Bed-Load Q_B (tons/d)	Cross-Sec. Area A (ft^2)	Mean Depth \bar{d} (ft)	Mean Vel. U (ft/s)
16 verticals	22,083	1,204	0.54±0	31,554	11.5	0.700
8 verticals	21,974	1,146	0.77±0	31,131	11.3	0.706
Percentage difference	+0.5%	+4.8%	---	+1.3%	+1.7%	-0.9%

It is seen that doubling the number of sampling stations, from 8 to 16, has an effect on the computed quantities that is within the accuracy of the individual measurements. Accordingly, it was concluded that the 8 to 10 sampling stations utilized in the data collection for each major section were adequate to yield reliable results.

4. Longitudinal distributions of averaged flow and sediment-transport quantities. The foregoing discussion was centered around the lateral distributions of the flow and the sediment-transport quantities. However, the longitudinal or streamwise distributions of the averages of these quantities over the cross sections are also of central importance to the understanding of the sediment-transport character of the river and to the framing of an improved sediment-management strategy for the study reaches. Figure 36 shows the longitudinal variations of mean unit discharge ($q=Q/W$), unit bed-load discharge ($q_B=Q_B/W$), and mean diameter of bed material (\bar{D}_{50}) calculated from the

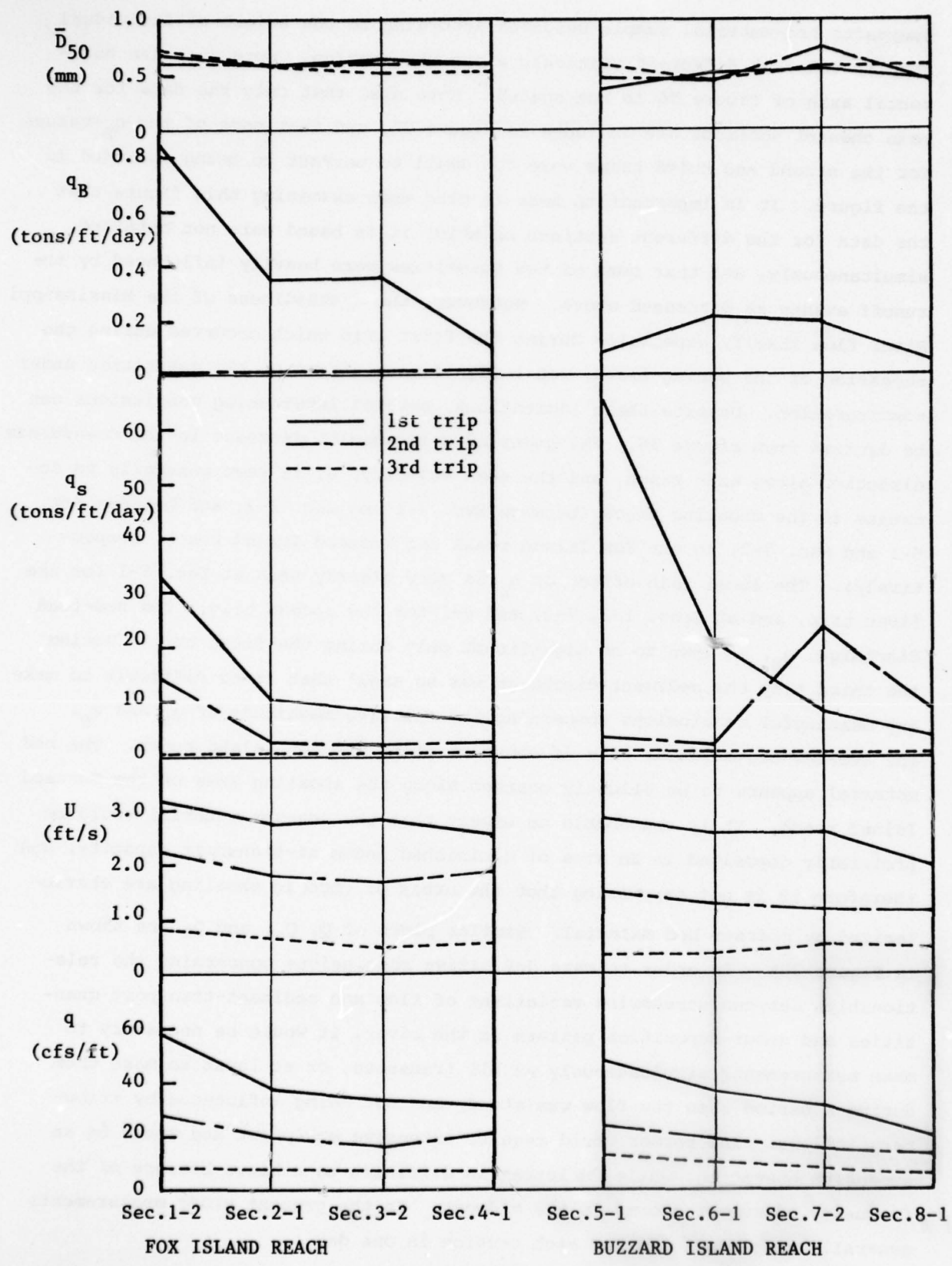


Figure 36. Longitudinal variations of q , U , q_s , q_B , and \bar{D}_{50}

57

composite bed-material sample weighted according to the weight of individual samples taken at different verticals along the section. Note that the horizontal axis of figure 36 is not scaled. Note also that only the data for the main channel sections are included in figure 36, and that some of the q_B -values for the second and third trips were too small to warrant being included in the figure. It is important to bear in mind when examining this figure that the data for the different sections on which it is based were not obtained simultaneously, and that some of the quantities were heavily influenced by the runoff events as discussed above. Moreover, the unsteadiness of the Mississippi River flow itself, especially during the first trip which occurred during the recession of the spring flood, had a significant effect on the quantities under consideration. Despite these limitations, several interesting conclusions can be derived from figure 36. The quantity q is seen to decrease in the downstream direction along each reach, and the mean velocity, U , is seen generally to decrease in the shoaling areas (between Sec. 2-1 and Sec. 3-2, and between Sec. 6-1 and Sec. 7-2, in the Fox Island reach and Buzzard Island reach, respectively). The local rain effect on q_s is very clearly seen at Sec. 5-1 for the first trip, and at Secs. 1-2, 7-2, and 8-1 for the second trip. The bed-load discharge, q_B , is seen to be significant only during the first trip. During the third trip the sediment discharge was so small that it is difficult to make any meaningful conclusions concerning the relative magnitude of q_s and q_B . The average bed-material size is constant along the Fox Island reach. The bed material appears to be slightly coarser along the shoaling area of the Buzzard Island reach. It is reasonable to expect that the coarser material would be preferably deposited in an area of diminished sediment-transport capacity, and therefore it is not surprising that the areas of chronic shoaling are characterized by coarser bed material. Similar plots of Q , Q_s , and Q_B are shown in figure 36A. In order to make definitive conclusions concerning the relationships between streamwise variations of flow and sediment-transport quantities and scour-deposition pattern in the river, it would be necessary to make measurements simultaneously at all transects, or at least to make them during a period when the flow was steady and not being influenced by tributary inflows. The former would require extensive equipment and would be an expensive operation, while the latter is difficult to achieve because of the frequency of summer storms in the Midwest. In the present study measurements generally were completed for each section in one day.

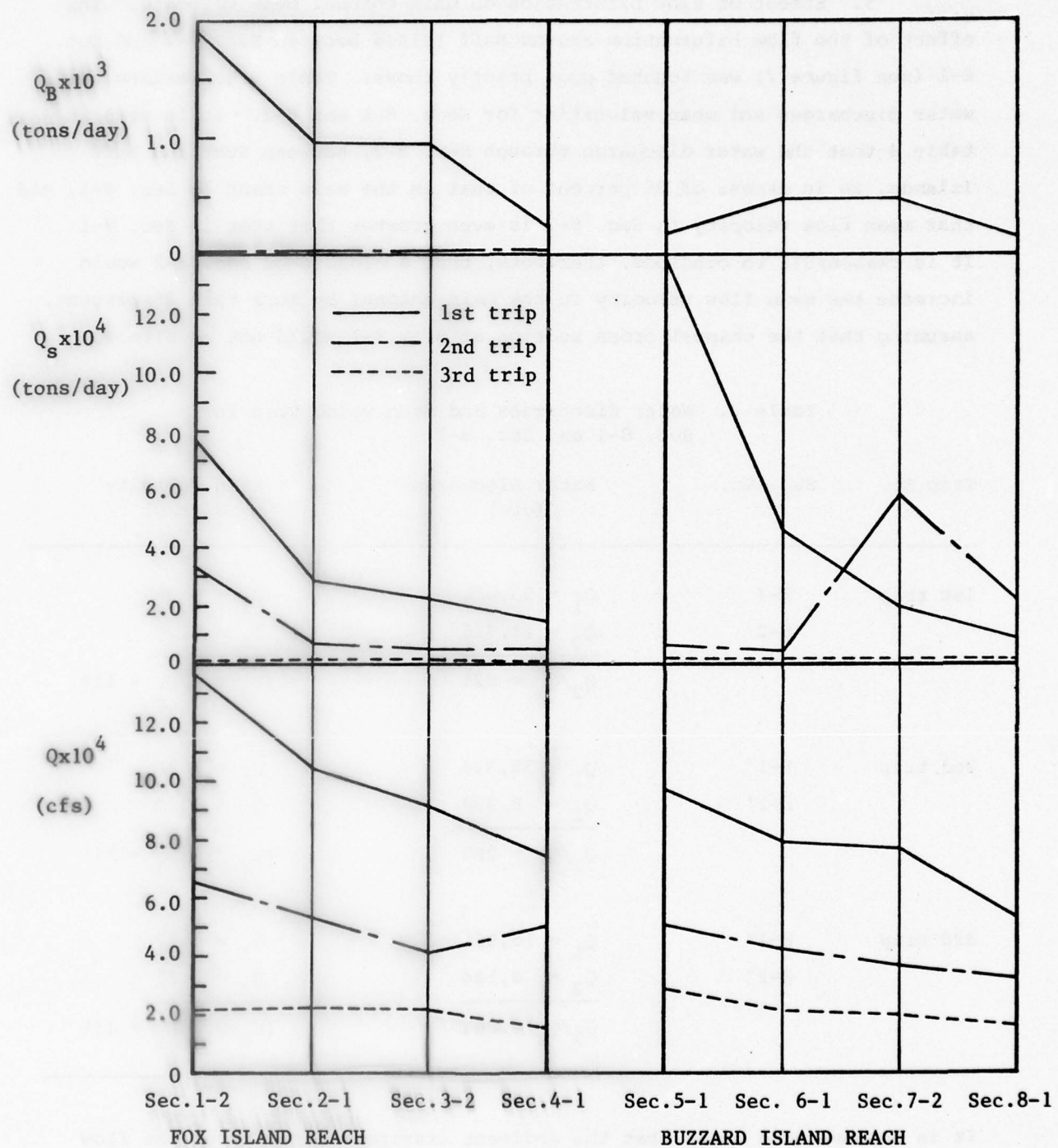


Figure 36A. Longitudinal variations of Q , Q_s , and Q_B

5. Effect of flow bifurcation on main-channel mean velocity. The effect of the flow bifurcation around Huff Island between Sec. 7-2 and Sec. 8-1 (see figure 7) was touched upon briefly above. Table 4 summarizes the water discharges and mean velocities for Secs. 8-1 and 8-2. It is seen in table 4 that the water discharge through Sec. 8-2, between Hunt and Huff Islands, is in excess of 25 percent of that in the main channel, Sec. 8-1, and that mean flow velocity in Sec. 8-2 is even greater than that in Sec. 8-1. It is reasonable to conclude, therefore, that a closure of Sec. 8-2 would increase the mean flow velocity in the main channel by more than 25 percent, assuming that the channel cross section at Sec. 8-1 would not be altered.

Table 4. Water discharges and mean velocities in Sec. 8-1 and Sec. 8-2

Trip No.	Sec. No.	Water Discharge Q (cfs)	Mean Velocity U (ft/s)
1st trip	8-1	$Q_1 = 53,084$	$U_1 = 1.98$
	8-2	$Q_2 = 11,726$	$U_2 = 2.20$
		$Q_2/Q_1 = 22\%$	$(U_2-U_1)/U_1 = 11\%$
2nd trip	8-1'	$Q_1 = 32,334$	$U_1 = 1.16$
	8-2'	$Q_2 = 8,994$	$U_2 = 1.29$
		$Q_2/Q_1 = 28\%$	$(U_2-U_1)/U_1 = 11\%$
3rd trip	8-1"	$Q_1 = 15,931$	$U_1 = 0.52$
	8-2"	$Q_2 = 4,144$	$U_2 = 0.61$
		$Q_2/Q_1 = 26\%$	$(U_2-U_1)/U_1 = 17\%$

It is demonstrated below that the sediment transport capacity of the flow increases markedly with mean velocity. Therefore, it is reasonable to expect that the higher mean velocity resulting from the channel closure at Sec. 8-2 would lead to a significant reduction in the shoaling and in the

dredging requirements along the Buzzard Island reach. Here it should be noted that a submerged dam existed between Huff and Hunt Islands for many years; however, now has deteriorated to the point of being practically nonexistent. Also, there is a deep pool (or bendway) just downstream from Sec. 8-1, which could accommodate some of the sediment which might be transported downstream by any enhancement in the sediment-transport capacity of the stream in the Buzzard Island reach. Observations similar to the foregoing also were made at Sec. 6-1 and Sec. 6-2. The water discharge through Sec. 6-2 was found to be more than 10 percent of that through Sec. 6-1. Therefore, it was concluded that the closure of Sec. 6-2 would enhance the mean flow velocity and the sediment-transport capacity of the main channel in that reach, and thereby would diminish the shoaling that characterizes the river just to the east of Buzzard Island. However, the effect of this closure was expected to be less marked than that of the closure of Sec. 8-2 would be. On the basis of the sediment-transport relation derived from the field data presented below, it was concluded that an increase in the mean velocity of 25 percent of the main channel would roughly double the bed-load transport rate in the main channel. In this connection it should be noted that the unit sediment-transport rate tends to be larger near the right bank, in the main channel, at Sec. 8-1. In the Fox Island reach it was found that the flow out of the main channel, around Hackley Island and through Sec. 3-3, amounted to approximately 10 percent of that in the main channel, through Sec. 3-2. Therefore, closure of Sec. 3-2 likely would be of significant benefit in diminishing the dredging requirements near Fox Island.

6. Effect of rainstorms on the Mississippi River sediment-transport characteristics. The effect of the increased sediment loads imposed on the Mississippi River by the inflow from the Des Moines River following the rainstorms which occurred during the first and second trips were cited above; these appeared at Sec. 5-1 for the first trip (figure 16), and at Secs. 1-2', 7-2', and 8-1' for the second trip (figures 20, 26, and 27, respectively). To facilitate close examination of the impact of the sediment inflows, the measured water discharges, Q , and suspended sediment discharges, Q_s , across the transects in the Mississippi and Des Moines Rivers are tabulated in table 5. The values of Q and Q_s for the Mississippi River are the totals for the main channel and the subchannels around the islands. Except for three values, the

Table 5. Water and suspended-load discharges through the Mississippi River and the Des Moines River study reaches

Trip No.	Sec. No.	Date	Water Disch. in Miss. River	Sus.-Load Disch. in Miss. River	Water Disch. in Des M.R.	Sus.-Load Disch. in Des M.R.
			Q (cfs)	Q _s (tons/day)	Q (cfs)	Q _s (tons/day)
1st Trip	1	050776	150,713	85,208	27,600	31,363
	2	051176	106,718	28,910	17,500	744(?)
	3	051276	99,573	24,381	17,000	5,209
	4	051476	80,620	16,381	12,300	5,452
	5	051876	100,672	139,880 (Rain)	21,300	130,115 (Rain)
	6	051976	89,679	47,973	19,400	34,249
	7	052176	87,446	22,150	13,950	10,668
	8	052576	71,773	11,377	10,800	5,074
	9	051376	---	---	10,797	5,149 (Meas'd)
2nd Trip	1	061776	67,186	34,199 (Rain)	16,100	31,786 (Rain)
	2	062176	53,429	7,154	7,980	4,922
	3	062276	45,903	5,753	6,540	3,840
	4	062376	54,620	6,228	5,780	3,449
	5	062476	52,175	7,908	4,670	4,540
	6	062576	47,973	6,157	3,890	3,631
	7	070176	42,032	60,174 (Rain)	9,740	56,757 (Rain)
	8	070276	45,534	27,739 (Rain)	9,610	21,640 (Rain)
	9	061876	---	---	11,603	22,395 (Meas'd)
3rd Trip	1	083176	22,681	1,495	400	1,039
	2	090176	22,083	1,204	400	747
	3	090276	23,646	1,359	440	654
	4	090376	17,899	873	400	382
	5	081776	29,895	1,756	730	832
	6	081876	25,353	1,498	760	508
	7	081976	23,626	1,456	730	521
	8	082076	22,489	1,104	1,170	478
	9	090776	---	---	222	3 (Meas'd)

water discharges listed for the Des Moines River were measured by COE(RI) at St. Francisville, Iowa, which is 15.1 mi upstream from the river mouth. The three discharge values determined from the measurements at Sec. 9-1 are listed opposite that section number in table 5, and are identified as having been measured. The values of Q_s for the Des Moines River were obtained by subtracting Q_s measured by COE(RI) at Keokuk (Lock and Dam 19) from those measured in the present study at the different transects. It was assumed that there was no sediment input to the river between the confluence and the study areas. The contribution of the sediment input from the Des Moines River to Q_s in the study reaches is readily apparent in table 5. On 18 May, 17 June, 1 July, and 2 July 1976, Q_s from the Des Moines river is seen to have amounted to 93 percent, 93 percent, 94 percent, and 78 percent, respectively, of the total suspended load discharge measured at the Mississippi River transects. It is also seen that Q_s in the Des Moines River increased dramatically, by a factor of approximately 24, between 14 May and 18 May 1976, after which it decreased by a factor of approximately 4 in one day.

The Des Moines River data on Q and Q_s listed in table 5 are plotted in figures 37; the points which were heavily influenced by rainstorms are identified by the sampling dates noted by them. The figure reveals a power-law relation between Q and Q_s from which the rain influenced values deviate, as could be expected, significantly. The least-squares power-law relationship between Q_s (tons/day) and Q (cfs) is given by

Rainstorms deliver large quantities of fine sediment to the Des Moines River from its heavily cultivated watershed, and the amount of fine material carried by the river depends primarily on its availability rather than on an equilibrium relationship between the sediment-transport capacity of the flow and the availability of the material in the bed. Therefore, it is to be expected that dramatic increases in the Des Moines River suspended load will follow rainstorms. Figure 38 is a comparative plot of the Des Moines River channel cross section at Sec. 9-1. During the second trip, which followed the bulk of the spring runoff, the channel bed was found to have been scoured to significantly below its earlier level. During the third trip, which was made after

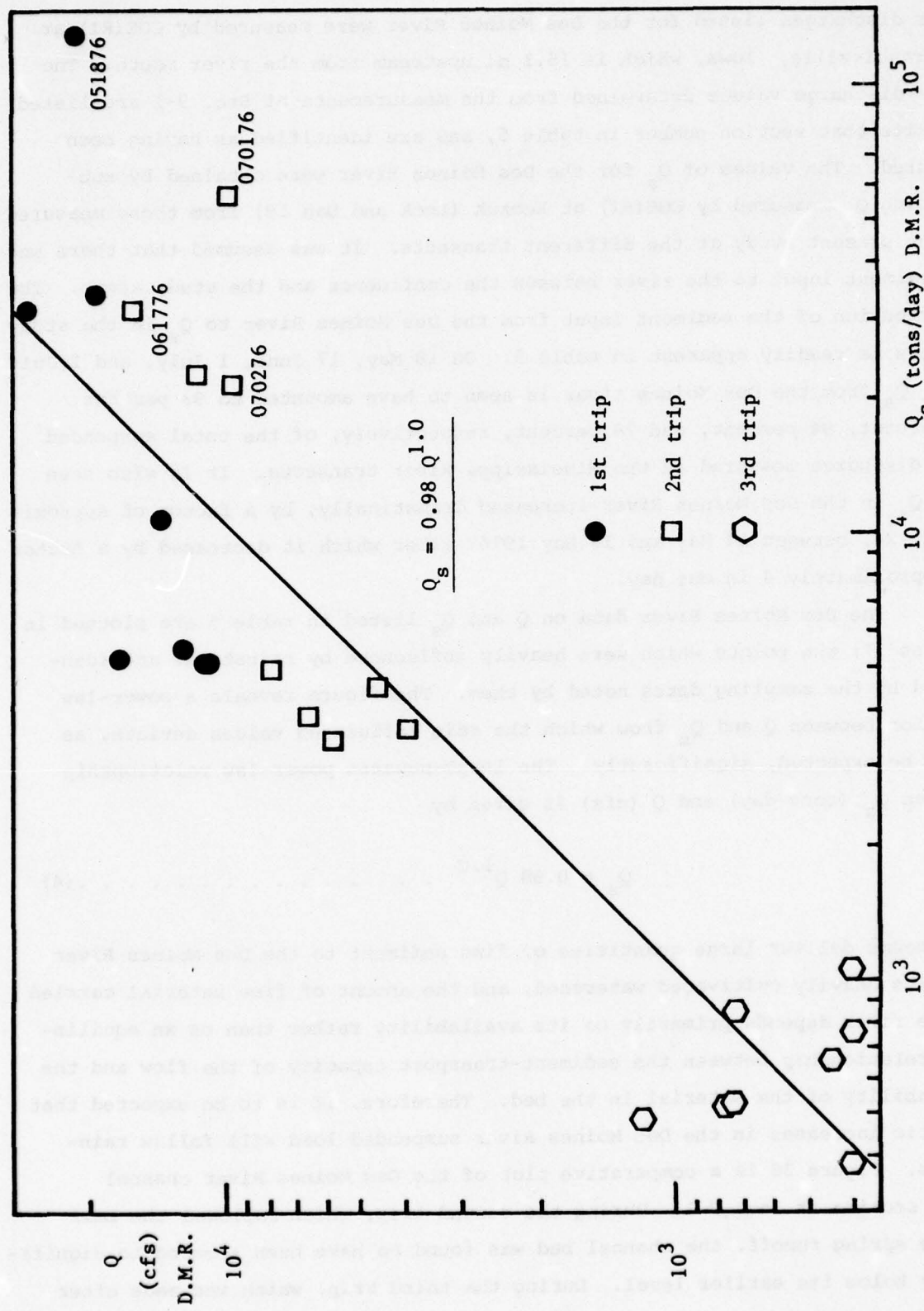


Figure 37. Relationship between Q and Q_s for the Des Moines River

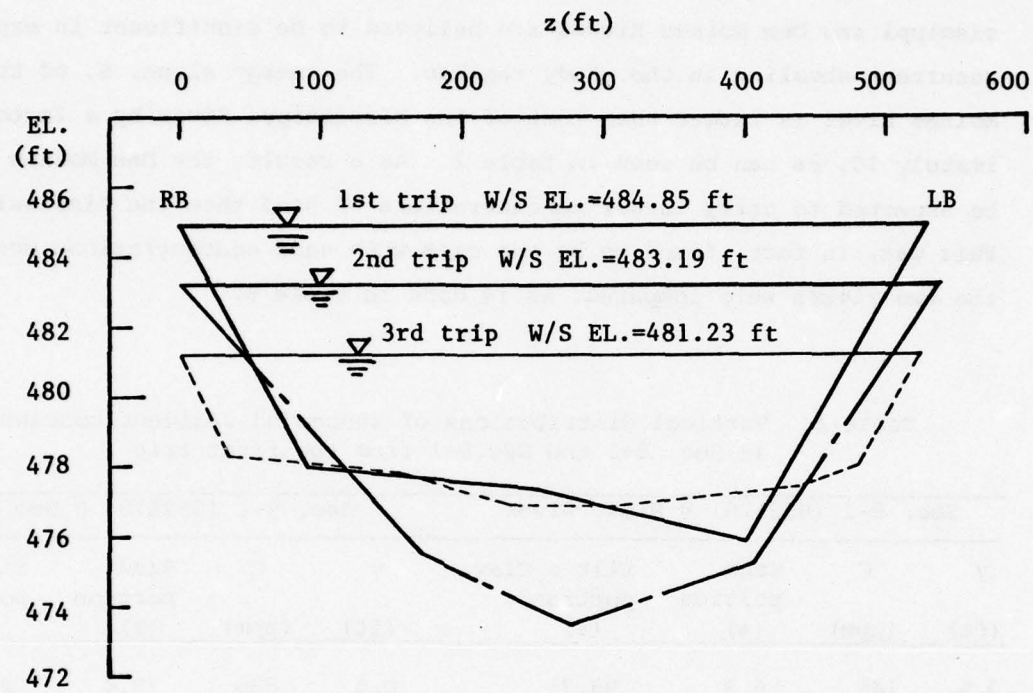


Figure 38. Variations in cross-sectional bed profile for the Des Moines River

an extended period of low flow, the river bed nearly had recovered the elevation measured during the first trip. Again, the bed-elevation fluctuations are comparable in magnitude to those of the water surface. Alluvial streams are truly flows with only free surfaces.

7. Sediment transport characteristics of the Mississippi and Des Moines Rivers. Differences between the sediment transport characteristics of the Mississippi and Des Moines Rivers are believed to be significant in explaining the recurrent shoaling in the study reaches. The energy slope, S , of the Des Moines River is larger than that of the Mississippi River by a factor of approximately 10, as can be seen in table 2. As a result, the Des Moines River can be expected to carry larger concentrations of sand than the Mississippi River. This was, in fact, found to be the case when sand concentrations measured in the two rivers were compared, as is done in table ..

Table 6. Vertical distributions of suspended sediment concentrations at Sec. 8-1 and Sec. 9-1 from the first trip

Sec. 8-1 (052576) @ Miss. River				Sec. 9-1 (052676) @ Des M. River			
Y (ft)	C (ppm)	Sand portion (%)	Silt & Clay portion (%)	Y (ft)	C (ppm)	Sand portion (%)	Silt & Clay portion (%)
0.5	149	6.3	93.7	0.5	836	78.4	21.6
1.0	104	8.6	91.4	1.0	344	51.2	48.8
1.5	99	9.3	90.7	1.5	300	59.0	41.0
2.0	60	9.9	90.1	2.0	283	42.1	57.9
3.0	112	8.8	91.2	3.0	287	41.4	58.6
4.0	81	7.8	92.2	4.0	265	38.6	61.4
5.0	59	9.2	90.8	5.0	220	26.6	73.4
7.0	56	9.9	90.1	7.0	198	14.0	86.0
10.0	83	3.2	96.8				
d=10.2 ft				d=7.8 ft			

Note that the data for Sec. 9-1 were obtained from a vertical located 276 ft from the right bank, while those for Sec. 8-1 are the results of the random sampling at different verticals along the section. At Sec. 9-1 in the Des Moines River, more than three-fourths of the suspended sediment was found to

be sand at the lowest sampling point ($y=0.5$ ft). With increasing distance above the bed, the sand fractions steadily diminished, due to the higher fall velocity of sand particles compared to those of the silt and clay fractions. However, even near the free surface ($y=7.0$ ft), 14 percent of this suspended sediment sample was sand. On the other hand, at Sec. 8-1, in the Mississippi River, the sand fraction of the suspended sediment samples never amounted to more than 10 percent, indicating that the suspended load of the Mississippi River was dominated by the so-called washload. During the second and third trips, no measurable quantity of sand was found in the Mississippi River suspended sediment samples.

Figures 39 illustrate the difference in the sediment-suspension capabilities of the two rivers. Therein, the suspended-sediment concentration profiles measured at Sec. 1-2 and Sec. 9-1 during the three sampling trips are compared. These data were measured at verticals located approximately 600 ft and 300 ft from the right bank of the Mississippi and Des Moines Rivers, respectively. For each plot the logarithmic slope of the best-fit straight line through the points, z , is given; this quantity also is known as the Rouse number, and arises in the theory of sediment suspension (Vanoni 1975). The quantity z , which is given by

where β is the ratio between the turbulence exchange coefficients for sediment and momentum; w is the particle fall velocity; κ is Kármán's constant; and u_* is the shear velocity characterizes the sediment suspension. Smaller values of z are associated with more uniform vertical distributions of suspended sediment. It is seen in figures 39 that the suspended sediment is quite uniformly distributed vertically in the Mississippi River, while the sediment suspension in the Des Moines River is characterized by relatively strong vertical concentration gradients. This difference results in a large measure from the aforementioned fact that the suspended load in the Mississippi River is dominated by material in the clay and silt range, which has a very low fall velocity, and hence small z and weak vertical concentration gradients. Additionally, the smaller value of u_* for the Mississippi River, which is a

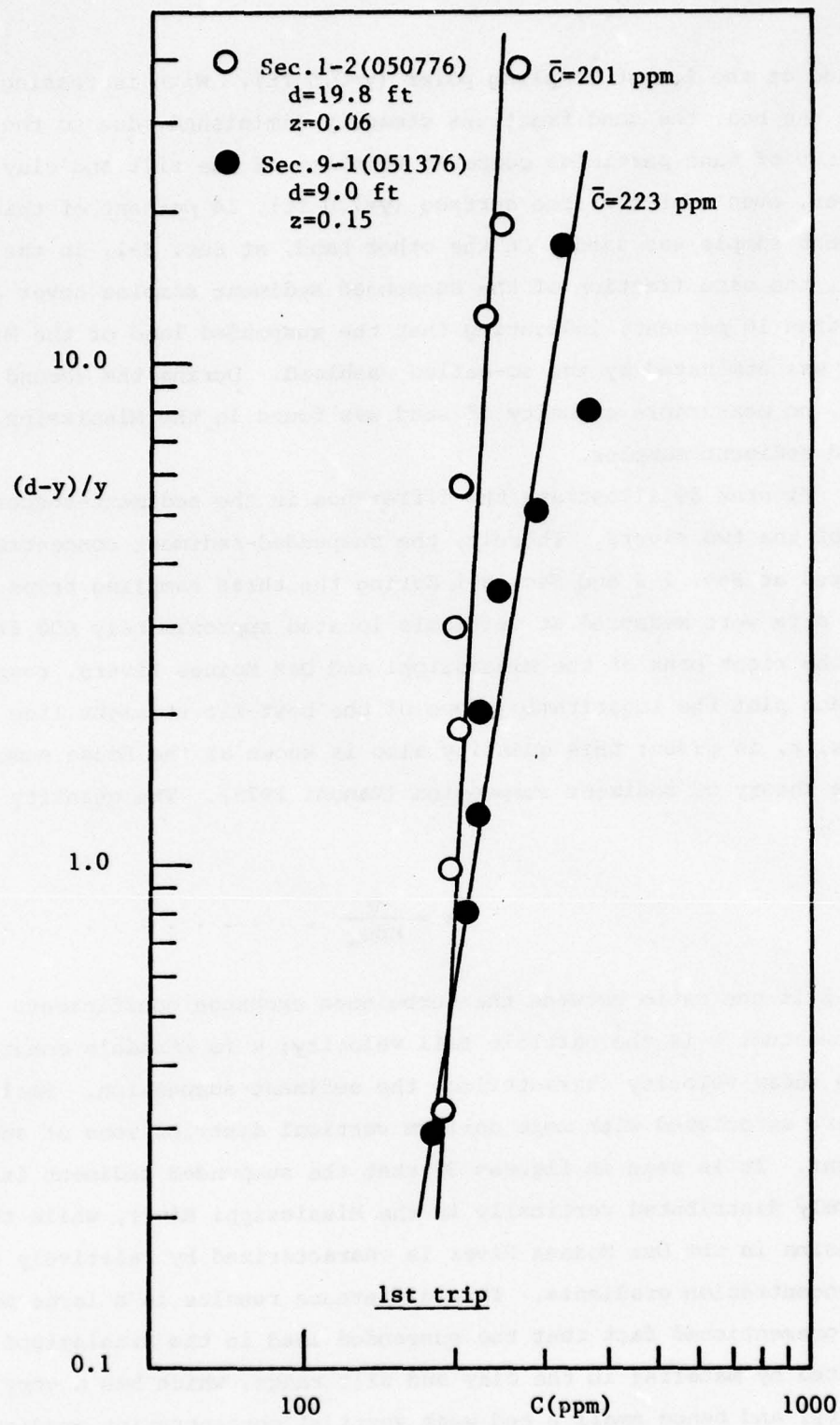


Figure 39. Typical vertical distributions of suspended-sediment concentration obtained at Sec. 1-2 and Sec. 9-1 (1st trip)

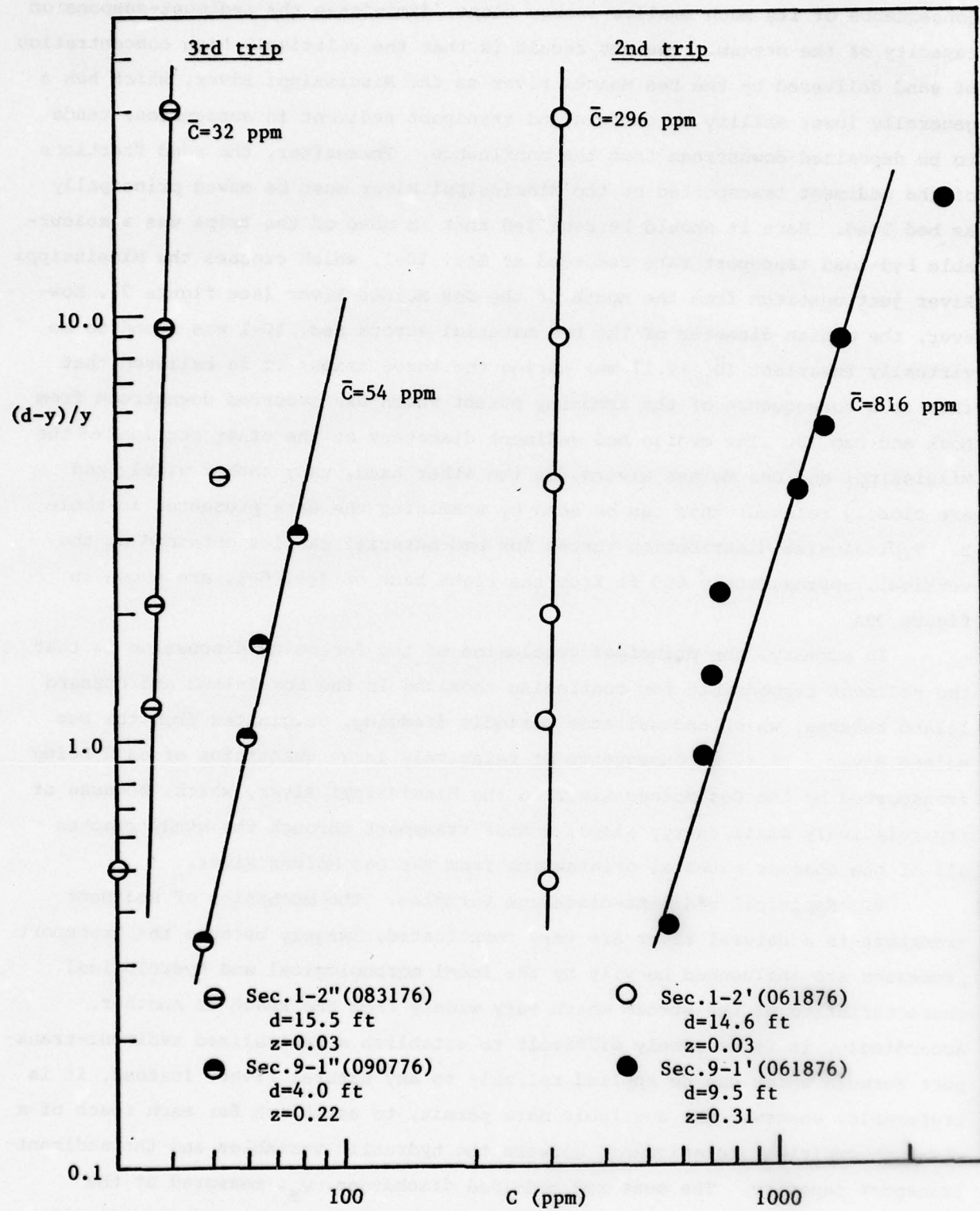


Figure 39. (Cont'd) (2nd and 3rd trips)

consequence of its much smaller energy slope, diminishes the sediment-suspension capacity of the stream. The net result is that the relatively high concentration of sand delivered by the Des Moines River to the Mississippi River, which has a generally lower ability to entrain and transport sediment in suspension, tends to be deposited downstream from the confluence. Thereafter, the sand fractions of the sediment transported by the Mississippi River must be moved principally as bed load. Here it should be recalled that in none of the trips was a measurable bed-load transport rate recorded at Sec. 10-1, which crosses the Mississippi River just upstream from the mouth of the Des Moines River (see figure 7). However, the median diameter of the bed material across Sec. 10-1 was found to be virtually invariant ($D_{50} = 2.17$ mm) during the three trips; it is believed that this is a consequence of the armoring effect which has occurred downstream from Lock and Dam 19. The median bed sediment diameters at the other sections of the Mississippi and Des Moines Rivers, on the other hand, vary rather widely and are closely related; this can be seen by examining the data presented in table 2. Typical size distribution curves for bed-material samples obtained at the vertical, approximately 600 ft from the right bank of Sec. 6-1, are shown in figure 39A.

In summary, the principal conclusion of the foregoing discussion is that the sediment responsible for continuing shoaling in the Fox Island and Buzzard Island reaches, which necessitates periodic dredging, originates from the Des Moines River. It is a consequence of relatively large quantities of sand being transported by the Des Moines River to the Mississippi River, which, because of its relatively small energy slope, cannot transport through the study reaches all of the coarser material originating from the Des Moines River.

8. Empirical sediment-discharge formulas. The mechanics of sediment transport in a natural river are very complicated, largely because the transport processes are influenced heavily by the local morphological and hydrological characteristics of the stream which vary widely from one reach to another. Accordingly, it is extremely difficult to establish a generalized sediment-transport formula which can be applied reliably to any natural river. Instead, it is preferable, whenever the available data permit, to establish for each reach of a river an empirical relationship between the hydraulic variables and the sediment-transport capacity. The measured bed-load discharges, Q_B , measured at the different sections in the main channel are shown plotted against mean velocity, U , in figure 40. It is seen that there is a very strong correlation between Q_B (tons/day) and U (ft/s), which was given quantitative expression by the means

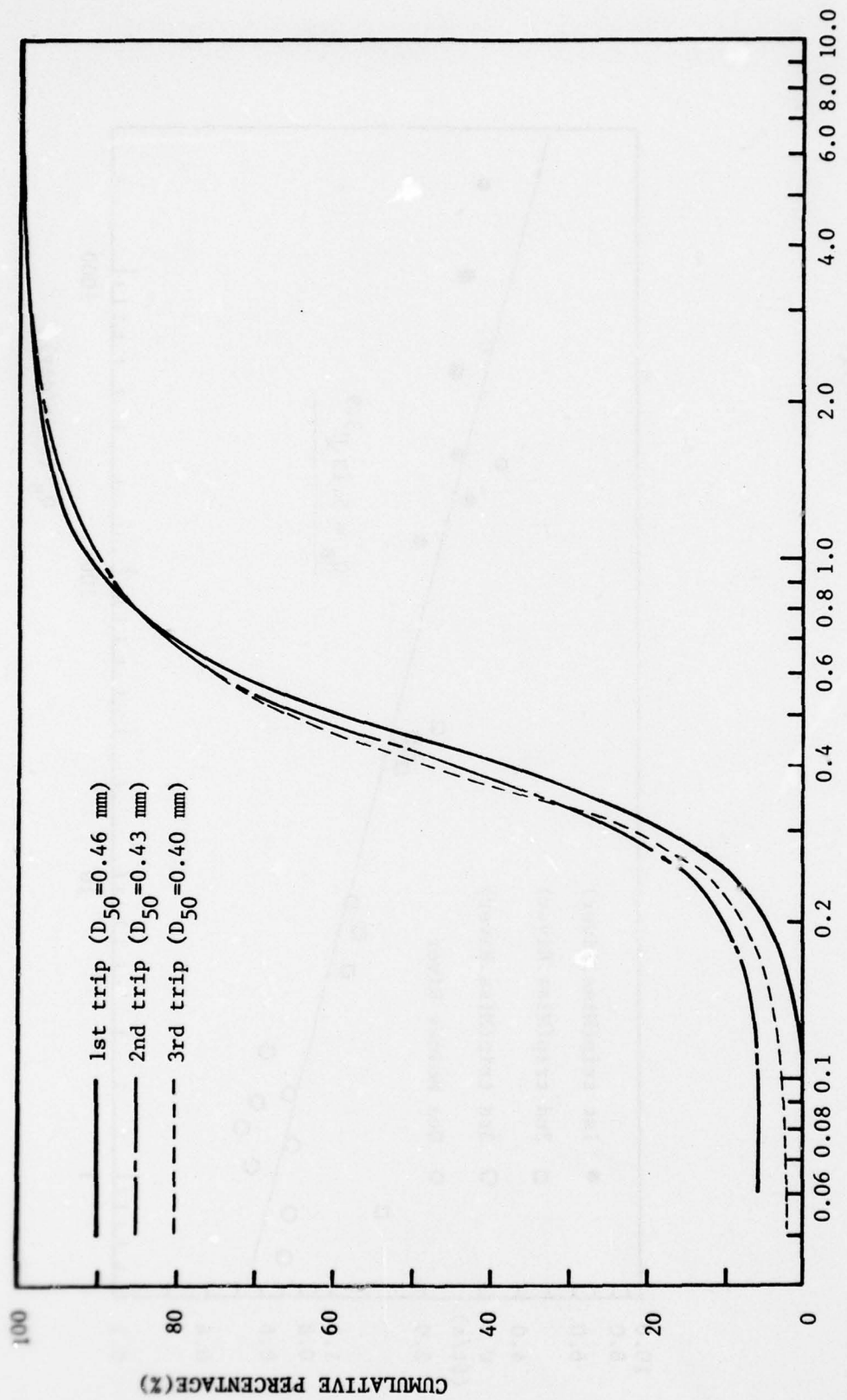


Figure 39A. Typical size distribution curves for bed-material samples obtained at Sec. 6-1
(approximately 600 ft from the right bank)

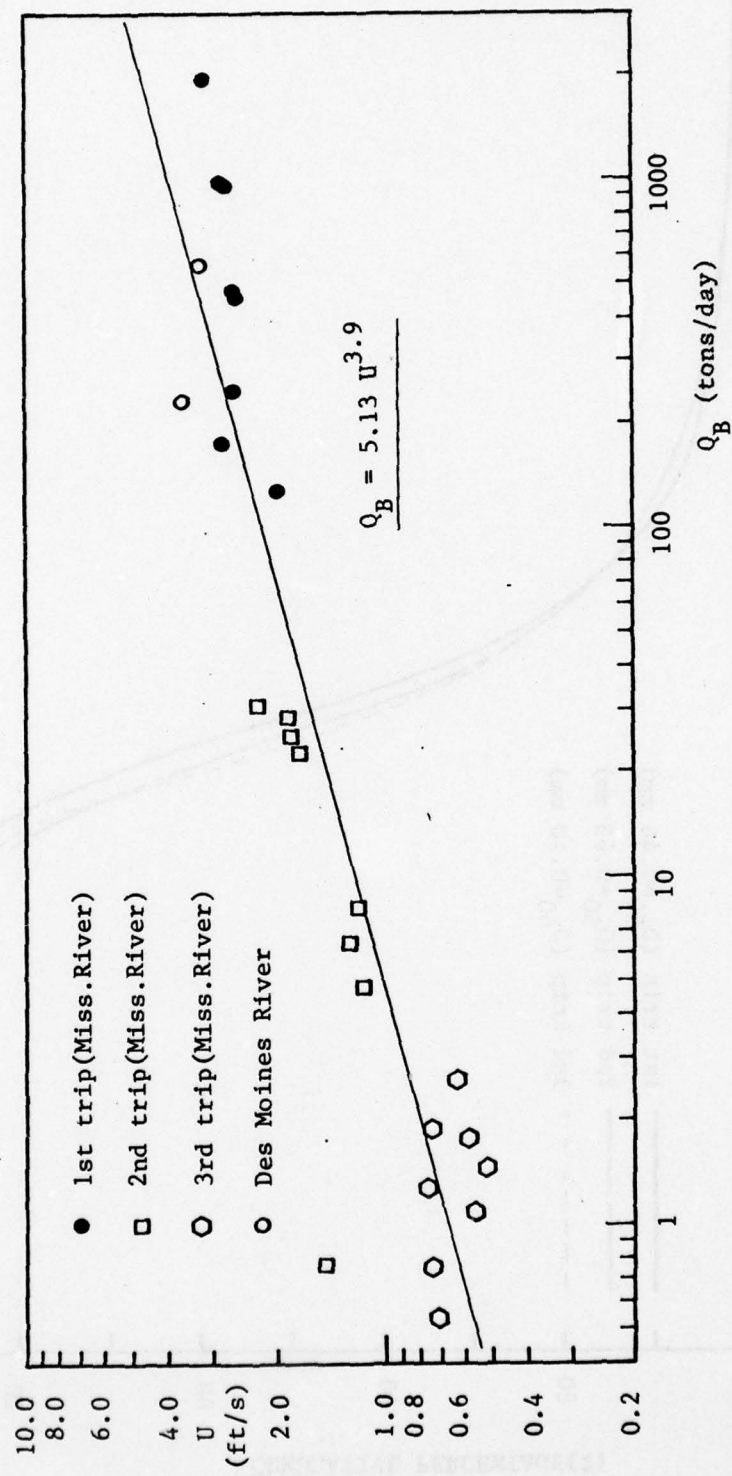


Figure 40. Relationship between U and Q_B

of the least-squares method, with the result

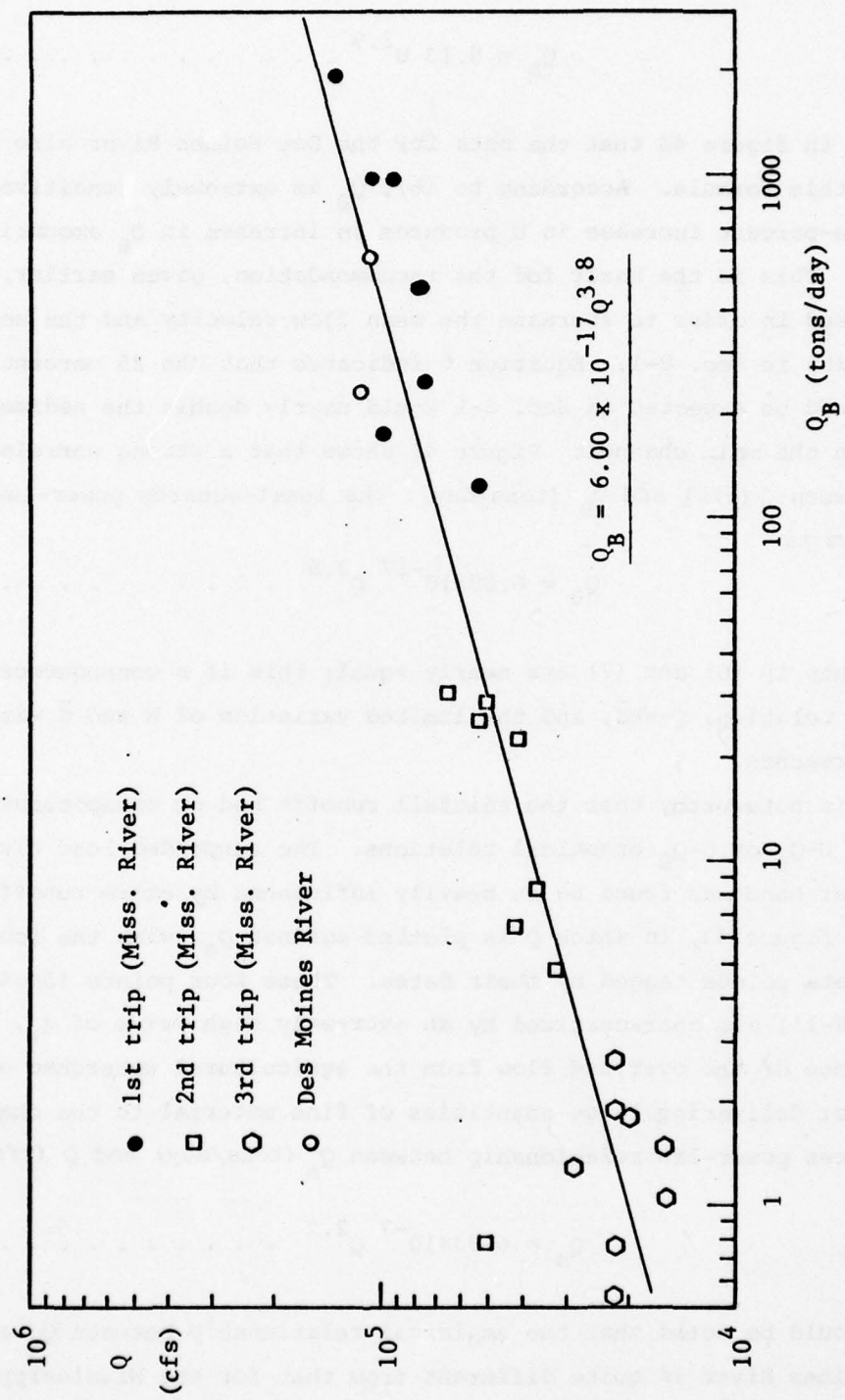
It is seen in figure 40 that the data for the Des Moines River also are in agreement with this formula. According to (6), Q_B is extremely sensitive to changes in U ; a one-percent increase in U produces an increase in Q_B amounting to nearly 4 percent. This is the basis for the recommendation, given earlier, that Sec. 8-2 be closed in order to increase the mean flow velocity and the sediment transport capacity in Sec. 8-1. Equation 6 indicates that the 25 percent increase in U which could be expected in Sec. 8-1 would nearly double the sediment transport capacity in the main channel. Figure 41 shows that a strong correlation also exists between Q (cfs) and Q_B (tons/day). The least-squares power-law relation between them is

$$Q_B = 6.00 \times 10^{-17} Q^{3.8} \quad \dots \dots \dots \dots \dots \dots \dots \quad (7)$$

The exponents in (6) and (7) are nearly equal; this is a consequence of the continuity relation, $Q = W\bar{d}$, and the limited variation of W and \bar{d} with Q along the study reaches.

It is noteworthy that the rainfall runoffs had no conspicuous effect on either the $U-Q_B$ or $Q-Q_B$ graphical relations. The suspended-load discharge, Q_s , on the other hand was found to be heavily influenced by storm runoffs; this is evident in figure 42, in which Q is plotted against Q_s , with the four rain affected data points tagged by their dates. These four points (Secs. 5-1, 1-2', 7-2', and 8-1') are characterized by an extremely high value of q_s , which is a consequence of the overland flow from the agricultural watershed of the Des Moines River delivering large quantities of fine material to the channel. The least-squares power-law relationship between Q_s (tons/day) and Q (cfs) is

Here it should be noted that the empirical relationship between Q_s and Q for the Des Moines River is quite different from that for the Mississippi River [compare (4) and (8)], while the relationship between Q_B and Q or U for the two rivers are practically indistinguishable.



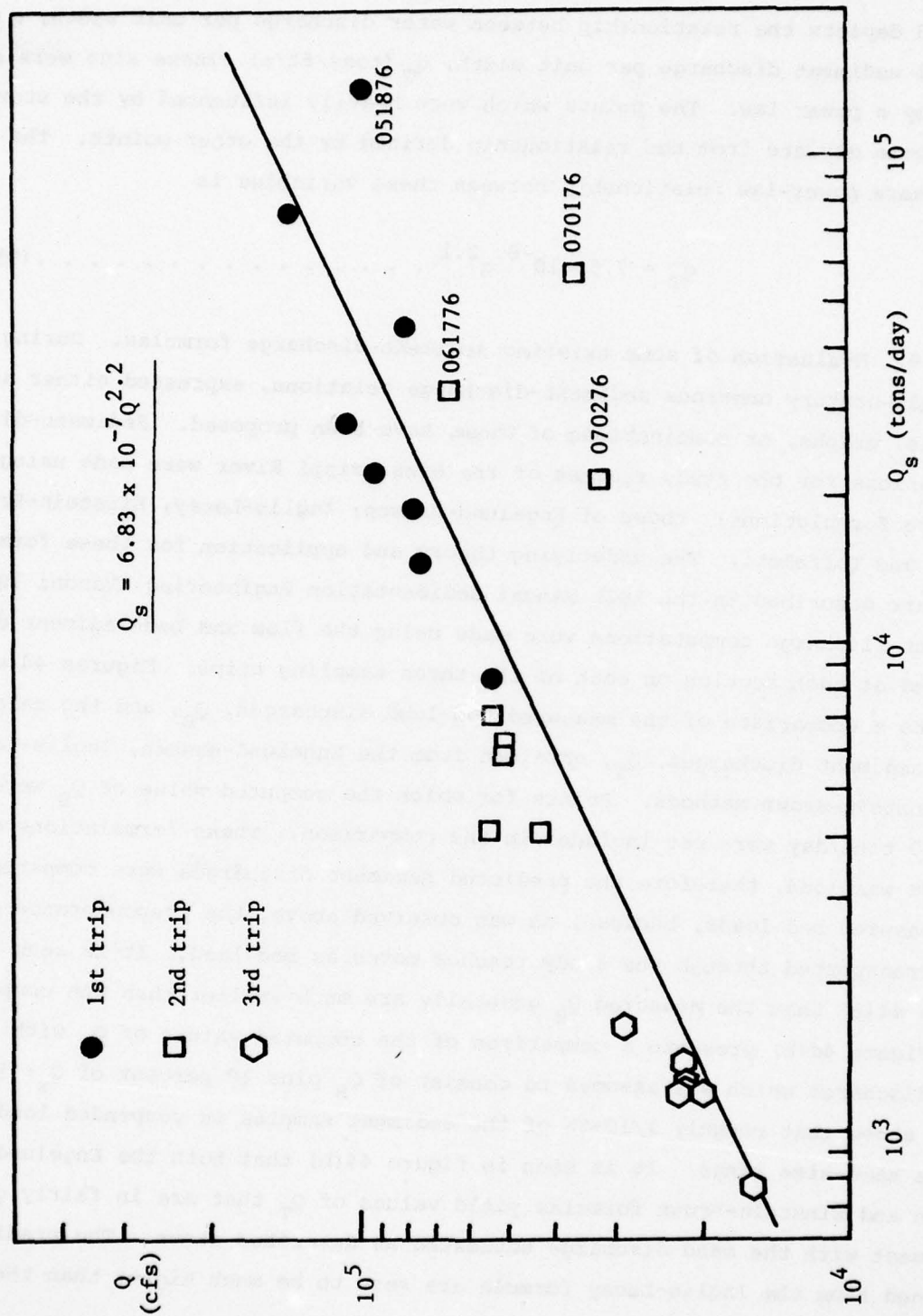


Figure 42. Relationship between Q and Q_s

Figure 43 depicts the relationship between water discharge per unit width, q (cfs/ft), and total sediment discharge per unit width, q_T (tons/ft/s). These also were seen to be related by a power law. The points which were heavily influenced by the storm runoff again deviate from the relationship defined by the other points. The least-square power-law relationship between these variables is

9. Evaluation of some existing sediment-discharge formulas. During the past half-century numerous sediment-discharge relations, expressed either as formulas, graphs, or combinations of these, have been proposed. Sediment-discharge calculations for the study reaches of the Mississippi River were made using five of these formulations: those of Engelund-Hansen; Inglis-Lacey; Einstein-Brown; Colby; and Toffaleti. The underlying theory and application for these formulations are described in the ASCE Manual Sedimentation Engineering (Vanoni 1975). Sediment-discharge computations were made using the flow and bed-sediment data obtained at each section on each of the three sampling trips. Figures 44(a) presents a comparison of the measured bed-load discharges, Q_B , and the calculated total sediment discharges, Q_T , obtained from the Engelund-Hansen, Inglis-Lacey, and Einstein-Brown methods. Points for which the computed value of Q_B were less than 10 tons/day were not included in the comparison. These formulations do not include washload; therefore the predicted sediment discharges were compared to the measured bed loads, because, as was observed above, the preponderance of the sand transported through the study reaches moves as bed load. It is seen in figure 44(a) that the measured Q_B generally are much smaller than the computed Q_T . Figure 44(b) presents a comparison of the computed values of Q_T with a sand discharge which was assumed to consist of Q_B plus 10 percent of Q_S ; it was noted above that roughly 1/10-th of the sediment samples as suspended load was in the sand-size range. It is seen in figure 44(b) that both the Engelund-Hansen and Einstein-Brown formulas yield values of Q_T that are in fairly good agreement with the sand discharge estimated as described above. The predictions obtained from the Inglis-Lacey formula are seen to be much higher than the estimated sand discharge.

Figure 45(a) presents a graphical comparison of the predicted measured total sediment discharge and that computed using the Toffaleti method. The

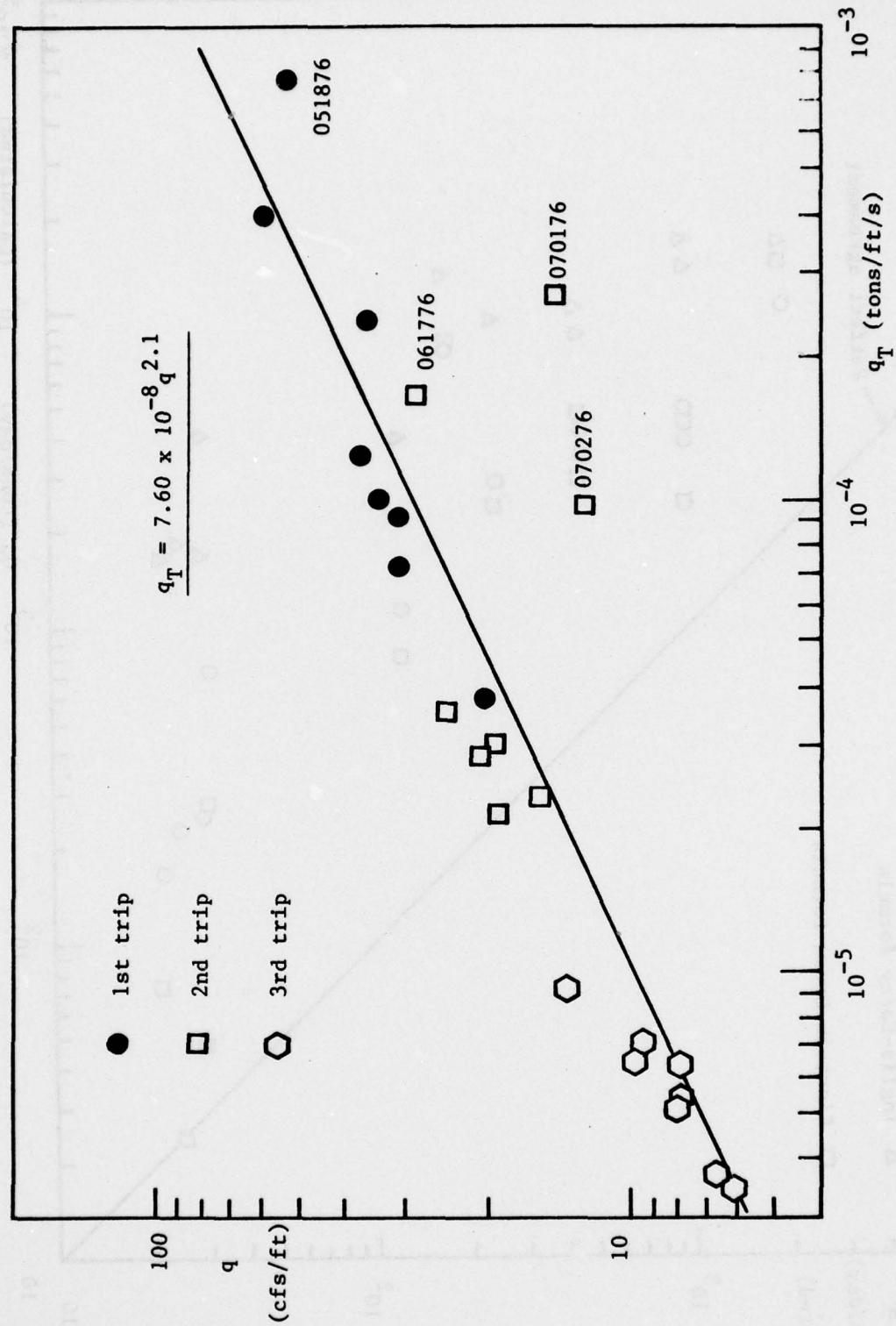


Figure 43. Relationship between q and q_T

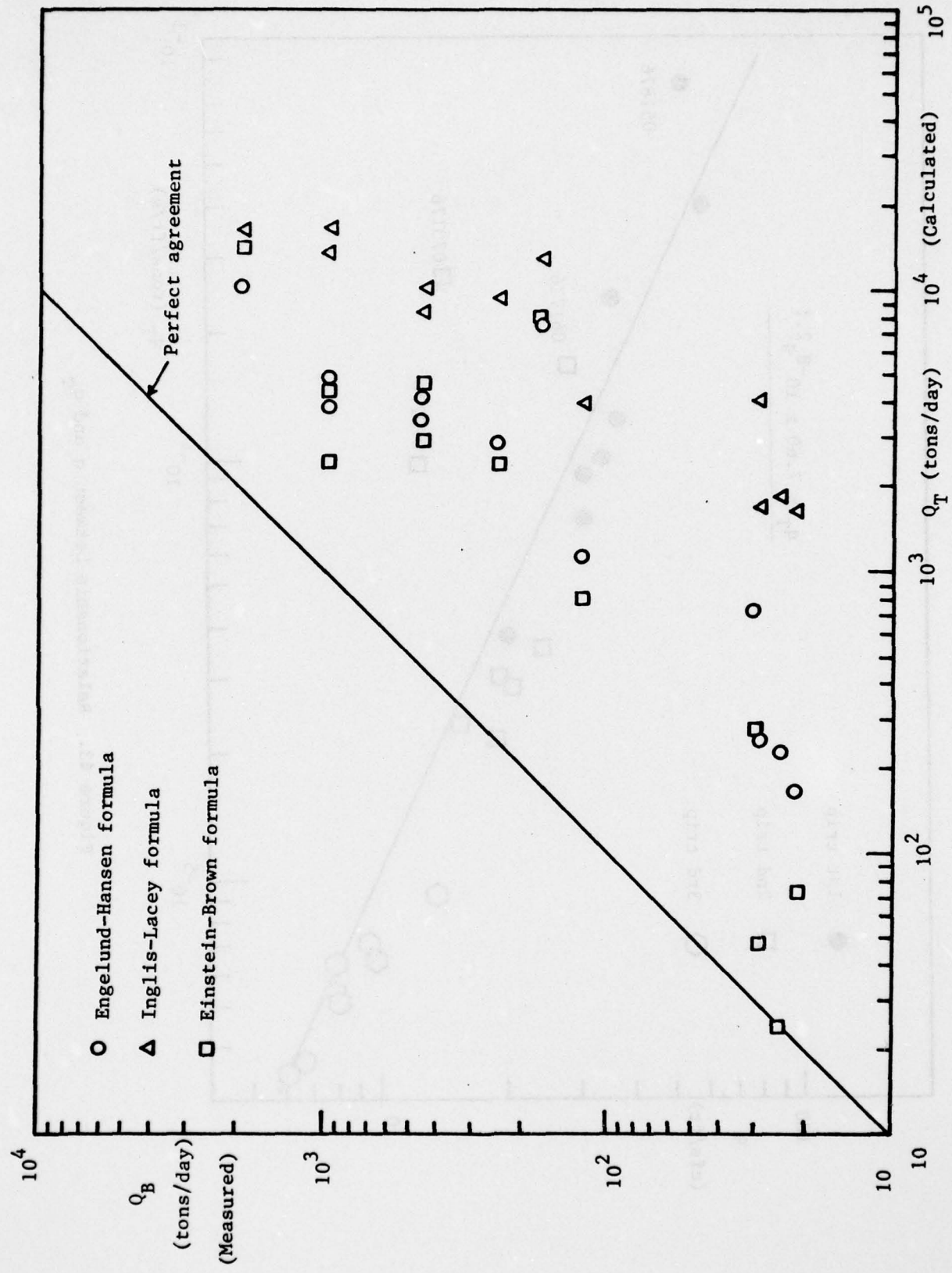
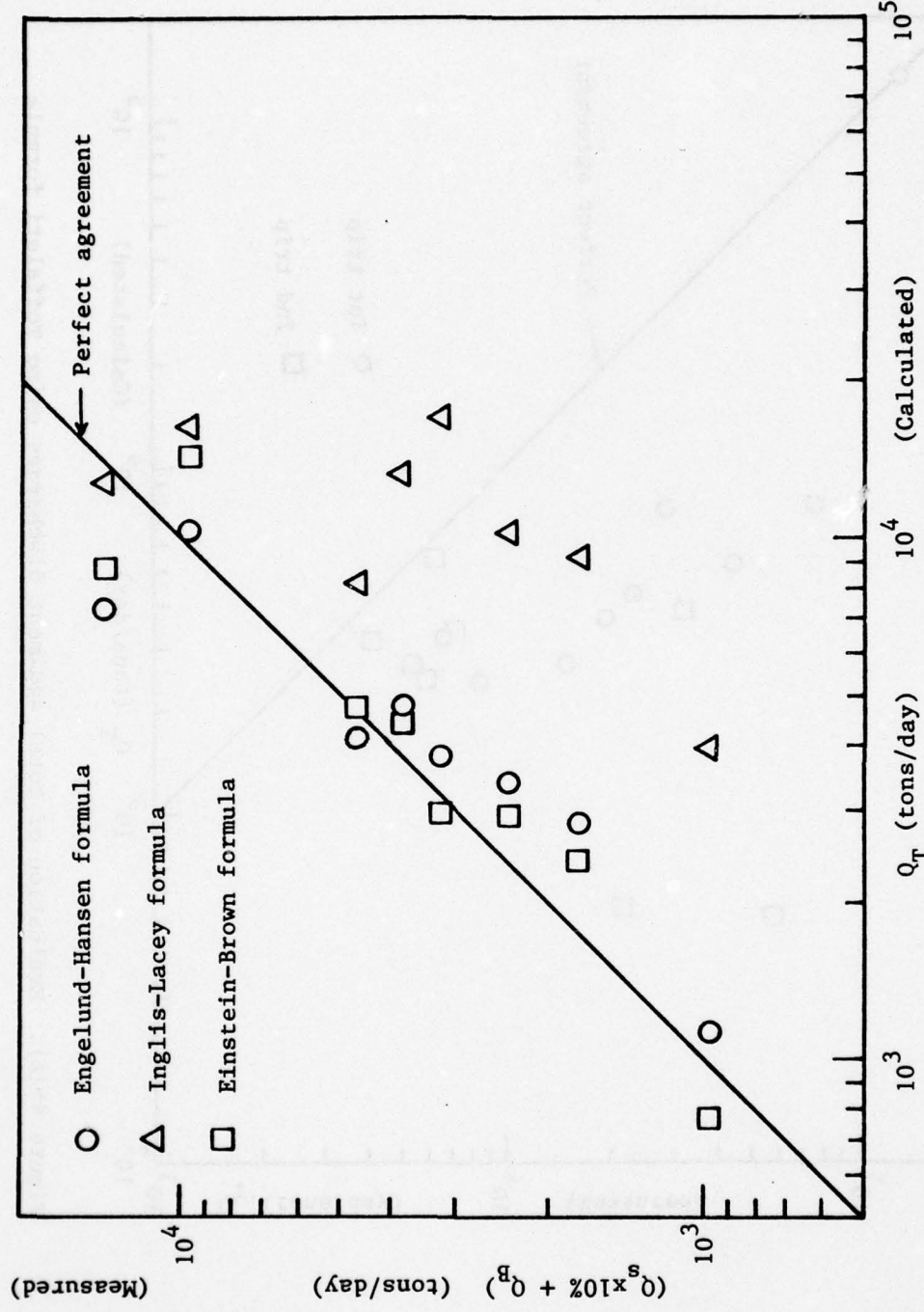


Figure 44(a). Evaluation of sediment-discharge formulas (Engelund-Hansen, Inglis-Lacey, and Einstein-Brown formulas)



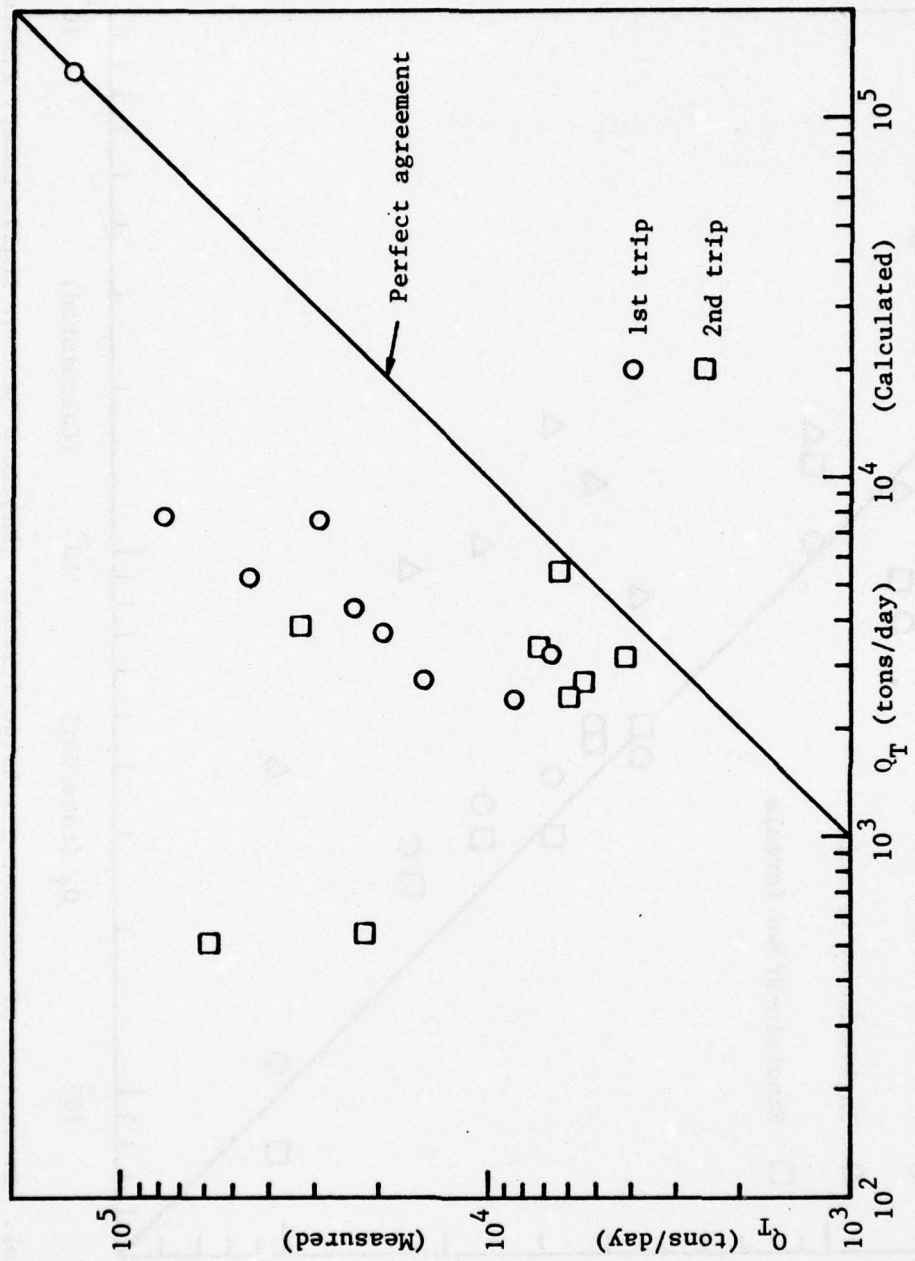


Figure 45(a). Evaluation of total sediment discharges using Toffaleti formula

predicted values of Q_T are seen to be much smaller than the measured ones, a consequence of the large quantities of washload carried by the Mississippi River in the study area. A comparison also was made between the values of Q_B predicted by Toffaleti's method and those which were measured. The result is shown in figure 45(b). As before, points for which the computed Q_B was less than 10 tons/day were not included. It is seen that the Toffaleti predictor yields bed-load discharges which are somewhat larger than the measured. It is noteworthy that the Toffaleti values Q_B are practically constant over the range of variables encountered.

Figure 46 presents a comparison of measured total sediment discharge, Q_T , and values computed using Colby's relation. The figure includes data from only the first trip, because the mean velocities prevalent during the second and third trips were below the range covered by the Colby relation. It is seen in figure 46 that Colby's method underestimates Q_T ; this is believed to be due primarily to the large quantity of washload present in the total load.

In summary, it can be concluded that the available techniques for predicting either the bed load or the total load of the study reaches of the Mississippi River do not yield reliable results. The empirical relations set forth above are believed to be far more reliable, and it is recommended that they rather than any of the generalized sediment-transport formulations be used in estimating the sediment-transport capacity of the river in the study area.

IV. SUMMARY AND CONCLUSIONS

The principal conclusions derived from this investigation may be summarized as follows:

1. The vertical distributions of velocity in the study reaches are adequately described by logarithmic relations of the Kármán-Prandtl type. However, the Kármán constant, κ , was found to vary widely with changes in mean suspended sediment concentration, especially at the lower values. At higher concentrations, in the range from about 400 ppm to 900 ppm, κ stabilizes at a value slightly in excess of 0.4.

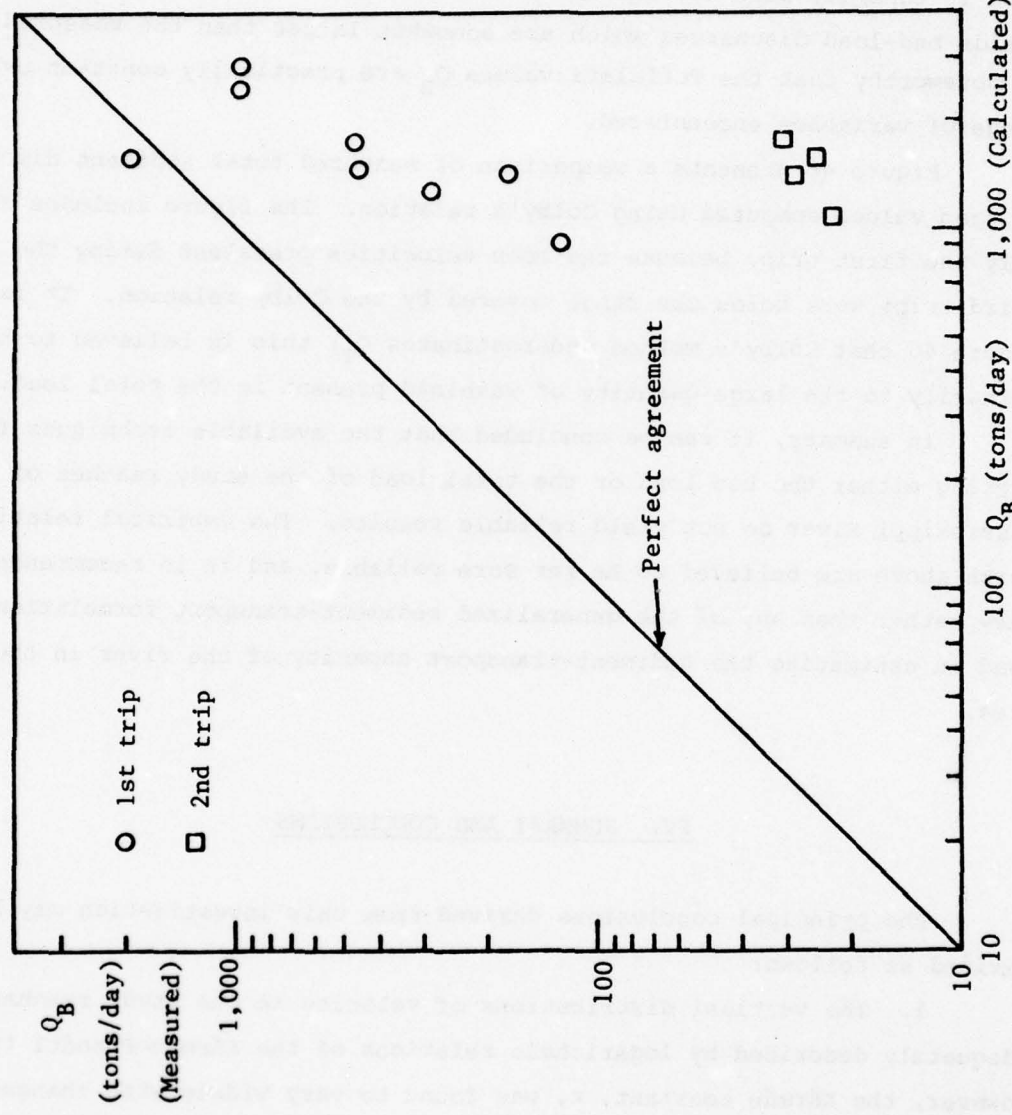


Figure 45(b). Evaluation of bed-load discharges using Toffaletti formula

and basin bottom and which includes the bottom of the river and the bed of the river. The total sediment discharge of the river can be calculated by the following equation, which is derived from the Colby's relation:

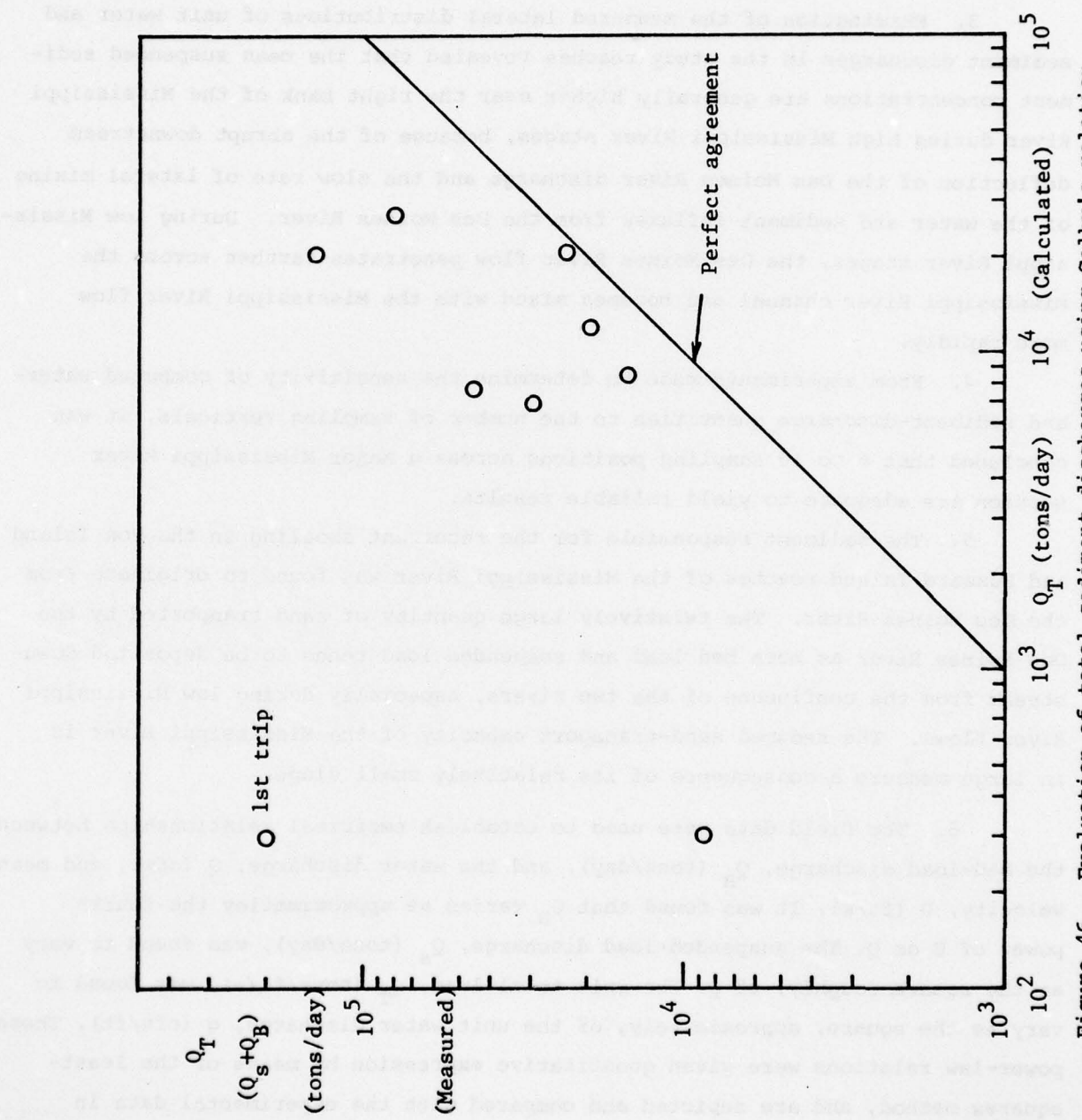


Figure 46. Evaluation of total sediment discharges using Colby's relation

2. During the study period (May-September 1976) the channel cross sections in the Buzzard Island reach were found to be more stable than those in the Fox Island reach. In the latter the bed-elevation changes were comparable in magnitude to the stage variations.

3. Examination of the measured lateral distributions of unit water and sediment discharges in the study reaches revealed that the mean suspended sediment concentrations are generally higher near the right bank of the Mississippi River during high Mississippi River stages, because of the abrupt downstream deflection of the Des Moines River discharge and the slow rate of lateral mixing of the water and sediment influxes from the Des Moines River. During low Mississippi River stages, the Des Moines River flow penetrates farther across the Mississippi River channel and becomes mixed with the Mississippi River flow more rapidly.

4. From experiments made to determine the sensitivity of computed water- and sediment-discharge quantities to the number of sampling verticals, it was concluded that 8 to 10 sampling positions across a major Mississippi River section are adequate to yield reliable results.

5. The sediment responsible for the recurrent shoaling in the Fox Island and Buzzard Island reaches of the Mississippi River was found to originate from the Des Moines River. The relatively large quantity of sand transported by the Des Moines River as both bed load and suspended load tends to be deposited downstream from the confluence of the two rivers, especially during low Mississippi River flows. The reduced sand-transport capacity of the Mississippi River is in large measure a consequence of its relatively small slope.

6. The field data were used to establish empirical relationships between the bed-load discharge, Q_B (tons/day), and the water discharge, Q (cfs), and mean velocity, U (ft/s). It was found that Q_B varies as approximately the fourth power of U or Q . The suspended-load discharge, Q_s (tons/day), was found to vary as the square, roughly, of Q . The unit total load, q_T (tons/ft/s), was found to vary as the square, approximately, of the unit water discharge, q (cfs/ft). These power-law relations were given quantitative expression by means of the least-squares method, and are depicted and compared with the experimental data in figures 40 through 43.

7. Between Secs. 7-2 and 8-1 the Mississippi River flow was found to bifurcate, with in excess of 25 percent of the water discharge passing through the secondary channel between Huff Island and Hunt Island. It was concluded

AD-A045 244

IOWA INST OF HYDRAULIC RESEARCH IOWA CITY
FIELD STUDY OF SEDIMENT TRANSPORT CHARACTERISTICS OF THE MISSIS--ETC(U)
JUL 77 T NAKATO, J F KENNEDY

F/G 8/8

UNCLASSIFIED

IIHR-201

NL

2 OF 2
AD
A045 244



END
DATE
FILMED
11-77
DDC

from examination of the field data that this flow bifurcation and the attendant velocity reduction downstream from it is responsible in large measure for the recurrent shoaling in the Buzzard Island reach. Closure of the channel between Huff and Hunt Islands would increase the flow velocity in the main channel (Sec. 8-1) by approximately 25 percent. According to the empirical sediment-discharge formulas, this would roughly double the sediment-transport capacity of the reach. Accordingly, it is recommended that the channel between Huff and Hunt Islands be closed.

8. In the Fox Island reach, it was found that approximately 10 percent of the flow passes through the secondary channel between Hackley Island and the Illinois shore. Closure of this narrow channel would increase the sediment-transport capacity of the main channel in this reach by approximately 40 percent, and should significantly reduce the magnitude of the shoaling problem in the Fox Island reach.

9. It should be noted that the quantities of sediment which must be dredged from the problem areas in the Fox Island and Buzzard Island reaches to maintain the 9-foot navigation depth are very small in comparison to the total quantity of sediment moving through the reach. Accordingly, remedial measures to alleviate the shoaling problem and reduce the dredging volume in these reaches should not give rise to deposition problems downstream.

10. Several existing generalized sediment-discharge predictors (Engelund-Hansen, Inglis-Lacey, Einstein-Brown, Colby, and Toffaleti) were evaluated by comparing sediment discharges computed from them with the measured values. None of the predictors was found to yield reliable results; this was mainly due to the fact that a large portion of sediment in transport in the study reaches consisted of fine sediment materials (silt and clay), and the sediment transport rate of coarse bed materials (mainly sand) was extremely low in testing the existing predictors. It was concluded that site-specific empirical sediment-discharge formulas based on good field data are far more reliable than the available published ones, and should be used whenever possible in framing sediment management strategies for natural streams.

LIST OF REFERENCES

GUY, H.P., 1969 Laboratory Theory and Methods for Sediment Analysis. U.S. Geological Survey, *Techniques of Water-Resources Investigations*, Book 5, Chapter C1.

GUY, H.P., & NORMAN, V.W., 1970 Field Methods for Measurement of Fluvial Sediment. U.S. Geological Survey, *Techniques of Water-Resources Investigations*, Book 3, Chapter C2.

ISFELD, E.O., HAY, D., & ROSSOUW, J., May 10-11, 1973 Field and Model Studies on a Siltation Problem in the FRASER RIVER. *Proceedings of the First Canadian Hydraulics Conference* held at the University of Alberta, Edmonton, Alberta, Canada, pp. 44-63.

LAGASSE, P.F., SIMONS, D.B., & CHEN, Y.H., January 26-28, 1976 Thalweg Disposal of Riverine Dredged Material. *ASCE Proceedings of the Specialty Conference on Dredging and its Environmental Effects held at Mobile, Alabama*, pp. 556-578.

SIMONS, D.B., ET AL. July, 1975 Environmental Inventory and Assessment of Navigation Pools 24, 25, and 26, Upper Mississippi and Lower Illinois Rivers -- A Geomorphic Study--. *Contract Report Y-75-3, U.S. Army Engineer Waterways Experiment Station*.

VANONI, V.A., 1975 Sedimentation Engineering. *ASCE Manuals and Reports on Engineering Practice -- No. 54*.